

AD-A080 810

NORTHROP RESEARCH AND TECHNOLOGY CENTER PALOS VERDES --ETC F/8 20/5
INVESTIGATION OF EFFICIENT CO LASER FREQUENCY TRIPLING. (U)

SEP 79 H KOMINE, E A STAPPAERTS, A S GERWER F29601-78-C-0068

UNCLASSIFIED

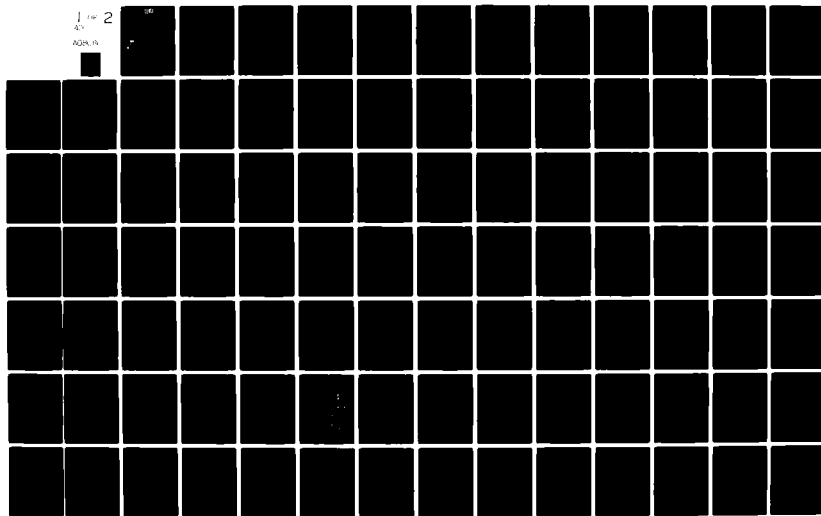
NRTC79-13R

AFWL-TR-79-71

NL

1 of 2

AD-A080 810



AFWL-TR-79-71

(2) LEVEL III

AD-E 200 437

AFWL-TR-
79-71

ADA 080810

INVESTIGATION OF EFFICIENT CO LASER FREQUENCY TRIPLING

H. Komine
E. A. Stappaerts
A. S. Gerwer

Northrop Corporation
Northrop Research and Technology Center
One Research Park
Palos Verdes Peninsula, CA 90274

September 1979

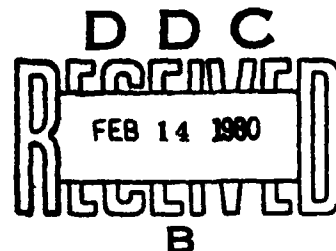
Final Report

DDC FILE COPY



Approved for public release; distribution unlimited.

THIS REPORT CONTAINS INFORMATION THAT IS UNCLASSIFIED.
THE COPY CONTAINED HEREIN CONTAINED A
SIGNIFICANT NUMBER OF PAGES WHICH DO NOT
REPRODUCE LEGIBLY.



AIR FORCE WEAPONS LABORATORY
Air Force Systems Command
Kirtland Air Force Base, NM 87117

79 12 17 116

This final report was prepared by the Northrop Research and Technology Center, Palos Verdes Peninsula, California, under Contract F29601-78-C-0068, Job Order 317J0522 with the Air Force Weapons Laboratory. Maj Jerry J. Perrizo (ALE) was the Laboratory Project Officer-in-Charge.

When US Government drawings, specifications, or other data are used for any purpose other than a definitely related Government procurement operation, the Government thereby incurs no responsibility nor any obligation whatsoever, and the fact that the Government may have formulated, furnished, or in any way supplied the said drawings, specifications, or other data, is not to be regarded by implication or otherwise, as in any manner licensing the holder or any other person or corporation, or conveying any rights or permission to manufacture, use, or sell any patented invention that may in any way be related thereto.

This report has been authored by a contractor of the United States Government. The United States Government retains a nonexclusive, royalty-free license to publish or reproduce the material contained herein, or allow others to do so, for the United States Government purposes.

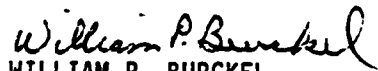
This report has been reviewed by the Information Office and is releasable to the National Technical Information Service (NTIS). At NTIS, it will be available to the general public, including foreign nations.

This technical report has been reviewed and is approved for publication.



JERRY J. PERRIZO
Major, USAF
Project Officer

FOR THE DIRECTOR



WILLIAM P. BURCKEL
Major, USAF
Chief, Pulsed Laser Branch



ARMAND D. MAIO
Colonel, USAF
Chief, Advanced Laser Technology Div

DO NOT RETURN THIS COPY. RETAIN OR DESTROY.

DISCLAIMER NOTICE

**THIS DOCUMENT IS BEST QUALITY
PRACTICABLE. THE COPY FURNISHED
TO DDC CONTAINED A SIGNIFICANT
NUMBER OF PAGES WHICH DO NOT
REPRODUCE LEGIBLY.**

UNCLASSIFIED

⑧ AFWL, SBIE

SECURITY CLASSIFICATION OF THIS PAGE (When Data Entered)

19 REPORT DOCUMENTATION PAGE		READ INSTRUCTIONS BEFORE COMPLETING FORM
1. REPORT NUMBER AFWL-TR-79-71, AD-E200 487	2. GOVT ACCESSION NO.	3. RECIPIENT'S CATALOG NUMBER
4. TITLE (and Subtitle) INVESTIGATION OF EFFICIENT CO LASER FREQUENCY TRIPLING.	5. TYPE OF REPORT & PERIOD COVERED Final Report	6. PERFORMING ORG. REPORT NUMBER NRTC 79-13R
7. AUTHOR(s) H. Komine, E. A. Stappaerts, A. S. Gerwer	8. CONTRACT OR GRANT NUMBER(s) F29601-78-C-0068	
9. PERFORMING ORGANIZATION NAME AND ADDRESS Northrop Research and Technology Center One Research Park Palos Verdes Peninsula, CA 90274	10. PROGRAM ELEMENT, PROJECT, TASK AREA & WORK UNIT NUMBERS 63605F/317J0522	
11. CONTROLLING OFFICE NAME AND ADDRESS Air Force Weapons Laboratory (ALP) Kirtland Air Force Base, NM 87117	12. REPORT DATE September 1979	
14. MONITORING AGENCY NAME & ADDRESS (if different from Controlling Office) 12 141	13. NUMBER OF PAGES 136	
	15. SECURITY CLASS. (of this report) UNCLASSIFIED	
	15a. DECLASSIFICATION, DOWNGRADING SCHEDULE	
16. DISTRIBUTION STATEMENT (of this Report) Approved for public release; distribution unlimited.		
17. DISTRIBUTION STATEMENT (of the abstract entered in Block 20, if different from Report)		
18. SUPPLEMENTARY NOTES		
19. KEY WORDS (Continue on reverse side if necessary and identify by block number) Frequency tripling, nonlinear susceptibilities, resonant enhancement schemes, sum frequency generation.		
20. ABSTRACT (Continue on reverse side if necessary and identify by block number) A thorough study on the feasibility of efficient CO laser frequency tripling in molecular gases has been completed. Computer code calculations of nonlinear susceptibilities and detailed analysis of efficiency limitations have been carried out for nine candidate molecules belonging to three different resonant enhancement schemes. The results of the study show that direct frequency tripling would yield small efficiencies. However, a two-step conversion process involving an intermediate frequency shifting may provide large enhancement factors for efficient two-photon resonant sum frequency generation.		

DD FORM 1 JAN 73 1473 EDITION OF 1 NOV 65 IS OBSOLETE

UNCLASSIFIED

SECURITY CLASSIFICATION OF THIS PAGE (When Data Entered)

407696

B

TABLE OF CONTENTS

1.0	SUMMARY	1
2.0	INTRODUCTION	3
3.0	THIRD HARMONIC AND SUM FREQUENCY GENERATION: NONLINEAR SUSCEPTIBILITY ANALYSIS AND CALCULATION	5
3.1	Third-Order Susceptibility $\chi^{(3)}$	7
3.2	Resonance Enhancement Schemes	9
3.3	Nonlinear Susceptibility $\chi^{(3)}$ Code	12
3.3.1	Type I Scheme	12
3.3.2	Type II Scheme	21
3.3.3	Type III Scheme	24
3.4	$\chi^{(3)}$ Calculation Results	30
3.4.1	Type I Scheme	30
3.4.2	Type II Scheme	39
3.4.3	Type III Scheme	41
4.0	EFFICIENCY LIMITATION AND PHASE-MATCHING ANALYSIS	44
4.1	Linear Processes	45
4.1.1	Absorption Coefficient and Refractive Index at Pump Frequencies	45
4.1.2	Absorption Coefficient and Refractive Index at Generated Frequencies	49
4.1.3	Population Transfer and Dynamic Phase Mismatch	52
4.1.4	Thermal Defocusing	53
4.2	Nonlinear Processes	54
4.2.1	Two-Photon Absorption	54
4.2.2	Quadratic Kerr Effect	55
4.2.3	Stimulated Raman Scattering	58
4.2.4	Three-Photon Absorption	62
4.2.5	Gas Breakdown	63
4.2.6	Pump Depletion	64
4.3	Optimum Scheme	65
5.0	MULTILINE THG AND SFG ANALYSIS	68
5.1	Efficient THG and SFG Optimization	68
5.2	Two-Step Frequency Conversion	69

TABLE OF CONTENTS (Continued)

6.0	EXPERIMENTAL PROGRAM	74
6.1	Approach	74
6.2	Experimental Facility	74
6.3	Parametric Study	78
7.0	CONCLUSION	79
8.0	REFERENCES	80
	APPENDIX A	83
	APPENDIX B	116

ACCESSION for		
NTIS	White Section	<input checked="" type="checkbox"/>
DDC	Buff Section	<input type="checkbox"/>
UNANNOUNCED		<input type="checkbox"/>
JUSTIFICATION		
BY		
DISTRIBUTION/AVAILABILITY CODES		
Dist. AVAIL. and/or SPECIAL		
A	23	CP

LIST OF FIGURES

FIGURE

1.	Three Types of Resonance Enhancement	10
2.	$\chi^{(3)}$ Flow Chart	20
3.	Nonlinear Susceptibility of CO^{18} for Third Harmonic Generation	37
4(a).	DCI Refractive Index vs Frequency	46
(b).	DCI Absorption Coefficient vs Frequency	46
5(a).	DBr Refractive Index vs Frequency	47
(b).	DBr Absorption Coefficient vs Frequency	47
6(a).	NO Refractive Index vs Frequency	48
(b).	NO Absorption Coefficient vs Frequency	48
7(a).	DF Refractive Index vs Frequency	50
(b).	DF Absorption Coefficient vs Frequency	50
8(a).	HCl Refractive Index vs Frequency	51
(b).	HCl Absorption Coefficient vs Frequency	51
9.	Normalized $ \chi^{\text{SFG}} $ vs HD Q(1) Two-Photon Resonance Frequency Detuning	70
10.	Normalized $ \chi^{\text{SFG}} $ vs Density	71
11.	Normalized χ^{KERR} and χ^{TPA} vs HD Q(1) Two-Photon Resonance Frequency Detuning	72
12.	Schematic of Two-Step CO Laser Sum Frequency Generation	73
13.	Sum Frequency Generation Experiment Block Diagram	75
14.	Fixed IR Source Block Diagram	75
15.	Tunable IR Source Block Diagram	76
16.	Schematic of Experimental Apparatus	78

LIST OF TABLES

TABLE

1.	Nonlinear Susceptibility $\chi^{(3)}$	8
2.	$\chi^{(3)}$ Formula	9
3.	Type I Scheme Optimum Pump Frequencies	11
4.	Type II Scheme Molecules: Two-Photon Resonance Frequency	11
5.	Product of Rotational Matrix Elements for $\Lambda = 0$ Molecules	14
6.	$W(J_a, J_b, J_c, J_d)$ for $\Lambda = 1$ Molecules	17
7.	$\xi_Q(a, b)$ in Terms of Mixing Coefficients and Reduced Rotational Matrix Elements	19
8.	Terms in the Ω -Path Summation	19
9.	Type II Nonlinear Susceptibility	25
10.	Type I Scheme Molecular Parameter References	30
11.	Type I $\chi^{(3)}$ Calculation Results: CO ¹⁸	31
12.	Type I $\chi^{(3)}$ Calculation Results: NO ¹⁶	32
13.	Type I $\chi^{(3)}$ Calculation Results: DCl ³⁵	33
14.	Type I $\chi^{(3)}$ Calculation Results: DCl ³⁷	34
15.	Type I $\chi^{(3)}$ Calculation Results: DBr ⁷⁹	35
16.	Type I $\chi^{(3)}$ Calculation Results: DBr ⁸¹	36
17.	Type I THG Survey Calculation	38
18.	Type II Scheme Molecular Parameter References	39
19.	Type II THG Survey Calculation	40
20.	Type III Scheme Molecular Parameter References	41
21.	Type III $\chi^{(3)}$ Calculation Results: HCl ³⁵	42
22.	Type III $\chi^{(3)}$ Calculation Results: DF	43
23.	Vibrational Raman Gain Coefficients	60
24.	Efficiency Limitation Analysis: Summary	66
25.	Coherent IR Source Parameters	77

1.0 SUMMARY

A detailed analysis on the feasibility of efficient CO laser frequency tripling in molecular gases has been carried out. The results of the study indicate that direct frequency tripling of multiline CO laser output leads to small conversion efficiencies based on the nonlinear susceptibilities and the efficiency limiting processes of the molecules surveyed. However, the analysis of the three resonance enhancement schemes shows that two-photon resonant SFG and THG in hydrogen molecules are potentially efficient frequency conversion processes if the pump frequencies can satisfy the resonance condition.

In the type I resonance enhancement scheme, pump absorption leading to dynamic phase mismatches is likely to be the primary efficiency limiting process. Since this scheme requires near-resonant conditions at one-, two-, and three-photon resonances, the pump absorption is always present and inherently restricts the application of the type I scheme to short pump pulses.

The type II scheme, which is based on two-photon resonance enhancement, avoids the dynamic phase mismatch caused by pump absorption. However, other competing nonlinear processes become significant at the high pump intensities required for efficient conversion. Although two-photon absorption, quadratic Kerr effect, and stimulated Raman scattering ultimately limit the efficiency, near unity THG and SFG conversion efficiencies are predicted under optimum conditions. The parameters that govern these conditions are the two-photon resonance frequency detuning and Kerr-induced phase shifts.

The type III scheme analysis and the related $\chi^{(3)}$ calculations which were performed utilizing three-photon resonances in a number of infrared-active molecules show that relatively small conversion efficiencies can be expected for this resonance enhancement scheme. The principal efficiency limitation in the type III scheme is optical gas breakdown at high pump intensities. The high pump intensities are necessary to compensate for relatively small nonlinear susceptibilities.

Efficient multiline frequency up-conversion of CO laser frequencies requires resonantly enhanced THG and/or SFG processes for a number of frequency combinations. The nonlinear medium must also allow simultaneous phase-matching for

different combinations of the pump frequencies. These requirements suggest that the type II scheme is more suitable for multiline pumping than the two other schemes. When the two-photon resonance condition is satisfied, the SFG nonlinear susceptibilities for various combinations of three pump frequencies are very similar. The type II candidate molecules such as H_2 and HD have very small dispersion at the pump and the generated frequencies. This property is desirable for the simultaneous phase-matching of the various pump frequency combinations.

Efficient CO laser output spans a frequency range between 1920 and 2030 cm^{-1} . Analysis of two-photon resonances in H_2 and HD indicates that the sum of two pump frequencies lies in between the strong Q-branch resonances of H_2 and HD. This leads to relatively small nonlinear susceptibilities for direct THG and SFG. Further investigation of competing effects shows that stimulated Raman scattering may be significant under certain conditions. In particular, stimulated rotational Raman scattering can become an efficient nonlinear process in H_2 . The Raman shifted frequencies may participate further in other nonlinear interactions such as induced two-photon absorption and sum frequency generation. The Raman-shifted frequencies in H_2 and the original pump frequencies closely match the Q-branch two-photon resonances in HD. This suggests that a two-step frequency conversion involving an initial Raman shifting in H_2 followed by sum frequency generation in HD is a potentially efficient process for multiline pumping. The two-step conversion process leads to output wavelengths in the 1.77 and 1.90 μm region.

These results indicate that two-photon resonantly enhanced sum frequency generation in HD is the most promising approach to up-convert multiline CO laser frequencies. In order to verify this feasibility, an experimental investigation of SFG in HD is recommended for future study. The investigation should consist of setting up an experimental facility to generate tunable IR frequencies in the 5-6 μm region and performing parametric SFG experiments using the generated frequencies.

2.0 INTRODUCTION

Efficient frequency up-conversion of high power infrared gas lasers is of considerable interest due to the advent of very efficient IR lasers. For example, the frequency conversion of CO laser output to shorter wavelengths would provide high power coherent radiation suitable for atmospheric transmission with smaller beam control and pointing optics. Recent experimental and theoretical studies indicate that IR laser frequency tripling in molecular media is indeed possible.¹⁻³ High conversion efficiencies at reasonable pump intensities are predicted using resonance enhancement of the third order nonlinear susceptibility due to vibrational states.¹⁻⁶

The resonance enhancement of frequency up-conversion processes is a widely used technique which is particularly useful for infrared laser frequency up-conversion in molecular media. The nonlinear medium may consist of infrared-active or Raman-active molecular species. In the IR-active molecules, the fundamental and overtone transitions provide one-, two-, and three-photon resonances in addition to contributions from the electronic states. The Raman-active molecules have energy level structures suitable for two-photon resonances. These resonances may yield a very significant enhancement of the nonlinear susceptibility leading to potentially high conversion efficiencies.

Several recent investigations have been devoted to frequency tripling of the CO₂ laser radiation. Although earlier results of these investigations were not promising, some very recent progress in the demonstration of CO₂ laser frequency tripling indicates that the experimental conversion efficiencies are approaching the theoretically predicted values.^{2,3,4} Analysis of the particular resonance enhancement schemes used in the CO₂ experiments shows that a similar technique is applicable to CO laser frequency tripling for generating high power coherent radiation at 1.7 μ m. Since the CO laser output consists of several frequencies, sum frequency generation may occur simultaneously with frequency tripling.

Because of the complexity created by the multitude of CO spectral lines, as many schemes as possible should be considered. For this reason, three different resonance enhancement schemes have been analyzed in terms of third harmonic

and sum frequency generation in several different molecular media. The basic concept of two of these schemes has been discussed in the literature.¹⁻⁶ Another scheme conceived at the Northrop Research and Technology Center (NRTC) involves a different type of resonance enhancement which may solve some of the problems inherent in the other schemes.

The details of the three schemes and the analysis and calculations of third-order susceptibilities for each of the schemes are described in Section 3. Section 4 discusses the efficiency limiting processes and phase-matching analysis, which are essential in understanding the optimum device performance characteristics and conversion efficiencies. Section 5 analyzes the effect of a multiline pump source on the third harmonic and sum frequency generation efficiencies and suggests a potentially efficient two-step frequency conversion scheme based on an intermediate frequency shifting technique. Recommendations for an experimental program aimed at verification of theoretical calculations are presented in Section 6.

3.0 THIRD HARMONIC AND SUM FREQUENCY GENERATION: NONLINEAR SUSCEPTIBILITY ANALYSIS AND CALCULATION

Optical third harmonic generation (THG) or frequency tripling is described by a microscopic nonlinear susceptibility tensor $\chi^{(3)}$ which relates the cubic power of the incident electric field amplitude to the generated polarization in the medium. More generally, the quantity $\chi^{(3)}$ relates a product of three electric field amplitudes to the generated polarization oscillating at the sum of the three field frequencies. This is referred to as sum frequency generation (SFG).

The theory of optical frequency mixing has been well established and experimentally verified. The basic quantity that enters into the equations which describe the THG and SFG processes is the macroscopic nonlinear polarization of the medium. For the case of three monochromatic (plane-wave) applied fields, the generated polarization at the sum frequency can be expressed as:⁷

$$P^{(3)}(z,t) = \frac{1}{2} P_s(z) e^{-i\omega_s t} + \text{c. c.} \quad (1)$$

$$\begin{aligned} \text{where} \quad P_s(z) &= \frac{N}{4} Z \chi_s^{(3)}(\omega_p, \omega_q, \omega_r) E_p(z) E_q(z) E_r(z) \\ &\times \exp[i(k_p + k_q + k_r)z] \end{aligned}$$

The factor Z is the number of distinguishable permutations of the applied field amplitudes: $Z = 6$ for three distinct (including sign) frequencies, $Z = 3$ for a pair of equal frequencies, and $Z = 1$ for $\omega_p = \omega_q = \omega_r$. The other quantities N and $\chi_s^{(3)}(\omega_p, \omega_q, \omega_r)$ are the total number density and microscopic (molecular) third-order susceptibility.

The macroscopic nonlinear polarization provides the source term for the wave equation governing the growth of the generated field. In the slowly-varying amplitude approximation, the wave equation reduces to:

$$\frac{\partial E_s(z)}{\partial z} = \frac{i \tau_l \omega_s}{2 n_s} P_s(z) e^{-i k_s z} \quad (2)$$

where

n_s = the refractive index at ω_s

$$k_s = \frac{n_s \omega_s}{c}$$

$\eta_1 = (\mu_0/\epsilon_0)^{1/2}$, the impedance of free space

Substitution of the expression for $P_s(z)$ from expression (1) into (2) yields

$$\frac{\partial E_s(z)}{\partial z} = \frac{i \eta_1 \omega_s N}{8 n_s} Z \chi_s^{(3)} E_p(z) E_q(z) E_r(z) e^{-i\Delta k z} \quad (3)$$

where the wave vector mismatch, Δk , is defined by

$$\Delta k \equiv k_s - (k_p + k_q + k_r) \quad (4)$$

If the depletion of the applied fields is neglected, equation (3) can be integrated directly over the interaction length, L :

$$E_s(L) = \frac{i \eta_1 \omega_s N L}{8 n_s} Z \chi_s^{(3)} E_p E_q E_r e^{-i\Delta k L/2} \text{sinc}(\Delta k L/2) \quad (5)$$

The electric field intensities are given by

$$I_\ell = \frac{n_\ell |E_\ell|^2}{2\eta_1} \quad (\ell = p, q, r) \quad (6a)$$

$$I_s = \frac{n_s |E_s|^2}{2\eta_1} \quad (6b)$$

Equations (5) and (6) are applicable to third harmonic generation as well as to sum frequency generation. For example, the third harmonic field at $\omega_s = 3\omega_1$ is given by

$$E_{3\omega_1}(L) = \frac{3\eta_1 \omega_1 N L}{8 n_s} \chi^{THG} E_1^3 e^{-i\Delta k L/2} \text{sinc}(\Delta k L/2) \quad (7)$$

Accordingly, the field intensity of the third harmonic is given by

$$I_{THG} = \frac{1}{16} \frac{\eta_1^4}{n_s n_1^3} (3\omega_1)^2 L^2 N^2 |\chi^{THG}|^2 I_1^3 \text{sinc}^2(\Delta k L/2) \quad (8)$$

where

I_{THG}	=	the field intensity at $3\omega_1$
I_1	=	the field intensity at ω_1
$\chi_{3\omega_1}^{\text{THG}}$	\equiv	$\chi_{3\omega_1}^{(3)}(\omega_1, \omega_1, \omega_1)$
	=	the nonlinear susceptibility for THG.

All of the parameters in Equation (8) are expressed in MKS units. In sum frequency generation ω_s may be either a sum of three different frequencies ($\omega_s = \omega_1 + \omega_2 + \omega_3$) or a sum of one frequency and twice another frequency (e.g., $\omega_s = 2\omega_1 + \omega_2$). The generated field intensities for these two cases are given by

$$I_{\text{SFG}} = \frac{9}{4} \frac{\tau_1^4}{n_s n_1 n_2 n_3} \omega_s^2 N^2 L^2 |\chi_s^{(3)}(\omega_1, \omega_2, \omega_3)|^2 I_1 I_2 I_3 \text{sinc}^2(\Delta k L / 2) \quad (9)$$

where $\omega_s = \omega_1 + \omega_2 + \omega_3$, and

$$I_{\text{SFG}}' = \frac{1}{16} \frac{\tau_1^4}{n_s n_1^2 n_2} (\omega_s')^2 N^2 L^2 |\chi_s^{(3)}(\omega_1, \omega_1, \omega_2)|^2 I_1^2 I_2^2 \times \text{sinc}^2(\Delta k L / 2) \quad (10)$$

where $\omega_s' = 2\omega_1 + \omega_2$.

Equations (8), (9), and (10) indicate that the generated intensities for THG and SFG depend on the molecular parameters through $\chi^{(3)}$ and Δk . Thus, efficient THG and SFG from CO laser output requires molecular species in which large values of $\chi^{(3)}$ can be obtained at the CO laser frequencies. Furthermore, the phase mismatch, $\Delta k L$, must be minimized in order to obtain a value of $\text{sinc}^2(\Delta k L / 2)$ which is as close to unity as possible. More detailed analyses of these important considerations are presented in the following sections.

3.1 Third Order Susceptibility $\chi^{(3)}$

The derivation of the nonlinear susceptibility tensor is based on density matrix perturbation calculations⁷ for atoms and molecules interacting with external electric fields. The formula for $\chi^{(3)}$ is given by the set of equations in Table 1. The application of the $\chi^{(3)}$ formula for molecules involves summation over intermediate states, as shown by the expressions in Table 2. In principle,

all of the rotational, vibrational, and electronic states of the molecule are required for the calculation. However, various approximations can be used to simplify the summations under certain conditions. For example, if the applied field frequencies or their combinations are nearly resonant with the molecular transition frequencies of the nonlinear medium, a large enhancement of the frequency factor results from the intermediate states associated with the resonances. This resonance enhancement not only gives large susceptibilities but also reduces the number of intermediate states which are necessary for accurate computation.

TABLE 1. NONLINEAR SUSCEPTIBILITY $\chi^{(3)}$

Process:

$$\omega_p + \omega_q + \omega_r \rightarrow \omega_s$$

$$\chi_s^{(3)}(\omega_p, \omega_q, \omega_r) = \mathbf{S} \left(\frac{-1}{6 \hbar^3} \right) \sum_{abcd} \rho_{aa}^{(0)} \mu_{ab} \mu_{bc} \mu_{cd} \mu_{da} F_{abcd}(\omega_1, \omega_2, \omega_3)$$

$\mathbf{S} \equiv$ sum over all permutations of $(\omega_p, \omega_q, \omega_r)$ for $(\omega_1, \omega_2, \omega_3)$

$\rho_{aa}^{(0)} \equiv$ population distribution of molecules

$\mu_{ij} \equiv$ electric dipole matrix element

$F_{abcd}(\omega_1, \omega_2, \omega_3) \equiv$ frequency factor

$$\begin{aligned} &= \frac{1}{(\omega_{ab} + i\Gamma_{ab} + \omega_1 + \omega_2 + \omega_3)(\omega_{ac} + i\Gamma_{ac} + \omega_2 + \omega_3)(\omega_{ad} + i\Gamma_{ad} + \omega_3)} \\ &+ \frac{1}{(\omega_{ab} - i\Gamma_{ab} - \omega_1)(\omega_{ac} + i\Gamma_{ac} + \omega_2 + \omega_3)(\omega_{ad} + i\Gamma_{ad} + \omega_3)} \\ &+ \frac{1}{(\omega_{ab} - i\Gamma_{ab} - \omega_1)(\omega_{ac} - i\Gamma_{ac} - \omega_1 - \omega_2)(\omega_{ad} + i\Gamma_{ad} + \omega_3)} \\ &+ \frac{1}{(\omega_{ab} - i\Gamma_{ab} - \omega_1)(\omega_{ac} - i\Gamma_{ac} - \omega_1 - \omega_2)(\omega_{ad} - i\Gamma_{ad} - \omega_1 - \omega_2 - \omega_3)} \end{aligned}$$

TABLE 2. $\chi^{(3)}$ FORMULA

$$\chi^{(3)} = S\left(\frac{-1}{6\hbar^3}\right) \sum_{[Y]} \sum_{[v]} \phi_v \sum_J f_J \sum_{[K]} \phi_r(K) F_{abcd}$$

$$\phi_v = \mu_{ab}^v \mu_{bc}^v \mu_{cd}^v \mu_{da}^v \quad \text{with } v_a = 0$$

$$f_J = Q^{-1} (2J + 1) e^{-E(J)/kT} \quad (Q = \text{partition function})$$

$$\phi_R = \frac{1}{2J+1} \sum_{[K]} \mu_{ab}^R \mu_{bc}^R \mu_{cd}^R \mu_{da}^R$$

$$[K] = \text{set of } (J_a, J_b, J_c, J_d) \text{ allowed by the selection rules} \\ \text{with } J_a = J$$

$$F_{abcd} = \text{frequency factor determined by } (\omega_1, \omega_2, \omega_3) \text{ and} \\ \text{molecular transition frequencies}$$

3.2 Resonance Enhancement Schemes

The resonance enhancement schemes considered for CO laser frequency tripling are based on one, two, and/or three photon resonances in infrared-active and Raman-active diatomic molecules. Figure 1 illustrates the three different schemes. The difference between the transition resonance frequency and the pump frequency or the combination of the pump frequencies is the frequency detuning which determines the resonance enhancement of the frequency factor.

The type I scheme utilizes near-resonant frequency detunings at the fundamental and the first two overtone transitions corresponding to the vibrational levels $v = 1, 2$, and 3 . The candidate molecules are IR active species with fundamental frequencies near 2000 cm^{-1} . Table 3 lists the molecules and the optimum THG pump frequency ranges for two and three photon resonance enhancement.

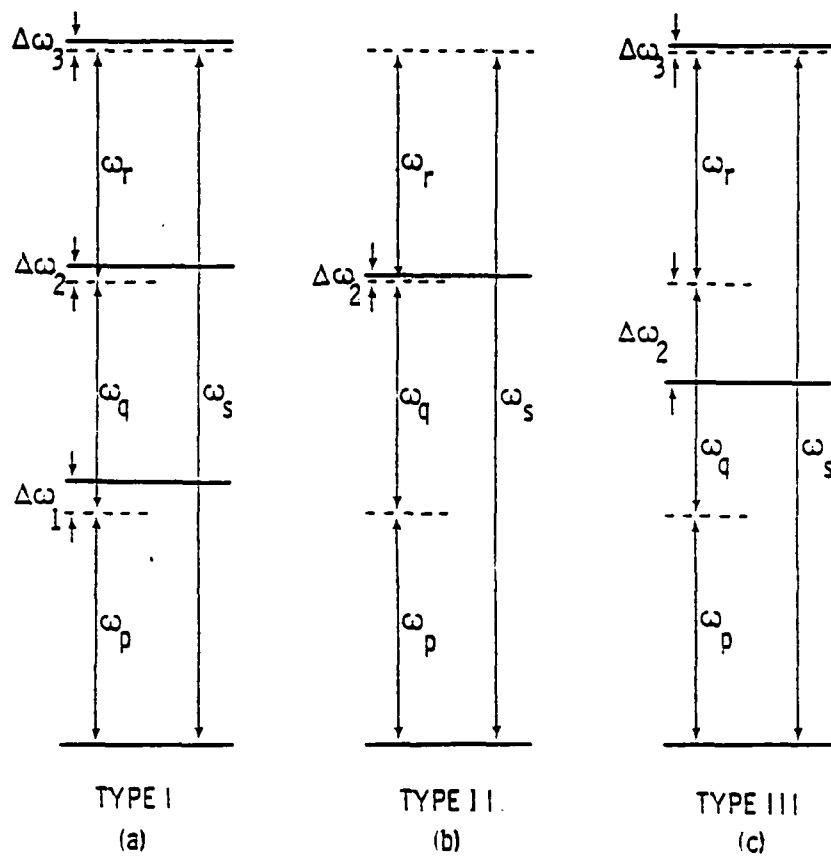


FIGURE 1. THREE TYPES OF RESONANCE ENHANCEMENT

TABLE 3. TYPE I SCHEME OPTIMUM PUMP FREQUENCIES

Molecule	THG Optimum Pump Frequency Range (cm ⁻¹)	
	2 Photon Resonant	3-Photon Resonant
CO ₁₈	2050 - 2065	2055 - 2060
DC ₂ ^{35,37}	1990 - 2025	2005 - 2020
DBr ^{79,81}	1860 - 1890	1805 - 1810
NO	1840 - 1890	1830 - 1860

The type II scheme is based on two-photon resonance in Raman-active molecules. The candidate molecules and the optimum two-photon resonant pump frequencies are listed in Table 4.

TABLE 4. TYPE II SCHEME MOLECULES
Two-Photon Resonance Frequency

Molecule	Two-Photon Transition		Optimum Pump Frequency (cm ⁻¹)
	Branch (J)	ω (cm ⁻¹)	
H ₂	Q(0)	4161.1	2080.55
	Q(1)	4155.2	2077.60
	Q(2)	4143.3	2071.65
	Q(3)	4125.3	2062.65
	Q(4)	4101.2	2050.60
	O(2)	3806.8	1903.40
	O(3)	3568.4	1784.20
HD	Q(0)	3632.1	1816.05
	Q(1)	3628.2	1814.10
	Q(2)	3620.5	1810.25
	Q(3)	3608.9	1804.45
	Q(4)	3593.3	1796.65
	S(0)	3887.5	1943.75
	S(1)	4051.8	2025.90
HF	Q(0)	3961.54	1980.77
	Q(1)	3960.00	1980.00
	Q(2)	3956.90	1978.45
	Q(3)	3952.26	1976.13
	Q(4)	3946.06	1973.03
	Q(5)	3938.30	1969.15

The type III scheme derives three-photon resonance enhancement from small frequency detunings at the $v = 2$ excited vibrational state of the molecule. The candidate molecules are DF and HCl, both of which have first overtone transitions in the 5500 to 5800 cm^{-1} range.

3.3 Nonlinear Susceptibility $\chi^{(3)}$ Code

A general third order nonlinear susceptibility code for infrared-active molecules has been developed using vibration-rotation transitions in the ground electronic state of the molecule. The code is based on the $\chi^{(3)}$ formula given in Table 2, and is capable of calculating nonlinear susceptibilities for THG, SFG, quadratic Kerr effect, two-photon absorption, and stimulated Raman effect for the type I and type III scheme molecules. The necessary input parameters are the equilibrium molecular energy level constants, gas temperature, the number of vibrational and rotational intermediate states, the dipole matrix elements, and the three pump frequency values. For the type III calculation, the code computes only the near-resonant contributions from the R-branch overtone transitions. The $\chi^{(3)}$ code consists of the pump and the generated frequencies as well as the real part, the complex part, and the modulus of the nonlinear susceptibility tensor.

The $\chi^{(3)}$ calculation for the type II resonance enhancement scheme involves virtual vibronic transitions in Raman-active molecules. According to the literature, the perturbation calculation requires extensive computation involving vibronic matrix elements which are not generally available. However, $\chi^{(3)}$ values may be obtained from differential Raman scattering cross section data and appropriate frequency factor scaling.⁵ This procedure is believed to be a reliable method.

The details of the $\chi^{(3)}$ program structure and the procedures used in the computation are described in the following sections.

3.3.1 Type I Scheme

The calculation of nonlinear susceptibilities for molecular media in principle requires a knowledge of all of the energy levels and of all of the transition matrix elements for the molecules of the nonlinear medium. When resonance

enhancement occurs, however, a knowledge of only a small group of intermediate states may be sufficient to determine good approximate values of $\chi^{(3)}$. The accuracy of this approximation depends on the frequency detunings. Thus a reliable resonance enhancement calculation requires a precise knowledge of the molecular energy level scheme. The molecular constants taken from spectroscopic data are generally adequate for computing frequency detunings to within approximately 1 cm^{-1} .

The equations for computing the molecular energy levels are summarized below.^{8,9} Each level is characterized by vibrational and rotational quantum numbers. The total energy, $T(v, J)$ is expressed as a sum of the vibrational term, $G(v)$, and the rotational term, $F_v(J)$.

$$T(v, J) = G(v) + F_v(J) \quad (11)$$

$$G(v) = \omega_e(v + \frac{1}{2}) - \omega_e x_e(v + \frac{1}{2})^2 + \omega_e y_e(v + \frac{1}{2})^3 + \omega_e z_e(v + \frac{1}{2})^4 + \dots \quad (12)$$

$$F_v(J) = B_v J(J+1) - D_v [J(J+1)]^2 + H_v [J(J+1)]^3 + \dots (\lambda=0) \quad (13)$$

$$F_v(J) = -D_v + (-1)^i \left[\frac{A_v}{2} + B_{vi}(J + \frac{1}{2})^2 - D_{vi}(J + \frac{1}{2})^4 + H_{vi}(J + \frac{1}{2})^6 + \dots \right] \quad (14)$$

($i \neq 0$)

where

$$B_v = B_e - \alpha_e(v + \frac{1}{2}) + \gamma_e(v + \frac{1}{2})^2 + \dots \quad (15)$$

$$D_v = D_e - \beta_e(v + \frac{1}{2}) + \dots \quad (16)$$

$$H_v = H_e + \dots \quad (17)$$

$$A_v = \lambda_v B_v \quad (18)$$

$$\lambda_v = A_v - 2B_v - 2B_v^2/A_v + \dots \quad (19)$$

$$B_{vi} = B_v + D_v + (-1)^i B_v [\lambda_v + 2\lambda_v^2 + \dots] \quad (20)$$

$$D_{vi} = D_v + (-1)^i B_v [\lambda_v^3 + 6\lambda_v^4 + \dots] \quad (21)$$

$$H_{vi} = H_v + (-1)^i B_v [2\lambda_v^5 + 20\lambda_v^6 + \dots] \quad (22)$$

The transition frequency between any two levels can be calculated using Equations (15) through (22). The calculated frequencies can then be used to compute the frequency denominator term in Table 1.

Direct calculation of the nonlinear susceptibility requires a variety of summations according to Table 2. Since the molecular states are labeled by vibrational (v) and rotational (J) quantum numbers, an explicit form of the expression in Table 2 requires the calculation of

$$\phi_R(J_a, J_b, J_c, J_d) = \frac{1}{2J+1} \sum_{m_a} \sum_{m_b} \sum_{m_c} \sum_{m_d} [\langle J_a m_a | \cos\theta | J_b m_b \rangle \langle J_b m_b | \cos\theta | J_c m_c \rangle \langle J_c m_c | \cos\theta | J_d m_d \rangle \langle J_d m_d | \cos\theta | J_a m_a \rangle] \quad (23)$$

In Equation (23) the indices b , c , and d denote the vibrational or vibronic quantum numbers of the intermediate states. The variables (J_b, J_c, J_d) are the rotational quantum numbers of the intermediate states. The frequency denominator term $F_{abcd}(J_a, J_b, J_c, J_d)$, indicates the dependence of $\chi^{(3)}$ on vibrational and rotational energy levels. Equation (23) gives the product of the rotational matrix elements. The selection rules for linearly polarized fields are $\Delta J = \pm 1$ and $\Delta m = 0$ for a molecular state with $\Lambda = 0$, and $\Delta J = 0, \pm 1$ and $\Delta m = 0$ for a molecular state with $\Lambda = 1$. Using these selection rules, $\phi_R(J_a, J_b, J_c, J_d)$ can be calculated for allowed values of J_b, J_c, J_d . The results for the $\Lambda = 0$ case are summarized in Table 5.

TABLE 5. PRODUCT OF ROTATIONAL MATRIX ELEMENTS
FOR $\Lambda = 0$ MOLECULES

Path	J_b	J_c	J_d	$\phi_R(J_a, J_b, J_c, J_d)_{J_a=J}$
1	$J-1$	$J-2$	$J-1$	$\frac{2J(J-1)}{15(2J-1)(2J+1)}$
2	$J-1$	J	$J-1$	$\frac{J(4J^2+1)}{15(2J-1)(2J+1)^2}$
3	$J+1$	J	$J-1$	$\frac{2J(J+1)}{15(2J+1)^2}$
4	$J-1$	J	$J+1$	$\frac{2J(J+1)}{15(2J+1)^2}$
5	$J+1$	J	$J+1$	$\frac{(J+1)(4J^2+8J+5)}{15(2J+3)(2J+1)^2}$
6	$J+1$	$J+2$	$J+1$	$\frac{2(J+1)(J+2)}{15(2J+3)(2J+1)}$

The experimental data on vibrational matrix elements are available for a number of infrared-active diatomic molecules. In most cases $\Delta v = \pm 1$ transitions are well approximated by the harmonic oscillator matrix elements which are given by

$$\langle v | \mu | v-1 \rangle = \sqrt{v} \langle 1 | \mu | 0 \rangle \quad (24)$$

The matrix elements for overtone transitions ($\Delta v = 2$ and 3) may be expressed as

$$\mu_{v,0} = S_{v,0} \mu_{1,0} \quad (25)$$

where $S_{v,0}$ is the strength relative to the fundamental ($0 \rightarrow 1$) transition. Typically, $S_{2,0} \approx 10^{-1}$ and $S_{3,0} \approx 5 \times 10^{-3}$.

The population distribution in the rotational states is represented by a factor f_J . For a gaseous medium in thermal equilibrium the distribution is considered Boltzmann. The quantity Q_{Rot} is the rotational partition function which is defined as

$$Q_{\text{Rot}} = \sum_{J=0}^{\infty} (2J+1) \exp(-hc F_0(J)/kT) \quad (26)$$

For $hc B_0 \ll kT$, Q_{Rot} may be approximated by

$$Q_{\text{Rot}} \cong \frac{kT}{hc B_0} \quad (27)$$

The summations involving vibrational quantum numbers and frequency permutations which are needed for the $\Lambda = 1$ case are exactly the same as the summations that are required for the $\Lambda = 0$ case. However, since the rotational states have two sets of levels ($\Omega = \frac{1}{2}, \frac{3}{2}$), two distinct summations over J must be performed.

$$\chi^{(3)} \propto \sum_v \sum_{bcd} \mu^4 \left[\sum_{J=\frac{1}{2}} (\Omega = \frac{1}{2}) + \sum_{J=\frac{3}{2}} (\Omega = \frac{3}{2}) \right] \quad (28)$$

In each summation over J , there are nineteen different paths to be summed as a result of allowed values of (J_b, J_c, J_d) .

$$\sum_{J=\frac{1}{2}} (\Omega = \frac{1}{2}) = \sum_{J=\frac{1}{2}} f_J (\Omega = \frac{1}{2}) \sum_{J_b J_c J_d} \phi(J_a, J_b, J_c, J_d) F_{abcd} \quad (29)$$

In each path of rotational quantum numbers, the Ω values of the intermediate states can be either $\frac{1}{2}$ or $\frac{3}{2}$, making eight different contributions to each set of (J_a, J_b, J_c, J_d)

$$\sum_{abcd} \phi(J_a, J_b, J_c, J_d) F_{abcd} = \sum_{\text{path}(J)} (-1)^s \frac{W(J_a, J_b, J_c, J_d)}{2 J_a + 1} \sum_{\text{path}(\Omega)} \psi(a, b, c, d) F_{abcd} \quad (30)$$

where $s = J_a + J_b + J_c + J_d$. $W(J_a, J_b, J_c, J_d)$ is defined by:

$$W(J_a, J_b, J_c, J_d) = \sum_{m_a} \sum_{m_b} \sum_{m_c} \sum_{m_d} \begin{pmatrix} J_a & 1 & J_b \\ -m_a & 0 & m_b \end{pmatrix} \begin{pmatrix} J_b & 1 & J_c \\ -m_b & 0 & m_c \end{pmatrix} \begin{pmatrix} J_c & 1 & J_d \\ -m_c & 0 & m_d \end{pmatrix} \begin{pmatrix} J_d & 1 & J_a \\ -m_d & 0 & m_a \end{pmatrix} \quad (31)$$

Using the properties of the summations involving products of 3j symbols¹⁰ expression (31) reduces to

$$W(J_a, J_b, J_c, J_d) = \frac{(-1)^{(-J_b+2J_c+J_d)}}{9} \left[(-1)^{J_b+J_d} \begin{Bmatrix} 1 & J_a & J_b \\ 1 & J_c & J_d \end{Bmatrix} + \sum_{k=0}^2 \begin{Bmatrix} J_c & 1 & J_b \\ 1 & J_a & k \end{Bmatrix} \begin{Bmatrix} J_c & 1 & J_d \\ 1 & J_a & k \end{Bmatrix} h(k) \right] \quad (32)$$

$$\text{where } h(k) = \frac{(-1)^k (2k+1)}{10} [3k^2 (k+1)^2 - 21k(k+1) + 20] \quad (33)$$

By specifying a particular set of rotational quantum numbers, expression (32) can be evaluated using 6j symbol formulas,¹⁰ and the results are summarized in Table 6.

The frequency factor is computed in the same way as was done for the $\Delta = 0$ case. The only difference is the formulae used for calculating molecular levels with quantum numbers $\{v, J, \Omega\}$.

The summation over intermediate Ω states can be written

$$\sum_{\text{path}(\Omega)} \psi(a, b, c, d) F_{abcd} = \sum_{\Omega_b} \sum_{\Omega_c} \sum_{\Omega_d} \xi(a, b) \xi(b, c) \xi(c, d) \xi(d, a) F_{abcd} \quad (34)$$

TABLE 6. $W(J_a, J_b, J_c, J_d)$
FOR $\Lambda = 1$ MOLECULES

Path	J_b	J_c	J_d	$W(J_a, J_b, J_c, J_d), (J_a=J)$
1	$J-1$	$J-2$	$J-1$	$\frac{2}{15} \frac{1}{(2J-1)}$
2	$J-1$	J	$J-1$	$\frac{1}{15} \frac{(4J^2+1)}{J(2J-1)(2J+1)}$
3	$J+1$	J	$J-1$	$\frac{2}{15} \frac{1}{(2J+1)}$
4	$J-1$	J	$J+1$	$\frac{2}{15} \frac{1}{(2J+1)}$
5	$J+1$	J	$J+1$	$\frac{1}{15} \frac{(4J^2+9J-5)}{(J+1)(2J+1)(2J+3)}$
6	$J+1$	$J+2$	$J+1$	$\frac{2}{15} \frac{1}{(2J+3)}$
7	J	J	$J-1$	$\frac{1}{15} \frac{(J-1)}{J(2J+1)}$
8	J	J	$J+1$	$\frac{1}{15} \frac{(J+2)}{(J+1)(2J+1)}$
9	J	$J-1$	J	$\frac{1}{15} \frac{(J-1)}{J(2J-1)}$
10	J	$J+1$	J	$\frac{1}{15} \frac{(J+2)}{(J+1)(2J+1)}$
11	$J-1$	J	J	$\frac{1}{15} \frac{(J-1)}{J(2J+1)}$
12	$J+1$	J	J	$\frac{1}{15} \frac{(J+2)}{J(2J+1)}$
13	$J-1$	$J-1$	$J-1$	$\frac{1}{15} \frac{(J+1)}{J(2J-1)}$
14	$J+1$	$J+1$	$J+1$	$\frac{1}{15} \frac{J}{(J+1)(2J+3)}$
15	J	$J-1$	$J-1$	$-\frac{1}{15} \left[\frac{(J+1)(J-1)}{J^2(2J+1)(2J-1)} \right]^2$
16	J	$J-1$	$J-1$	$-\frac{1}{15} \left[\frac{J(J+2)}{(J+1)^2(2J+1)(2J-3)} \right]^2$
17	$J-1$	$J-1$	J	$-\frac{1}{15} \left[\frac{(J+1)(J-1)}{J^2(2J-1)(2J-1)} \right]^2$
18	$J+1$	$J+1$	J	$-\frac{1}{15} \left[\frac{J(J+2)}{(J+1)^2(2J+1)(2J+3)} \right]^2$
19	J	J	J	$\frac{1}{15} \frac{(3J^2+3J-1)}{J(J+1)(2J-1)}$

The terms of the form $\xi(a,b)$ represent effective reduced matrix elements between states a and b when both states are expressed in the intermediate coupling scheme. In this coupling scheme, molecular states are expressed as linear combinations of unperturbed eigenfunctions with coefficients defined by the following relations:

$$|{}^2_{\pi_1 \frac{1}{2}}\rangle_{\text{INT}} = CA(v) |{}^2_{\pi_1 \frac{1}{2}}\rangle - CB(v) |{}^2_{\pi_3 \frac{1}{2}}\rangle \quad (35)$$

and

$$|{}^2_{\pi_3 \frac{1}{2}}\rangle_{\text{INT}} = CA(v) |{}^2_{\pi_1 \frac{1}{2}}\rangle + CB(v) |{}^2_{\pi_3 \frac{1}{2}}\rangle \quad (36)$$

where the mixing coefficients are given by:

$$\begin{aligned} CA(v) &= \frac{X_v - 2 + \lambda_v}{2 X_v} \\ \text{and} \quad CB(v) &= \frac{X_v + 2 - \lambda_v}{2 X_v} \\ X_v &= [\lambda_v(\lambda_v - 4) + 4(J + \frac{1}{2})^2]^{\frac{1}{2}} \\ \lambda_v &= A_v/B_v \end{aligned} \quad (37)$$

The rotational reduced matrix elements are also necessary to compute ξ . For $\Omega \neq 0$ cases, these matrix elements are given by¹¹

$$R_{\Omega}(J, J') = \begin{cases} \left[\frac{(J+1)^2 - \Omega^2}{J+1} \right]^{\frac{1}{2}} & \text{for } J' = J+1 \\ \left[\frac{(2J+1)\Omega^2}{J(J+1)} \right]^{\frac{1}{2}} & \text{for } J' = J \\ \left[\frac{J^2 - \Omega^2}{J} \right]^{\frac{1}{2}} & \text{for } J' = J-1 \end{cases} \quad (38)$$

The three different forms of ξ in terms of the expressions given in Equations (35) through (38) are given in Table 7.

TABLE 7. $\xi_{\alpha}(a,b)$ IN TERMS OF MIXING COEFFICIENTS
AND REDUCED ROTATIONAL MATRIX ELEMENTS

α	Ω_a	Ω_b	$\xi_{\alpha}(a,b)$
1	$\frac{1}{2}$	$\frac{1}{2}$	$CA(a) CA(b) R_{\frac{1}{2}}(J_a, J_b) + CB(a) CB(b) R_{\frac{3}{2}}(J_a, J_b)$
2	$\frac{1}{2}$	$\frac{3}{2}$	$CA(a) CA(b) R_{\frac{3}{2}}(J_a, J_b) + CB(a) CB(b) R_{\frac{1}{2}}(J_a, J_b)$
3	$\frac{1}{2}$	$\frac{3}{2}$	$CA(a) CB(b) R_{\frac{1}{2}}(J_a, J_b) - CA(b) CB(a) R_{\frac{3}{2}}(J_a, J_b)$

In Table 8, $\psi(a,b,c,d)$ is defined in terms of appropriate products of the effective reduced matrix elements, determined by the possible combinations (paths) of the quantum numbers, Ω_a , Ω_b , Ω_c , and Ω_d .

TABLE 8. TERMS IN THE Ω -PATH SUMMATION

Path	Ω_a	Ω_b	Ω_c	Ω_d	$\xi_{\alpha}(a,b) \xi_{\beta}^{\psi(a,b,c,d)}(b,c) \xi_{\gamma}(c,d) \xi_{\delta}(d,a)$			
					α	β	γ	δ
1	$\frac{1}{2}$	$\frac{1}{2}$	$\frac{1}{2}$	$\frac{1}{2}$	1	1	1	1
2	$\frac{1}{2}$	$\frac{1}{2}$	$\frac{3}{2}$	$\frac{3}{2}$	1	1	3	3
3	$\frac{1}{2}$	$\frac{1}{2}$	$\frac{3}{2}$	$\frac{1}{2}$	1	3	3	1
4	$\frac{1}{2}$	$\frac{1}{2}$	$\frac{3}{2}$	$\frac{3}{2}$	1	3	2	3
5	$\frac{1}{2}$	$\frac{3}{2}$	$\frac{1}{2}$	$\frac{1}{2}$	3	3	1	1
6	$\frac{1}{2}$	$\frac{3}{2}$	$\frac{1}{2}$	$\frac{3}{2}$	3	3	3	3
7	$\frac{1}{2}$	$\frac{3}{2}$	$\frac{3}{2}$	$\frac{1}{2}$	3	2	3	1
8	$\frac{1}{2}$	$\frac{3}{2}$	$\frac{3}{2}$	$\frac{3}{2}$	3	2	2	3
1	$\frac{3}{2}$	$\frac{3}{2}$	$\frac{1}{2}$	$\frac{1}{2}$	2	2	2	2
2	$\frac{3}{2}$	$\frac{3}{2}$	$\frac{1}{2}$	$\frac{3}{2}$	2	2	3	3
3	$\frac{3}{2}$	$\frac{3}{2}$	$\frac{3}{2}$	$\frac{1}{2}$	2	3	3	2
4	$\frac{3}{2}$	$\frac{3}{2}$	$\frac{3}{2}$	$\frac{3}{2}$	2	3	1	3
5	$\frac{3}{2}$	$\frac{3}{2}$	$\frac{3}{2}$	$\frac{1}{2}$	3	3	2	2
6	$\frac{3}{2}$	$\frac{3}{2}$	$\frac{3}{2}$	$\frac{3}{2}$	3	3	3	3
7	$\frac{3}{2}$	$\frac{3}{2}$	$\frac{1}{2}$	$\frac{1}{2}$	3	1	3	2
8	$\frac{3}{2}$	$\frac{3}{2}$	$\frac{1}{2}$	$\frac{3}{2}$	3	1	1	3

The expressions presented in this section constitute a general method for calculating third-order susceptibilities in IR-active molecules. Figure 2 shows a flow chart of the $\chi^{(3)}$ code based on these expressions. A listing of the computer program is given in Appendix A.

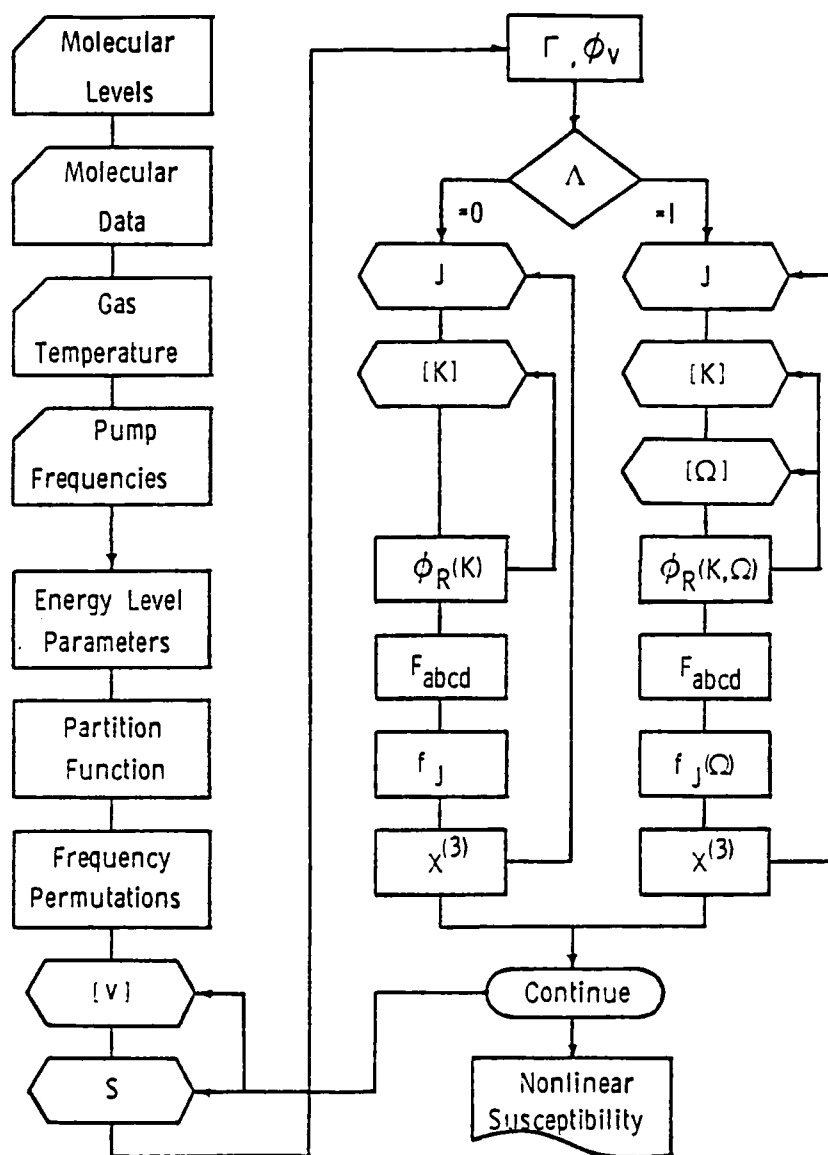


FIGURE 2. $\chi^{(3)}$ FLOW CHART

3.3.2 Type II Scheme

In the type II scheme, analysis of the $\chi^{(3)}$ formula shows that THG and SFG, stimulated Raman scattering (SRS), two-photon absorption (TPA), and quadratic Kerr effect share the same two-photon resonance and vibronic intermediate states. Consequently, the susceptibilities are related and may be evaluated from measured data on one of the processes. A direct relation between χ^{SRS} and differential Raman scattering cross section, $d\sigma/d\Omega$, enables the calculation of the various susceptibilities. The relation has been derived using the definitions of the scattering cross sections.^{12,13} A derivation consistent with the definition of $\chi^{(3)}$ of this report is outlined below.

The starting point is Placzek's definition of the "effective cross section" for scattered light due to a transition $k \rightarrow n$ in both scattering polarization directions:¹²

$$Q_{kn} = \frac{2^7 \pi^5}{3 \lambda_s^4} \sum_{\rho} |(C_{\rho\sigma})_{kn}|^2 \quad (39)$$

[Placzek's Equation (5.5a)]

where

$$(C_{\rho\sigma})_{kn} = \frac{1}{\hbar} \sum_r \frac{(M_{\sigma})_{kr} (M_{\rho})_{rn}}{\omega_{rk} - \omega} + \frac{(M_{\rho})_{kr} (M_{\sigma})_{rn}}{\omega_{rn} + \omega} \quad (40)$$

[Placzek's Equation (5.2)]

and $\sigma = 1, 2, \text{ or } 3$ corresponding to the $x, y, \text{ or } z$ directions of polarization for the incident radiation, respectively

$\rho = 1, 2, \text{ or } 3$ corresponding to the $x, y, \text{ or } z$ directions of polarization for the scattered radiation, respectively

$\lambda_s =$ the wavelength of the scattered radiation

$$(M_{\gamma})_{kr} = \int \psi_r^* \hat{M}_{\gamma} \psi_k d\tau$$

$\hat{M}_{\gamma} =$ the electric dipole operator of polarization specified by γ .

In the equation for $\chi^{(3)}$, the states are labeled as (a,b,c,d) , so that $k=|a,J_a,m_a\rangle$ and $n=|c,J_c,m_c\rangle$. Consider the case of parallel polarization ($\rho = \sigma$)

$$(Q_{a,J_a,m_a \rightarrow c,J_c,m_c})_{||} = \frac{2^7 \pi^5}{3 \lambda_s^4} |(C_{\sigma\sigma})_{a,J_a,m_a;c,J_c,m_c}|^2 \quad (41)$$

Summing over the degenerate m states and dividing by the degeneracy of the initial state (according to Equation (5.5b) of Placzek) yields

$$(Q_{a,J_a \rightarrow c,J_c})_{||} = \left(\frac{8\pi}{3}\right) k_s^4 \frac{1}{g_a} \sum_{m_a} \sum_{m_c} |(C_{\sigma\sigma})_{a,J_a,m_a;c,J_c,m_c}|^2 \quad (42)$$

where k_s = the wavevector for the scattered radiation ($= 2\pi/\lambda_s$).

The differential Raman scattering cross section $(d\sigma/d\Omega)$ at 90° to the direction of the incident radiation and at 90° to the polarization direction of the incident radiation has the maximum value $(d\sigma/d\Omega)_{\max}$. This is the value measured experimentally. The relationship between the total cross section, $(\sigma)_{\text{total}}$, and the differential cross section, $(d\sigma/d\Omega)_{\max}$, for the case of isotropic scattering is:¹³

$$(\sigma)_{\text{total}} = \frac{8\pi}{3} \left(\frac{d\sigma}{d\Omega}\right)_{\max} \quad (43)$$

where $(\sigma)_{\text{total}}$ is the $(Q_{a,J_a \rightarrow c,J_c})_{||}$ of Equation (42). Hence, the polarized $(d\sigma/d\Omega)$ is given by:

$$\left(\frac{d\sigma}{d\Omega}\right)_{||}^s = k_s^4 \frac{1}{g_a} \sum_{m_a} \sum_{m_c} |(C_{\sigma\sigma})_{a,J_a,m_a;c,J_c,m_c}|^2 \quad (44)$$

where the subscript s on $(d\sigma/d\Omega)^s$ indicates the cross section for the scattered (Stokes) radiation.

Analysis of the form of $\chi^{(3)}$ which is appropriate for Raman scattering shows that for $a,J_a \rightarrow c,J_c$ resonance:

$$\chi^{(3)}(\omega_p, -\omega_p, \omega_s) = \frac{-1}{6\hbar^3} \sum_{a,c} \sum_{m_a,m_c} \rho_{aa}^{(0)} \left| \sum_b \mu_{ab} \mu_{bc} A_{ab} \right|^2 \times -\frac{1}{i\Gamma} \quad (45)$$

where
$$A_{ab} = \frac{1}{\omega_{ab} + \omega_p} + \frac{1}{\omega_{ab} - \omega_s} \quad (46)$$

and Γ is the half-width at half-maximum corresponding to the $a, J_a \rightarrow c, J_c$ resonance. Note that

$$\omega_{ab} = -\omega_{ba}$$

and $\omega_{bc} = \omega_{bc} + \omega_{ac}$, or $\omega_{bc} = \omega_{ba} - \omega_{\text{Raman}}$

so that
$$-\omega_{ab} = \omega_{bc} + \omega_{\text{Raman}}$$

and
$$\omega_{ab} - \omega_s = -\omega_{bc} - \omega_p.$$

Rewriting Equation (46) using the last relation

$$A_{ab} = - \left[\frac{1}{\omega_{ba} - \omega_p} + \frac{1}{\omega_{bc} + \omega_p} \right]$$

Therefore,

$$\chi^{(3)}(\omega_p, -\omega_p, \omega_s) = \frac{-i}{6\hbar\Gamma} \sum_{a,c} \sum_{m_a} \sum_{m_c} \rho_{aa}^{(0)} |(C_{\sigma\sigma})_{a,J_a,m_a;c,J_c,m_c}|^2 \quad (47)$$

The expression for $\rho_{aa}^{(0)}$ is independent of m_a and is given by

$$\begin{aligned} \rho_{aa}^{(0)} &= \frac{1}{Q} \exp[-E_a/kT] \\ &= \frac{1}{g_a} f_a \end{aligned} \quad (48)$$

where Q is the rotational partition function for molecules of the Raman medium.

Thus,

$$\begin{aligned} \chi^{(3)}(\omega_p, -\omega_p, \omega_s) &= \frac{-i}{6\hbar\Gamma} \sum_a f_a \frac{1}{g_a} \sum_{m_a} \sum_{m_c} |(C_{\sigma\sigma})_{a,J_a,m_a;c,J_c,m_c}|^2 \\ &= \frac{-i}{6\hbar\Gamma} \sum_a f_a \frac{1}{k_s^4} \left(\frac{d\sigma}{d\Omega} \right)_\parallel^s \end{aligned} \quad (49)$$

For vibrational Raman scattering, the final state is essentially empty. Thus the summations over v_a and v_c reduce to a particular initial state ($v_a=0, J_a=J$)

$$\chi^{(3)}(\omega_p, -\omega_p, \omega_s) = \frac{-1}{6\hbar\Gamma} f_J \left[\frac{1}{k_s} \left(\frac{d\sigma}{d\Omega} \right)_\parallel^s \right] \quad (50)$$

Since $\chi^{\text{SRS}} = \text{Im} [\chi^{(3)}(\omega_p, -\omega_p, \omega_s)_{\Delta\omega=0}]$,

$$\chi^{\text{SRS}} = \frac{-1}{6} \left(\frac{1}{\hbar\Gamma} \right) \left[\frac{1}{k_s} \left(\frac{d\sigma}{d\Omega} \right)_\parallel^s \right] f_J \quad (51)$$

The quantities in expression (51) are defined in CGS units. By multiplying (51) by $(4\pi\epsilon_0)^2$ and expressing all quantities in MKS units, χ^{SRS} is obtained also in MKS units.

In order to relate χ^{SRS} of Equation (51) to other third-order susceptibilities, the $\chi^{(3)}$ formula given in Table 1 has been analyzed. The results are summarized in Table 9. Since the cross section is proportional to the fourth power of the Stokes wave vector, the peak values of $\chi^{(3)}$ (i.e. $\Delta\omega=0$) are nearly independent of frequency for radiation in the IR and visible regions. Thus, Raman scattering data obtained at a certain visible wavelength can be used to compute the peak values of $\chi^{(3)}$ for all of the third-order processes associated with the type II scheme.

3.3.3 Type III Scheme

The type III resonance enhancement scheme utilizes three-photon resonance via vibrational-rotational and vibronic intermediate states. A detailed study of the $\chi^{(3)}$ formula indicates that an exact calculation requires vibronic transition moments and Franck-Condon amplitudes for each of the excited electronic states coupled to the ground electronic state by electric dipole transitions. An extensive literature search provided only a small fraction of the necessary parameters for HCl and DF. Because of this lack of data, various approximations were considered in order to derive formulas that can be evaluated numerically with the existing data.

TABLE 9. TYPE II NONLINEAR SUSCEPTIBILITY

- $\chi^{(3)} = \text{Re}[\chi^{(3)}] + i \text{Im}[\chi^{(3)}]$
- $\text{Re}[\chi^{(3)}] = \text{Im}[\chi^{(3)}]_{\Delta\omega=0} \times \left[\frac{\Delta\omega\Gamma}{\Delta\omega^2 + \Gamma^2} \right]$
- $\text{Im}[\chi^{(3)}] = \text{Im}[\chi^{(3)}]_{\Delta\omega=0} \times \left[\frac{\Gamma^2}{\Delta\omega^2 + \Gamma^2} \right]$
- $\Delta\omega \equiv \omega_R - (\omega + \omega')$
- $\text{Im}[\chi^{(3)}]_{\Delta\omega=0} = \frac{A}{6} \left[\frac{(4\pi\epsilon_0)^2}{\hbar\Gamma} \right] \left[k^{-4} \left(\frac{d\sigma}{d\Omega} \right)_{||} \right] f_J$
- Process A

THG:	$3\omega \rightarrow \omega_S$	3
SFG:	$2\omega + \omega' \rightarrow \omega_S$	2
	$2\omega' + \omega \rightarrow \omega_S$	2
	$\omega + \omega' + \omega'' \rightarrow \omega_S$	1
TPA, Kerr at ω, ω'		1
SRS at ω, ω'		-1

Γ : Two-Photon Resonance Linewidth (HWHM)

$\left(\frac{d\sigma}{d\Omega} \right)_{||}$: Polarized Differential Raman Scattering Cross Section

k : Raman Stokes Radiation Wave Vector

f_J : Fractional Population Distribution

ω_R : Raman Frequency

The calculation of $\chi^{(3)}$ for candidate molecules in the type III resonance enhancement scheme involves three different kinds of pairs of the intermediate states $|c\rangle$ and $|d\rangle$: The two intermediate states may both be pure vibrational-rotational; one intermediate state may be pure vibrational-rotational and the other intermediate state may be vibronic, or both intermediate states may be vibronic. Pairs of intermediate states of the first kind have already been encountered in the calculation of $\chi^{(3)}$ for candidate molecules in the type I resonance enhancement scheme. Accordingly, the treatment of the contributions from pairs of intermediate state of the first kind has been discussed during the analysis of the type I resonance enhancement scheme and will not be repeated here. Parts of the intermediate states of the third kind lead to terms which are small because of the square of the electronic energy occurring in the denominator of these terms. Thus, pairs of intermediate states of the second kind will be considered in detail in the following discussion.

The third-order susceptibility for the type III resonance enhancement may be approximated as

$$\chi_{III}^{(3)} \cong \frac{-1}{\hbar^3} \sum_a \rho_{aa}^{(0)} \sum_{bc} \frac{\mu_{ab} \mu_{bc}}{\omega_{ab} + \omega_3 + i\Gamma_{ab}} \frac{1}{\omega_{ac} + \omega_2 + \omega_3} \sum_d \frac{\mu_{cd} \mu_{da}}{\omega_{ad} + \omega_3} \quad (52)$$

Consider the special case of three-photon resonance at $v_a=0$, $J_a=J$ and $v_b=2$, $J_b=J+1$ (0-2 R(J) transition)

$$\chi_{III,res}^{(3)} \cong \frac{-1}{\hbar^3} \rho_{aa}^{(0)} \frac{\mu_{02}}{\omega_{02} + \omega_3 + i\Gamma_{02}} \sum_c \sum_d \frac{\mu_{2c} \mu_{cd} \mu_{d0}}{(\omega_{0c} + \omega_2 + \omega_3)(\omega_{0d} + \omega_3)} \quad (53)$$

The summations over the intermediate states $|c\rangle$ and $|d\rangle$ must now be examined in the case where one of the two intermediate states is a vibronic state. Let "e" stand for a set of vibronic levels and "I" stand for the summations over the intermediate states.

$$I = \sum_d \sum_e \frac{\mu_{2e} \mu_{ed} \mu_{d0}}{(\omega_{0e} + \omega_2 + \omega_3)(\omega_{0d} + \omega_3)} + \sum_c \sum_e \frac{\mu_{2c} \mu_{ce} \mu_{e0}}{(\omega_{0c} + \omega_2 + \omega_3)(\omega_{0e} + \omega_3)} = I_1 + I_2 \quad (54)$$

where $|\omega_{0e}|$ is the electronic transition frequency, assumed to be much greater than any of the input frequencies. Analyzing the two terms in Equation (54) separately,

$$I_1 = \sum_e \left\{ \frac{\mu_{2e} \mu_{e0'} \mu_{0'0}}{(\omega_{0e} + \omega_2 + \omega_3)(\omega_{00'} + \omega_3)} + \frac{\mu_{2e} \mu_{e1'} \mu_{1'0}}{(\omega_{0e} + \omega_2 + \omega_3)(\omega_{01'} + \omega_3)} + \frac{\mu_{2e} \mu_{e2'} \mu_{2'0}}{(\omega_{0e} + \omega_2 + \omega_3)(\omega_{02'} + \omega_3)} \right\} \quad (55)$$

$$I_2 = \sum_e \left\{ \frac{\mu_{20'} \mu_{0'e} \mu_{e0}}{(\omega_{00'} + \omega_2 + \omega_3)(\omega_{0e} + \omega_3)} + \frac{\mu_{21'} \mu_{1'e} \mu_{e0}}{(\omega_{01'} + \omega_2 + \omega_3)(\omega_{0e} + \omega_3)} + \frac{\mu_{22'} \mu_{2'e} \mu_{e0}}{(\omega_{02'} + \omega_2 + \omega_3)(\omega_{0e} + \omega_3)} \right\} \quad (56)$$

where the primes indicate summation over rotational states.

Note that $|\omega_{0e}| \gg \omega$. This fact leads to the approximations $\omega_{0e} + \omega_2 + \omega_3 \cong \omega_{0e}$ and $\omega_{0e} + \omega_3 \cong \omega_{0e}$ which, when applied to Equations (54)-(56) yields

$$I \cong \sum_e \left[\frac{1}{\omega_{0e}} \left\{ \frac{\mu_{2e} \mu_{e0'} \mu_{0'0}}{\omega_{00'} + \omega} + \frac{\mu_{2e} \mu_{e1'} \mu_{1'0}}{\omega_{01'} + 2\omega} + \frac{\mu_{2e} \mu_{e2'} \mu_{2'0}}{\omega_{02'} + \omega} \right\} + \frac{1}{\omega_{0e}} \left\{ \frac{\mu_{20'} \mu_{0'e} \mu_{e0}}{\omega_{00'} + 2\omega} + \frac{\mu_{21'} \mu_{1'e} \mu_{e0}}{\omega_{01'} + 2\omega} + \frac{\mu_{22'} \mu_{2'e} \mu_{e0}}{\omega_{02'} + 2\omega} \right\} \right] \quad (57)$$

Next, the summation over vibronic intermediate states is carried out assuming that the quantity ω_{0e} may be energy averaged over the vibrational levels of the electronic state to yield the quantity $\bar{\omega}_e$ which is independent of the vibrational quantum numbers, v_e . Making this second approximation,

$$I \cong \sum_e \frac{1}{\bar{\omega}_e} \sum_{j_e} \sum_{v_e} \left\{ \frac{\mu_{2e} \mu_{e0'} \mu_{0'0}}{\omega_{00'} + \omega} + \frac{\mu_{22'} \mu_{2'e} \mu_{e0}}{\omega_{02'} + 2\omega} + \frac{\mu_{2e} \mu_{e1'} \mu_{1'0}}{\omega_{01'} + \omega} + \frac{\mu_{21'} \mu_{1'e} \mu_{e0}}{\omega_{01'} + 2\omega} + \frac{\mu_{2e} \mu_{e2'} \mu_{2'0}}{\omega_{02'} + \omega} + \frac{\mu_{20'} \mu_{0'e} \mu_{e0}}{\omega_{00'} + 2\omega} \right\} \quad (58)$$

where J_e and v_e are the rotational and vibrational quantum numbers of states in the excited electronic level manifold. The above approximation allows a simplification of the summation over vibrational levels of the electronic state. Note that the products of the matrix elements in Equation (58) have the general form $\mu_{2e} \mu_{ev'} \mu_{v'0}$ or $\mu_{2v'} \mu_{v'e} \mu_{e0}$. Thus, separating the rotational and vibrational parts of each matrix element, these two products can be explicitly written as

$$\mu_{2e} \mu_{ev'} \mu_{v'0} = \langle g, 2 | \mu | e, v_e \rangle \langle e, v_e | \mu | g, v' \rangle \langle g, v' | \mu | g, 0 \rangle R_1 \quad (59)$$

$$\mu_{2v'} \mu_{v'e} \mu_{e0} = \langle g, 2 | \mu | g, v' \rangle \langle g, v' | \mu | e, v_e \rangle \langle e, v_e | \mu | g, 0 \rangle R_2 \quad (60)$$

where R_1 and R_2 represent the appropriate product of rotational integrals. Both terms are of the form

$$\langle g, v'' | \mu | g, v' \rangle \langle g, v' | \mu | e, v_e \rangle \langle e, v_e | \mu | g, v \rangle R \quad (61)$$

The summation over $|e, v_e\rangle$ can thus be evaluated using the completeness property of the vibrational states in the manifold of the excited electronic state.

The product of the second and third factors in Equation (61) is performed first. The electronic part of the matrix element must be integrated. It is assumed that the individual matrix elements can be written¹⁴ as

$$\begin{aligned} \langle g, v' | \mu | e, v_e \rangle &= \langle v' | \mu_{ge} | v_e \rangle \\ \langle e, v_e | \mu | g, v \rangle &= \langle v_e | \mu_{eg} | v \rangle \end{aligned} \quad (62)$$

where $\mu_{ge} = \mu_{eg}^+$ is the dipole moment operator for the nuclear coordinates. The nuclear dipole moment operator can be expressed as a Taylor series expansion about the equilibrium internuclear separation, r_e :¹⁴

$$\mu_{ge}(r) = \mu_{ge}(r_e) + \left. \frac{\partial \mu_{ge}}{\partial r} \right|_{r_e} (r - r_e) + \frac{1}{2} \left. \frac{\partial^2 \mu_{ge}}{\partial r^2} \right|_{r_e} (r - r_e)^2 + \dots \quad (63)$$

Using the completeness property yields

$$\sum_{v_e} \langle v' | \mu_{ge} | v_e \rangle \langle v_e | \mu_{eg} | v \rangle = \langle v' | \mu_{ge} \mu_{eg} | v \rangle \quad (64)$$

Noting that $|\mu_{ge}|$ is real, the operator in Equation (64) may be reexpressed as

$$|\mu_{ge}|^2 = \mu_{ge} \mu_{eg} = D_{ge}^{(0)} + D_{ge}^{(1)} x + D_{ge}^{(2)} x^2 + D_{ge}^{(3)} x^3 + \dots \quad (65)$$

where x is the displacement of the atoms from their equilibrium positions (i.e. $x = r - r_e$) and the $D_{ge}^{(b)}$ are all real coefficients. These coefficients are related to certain derivatives of (63) according to:

$$D_{ge}^{(0)} = |\mu_{ge}^{(0)}|^2 \quad (66)$$

$$D_{ge}^{(1)} = \mu_{ge}^{(0)} \mu_{ge}^{(1)*} + \mu_{ge}^{(0)*} \mu_{ge}^{(1)} \quad (67)$$

$$D_{ge}^{(2)} = \mu_{ge}^{(0)} \mu_{ge}^{(2)*} + |\mu_{ge}^{(1)}|^2 + \mu_{ge}^{(0)*} \mu_{ge}^{(2)} \quad (68)$$

where

$$\mu_{ge}^{(k)} \equiv \left. \frac{\partial^{(k)} \mu_{ge}}{\partial r^{(k)}} \right|_{r_e} \quad (69)$$

The remaining integral in Equations (64) and (65) is of the form

$$A_{v',v}^{(k)} \equiv \langle v' | x^k | v \rangle \quad (70)$$

where $|v'\rangle$ and $|v\rangle$ are assumed to be normalized eigenfunctions of an anharmonic oscillator. Thus, Equations (59) and (60) can be evaluated according to:

$$\sum_{v_e} \mu_{2e} \mu_{ev'} \mu_{v'0} = \sum_{k=0}^2 D_{ge}^{(k)} A_{2,v'}^{(k)} \sum_{\ell=0}^2 \mu_{gg}^{(\ell)} A_{v',0}^{(\ell)} R_1 \quad (71)$$

$$\sum_{v_e} \mu_{2v'} \mu_{v'e} \mu_{e0} = \sum_{\ell=0}^2 \mu_{gg}^{(\ell)} A_{2,v'}^{(\ell)} \sum_{k=0}^2 D_{ge}^{(k)} A_{v',0}^{(k)} R_2 \quad (72)$$

Since the frequency denominators do not depend on J_e , the summations over rotational states are carried out first. Summation over J' must be performed explicitly using actual energy levels. Summation over m states can be performed by factoring the rotational part of the μ_{02} matrix element into R_1 and R_2 . This procedure yields precisely the function φ_R defined by Equation (23).

3.4 $\chi^{(3)}$ Calculation Results

The $\chi^{(3)}$ calculations for the three resonance enhancement schemes have been performed using the line selected CO laser frequencies corresponding to P(9), P(10), P(11), and P(12) transitions in the $[6 \rightarrow 5]$, $[5 \rightarrow 4]$, and $[4 \rightarrow 3]$ vibrational manifold. In addition, survey calculations have been carried out for each molecular species in order to determine the pump frequencies for which the nonlinear susceptibility is optimized. Nonlinear susceptibility values have been computed in CGS units; conversion to MKS units is obtained by multiplying the CGS value by a factor of 1.235×10^{-25} .

The following sections summarize the results of the calculations for each resonance enhancement scheme.

3.4.1 Type I Scheme

The candidate molecules studied for the type I scheme are CO^{18} , NO , $\text{DCl}^{35,37}$, and $\text{DBr}^{79,81}$. The spectroscopic constants, transition dipole moments, and linewidth data references for each molecule are listed in Table 10.

TABLE 10. TYPE I SCHEME MOLECULAR PARAMETER REFERENCES

Molecule	Spectroscopic Constants	Transition Dipole Moments	Linewidth
CO^{18}	[15]	[16]	[17]
NO	[18]	[19]	[20]
DCl^{35}	[21]	[22]	[23]
DBr^{79}	[24]	[25]	[26]

The spectroscopic constants for DCl^{37} were calculated from the DCl^{35} parameters using the isotope effect relations.²⁷ The same procedure was used to obtain the constants for DBr^{81} and DBr^{79} . The transition moments and linewidths for the isotopes were assumed to be the same.

The results of the $\chi^{(3)}$ code calculations using the line selected CO laser frequencies are listed in Tables 11 through 16. The tables indicate that χ^{THG} and χ^{SFG} values are in the range of 10^{-38} to $10^{-36} \text{ cm}^6/\text{erg}$ for CO^{18} and $\text{DCl}^{35,37}$, while the nonlinear susceptibilities of NO and $\text{DBr}^{79,81}$ are on the order of $10^{-38} \text{ cm}^6/\text{erg}$ and $10^{-40} \text{ cm}^6/\text{erg}$, respectively.

TABLE 11. TYPE I X⁽³⁾ CALCULATION RESULTS
MOLECULE: [CO¹⁸]

ω_s	P(9)	P(10)	P(11)	P(12)
$\omega_a + \omega_a + \omega_a$	1.79×10^{-37}	1.43×10^{-37}	1.22×10^{-37}	1.14×10^{-37}
$\omega_a + \omega_a + \omega_b$	2.40×10^{-37}	1.91×10^{-37}	1.62×10^{-37}	1.46×10^{-37}
$\omega_a + \omega_a + \omega_c$	2.26×10^{-38}	$1.94 \times 10^{-38}(1)$	1.64×10^{-38}	1.46×10^{-38}
$\omega_b + \omega_b + \omega_b$	3.38×10^{-38}	1.10×10^{-38}	4.41×10^{-39}	1.09×10^{-38}
$\omega_b + \omega_b + \omega_a$	1.83×10^{-37}	1.59×10^{-37}	1.41×10^{-37}	1.29×10^{-37}
$\omega_b + \omega_b + \omega_c$	2.64×10^{-38}	$1.91 \times 10^{-38}(1)$	1.70×10^{-38}	2.34×10^{-38}
$\omega_c + \omega_c + \omega_c$	2.35×10^{-39}	$1.05 \times 10^{-38}(1)$	4.55×10^{-39}	4.22×10^{-39}
$\omega_c + \omega_c + \omega_a$	3.12×10^{-38}	$3.10 \times 10^{-38}(1)$	2.64×10^{-38}	2.54×10^{-38}
$\omega_c + \omega_c + \omega_b$	2.94×10^{-38}	$2.15 \times 10^{-38}(1)$	1.68×10^{-38}	2.34×10^{-38}
$\omega_a + \omega_b + \omega_c$	1.19×10^{-37}	$9.56 \times 10^{-38}(1)$	8.37×10^{-38}	8.47×10^{-38}

$\omega_a = [4-3]$; $\omega_b = [5-4]$; $\omega_c = [6-5]$

(1) = One-Photon Resonance; (2) = Two-Photon Resonance; (3) = Three-Photon Resonance

TABLE 12. TYPE I x (3) CALCULATION RESULTS
MOLECULE: [NO¹⁶]

ω_s	P(9)	P(10)	P(11)	P(12)
$\omega_a + \omega_a + \omega_a$	1.09×10^{-39}	1.18×10^{-39}	1.29×10^{-39}	1.40×10^{-39}
$\omega_a + \omega_a + \omega_b$	1.32×10^{-39}	1.45×10^{-39}	1.56×10^{-39}	1.73×10^{-39}
$\omega_a + \omega_a + \omega_c$	1.69×10^{-39}	1.87×10^{-39}	2.08×10^{-39}	2.34×10^{-39}
$\omega_b + \omega_b + \omega_b$	1.92×10^{-39}	2.16×10^{-39}	2.31×10^{-39}	2.59×10^{-39}
$\omega_b + \omega_b + \omega_a$	1.59×10^{-39}	1.77×10^{-39}	1.90×10^{-39}	2.12×10^{-39}
$\omega_b + \omega_b + \omega_c$	2.46×10^{-39}	2.77×10^{-39}	3.05×10^{-39}	3.48×10^{-39}
$\omega_c + \omega_c + \omega_c$	3.90×10^{-39}	4.41×10^{-39}	5.23×10^{-39}	6.17×10^{-39}
$\omega_c + \omega_c + \omega_a$	2.59×10^{-39}	2.90×10^{-39}	3.33×10^{-39}	3.84×10^{-39}

$\omega_a = [4-3]$; $\omega_b = [5-4]$; $\omega_c = [6-5]$

(1) = One-Photon Resonance; (2) = Two-Photon Resonance; (3) = Three-Photon Resonance

TABLE 13. TYPE I x ⁽³⁾ CALCULATION RESULTS
MOLECULE: [DC₂³⁵]

ω_s	P(9)	P(10)	P(11)	P(12)
$\omega_a + \omega_a + \omega_a$	1.25×10^{-38}	6.17×10^{-38}	6.38×10^{-38}	1.52×10^{-37}
$\omega_a + \omega_a + \omega_b$	5.37×10^{-38}	7.15×10^{-38}	3.36×10^{-37}	6.82×10^{-38}
$\omega_a + \omega_a + \omega_c$	5.51×10^{-37}	$1.41 \times 10^{-37} (3)$	1.46×10^{-38}	2.07×10^{-37}
$\omega_b + \omega_b + \omega_b$	8.21×10^{-38}	4.90×10^{-38}	2.94×10^{-39}	$1.31 \times 10^{-37} (2)$
$\omega_b + \omega_b + \omega_a$	2.19×10^{-37}	$2.31 \times 10^{-37} (3)$	6.08×10^{-40}	$1.05 \times 10^{-37} (2)$
$\omega_b + \omega_b + \omega_c$	7.99×10^{-39}	$1.69 \times 10^{-38} (2)$	4.04×10^{-39}	$2.48 \times 10^{-38} (2)$
$\omega_c + \omega_c + \omega_c$	3.09×10^{-39}	3.54×10^{-39}	6.63×10^{-40}	1.92×10^{-39}
$\omega_c + \omega_c + \omega_a$	2.63×10^{-38}	3.63×10^{-38}	2.01×10^{-39}	6.22×10^{-38}
$\omega_c + \omega_c + \omega_b$	1.48×10^{-38}	$8.25 \times 10^{-39} (2)$	1.92×10^{-39}	$6.01 \times 10^{-39} (3)$
$\omega_a + \omega_b + \omega_c$	3.40×10^{-38}	$3.66 \times 10^{-38} (2)$	1.07×10^{-39}	5.05×10^{-38}

$\omega_a = [4-3]$; $\omega_b = [5-4]$; $\omega_c = [6-5]$

(1) = One-Photon Resonance; (2) = Two-Photon Resonance; (3) = Three-Photon Resonance

TABLE 14. TYPE I x⁽³⁾ CALCULATION RESULTSMOLECULE: [DCx³⁷]

ω_s	P(9)	P(10)	P(11)	P(12)
$\omega_a + \omega_a + \omega_a$	4.99×10^{-40}	1.31×10^{-38}	5.38×10^{-38}	4.18×10^{-38}
$\omega_a + \omega_a + \omega_b$	1.98×10^{-38}	3.30×10^{-37}	7.01×10^{-38}	5.91×10^{-38}
$\omega_a + \omega_a + \omega_c$	5.92×10^{-39}	1.17×10^{-37}	5.09×10^{-38}	1.38×10^{-38}
$\omega_b + \omega_b + \omega_b$	2.20×10^{-38}	3.65×10^{-38}	1.90×10^{-38}	3.69×10^{-39}
$\omega_b + \omega_b + \omega_a$	1.47×10^{-38}	4.55×10^{-38}	3.75×10^{-38}	3.82×10^{-38}
$\omega_b + \omega_b + \omega_c$	1.86×10^{-38}	8.92×10^{-39}	9.07×10^{-39}	4.02×10^{-39}
$\omega_c + \omega_c + \omega_c$	3.57×10^{-39}	2.17×10^{-39}	5.89×10^{-40}	$1.80 \times 10^{-39}(2)$
$\omega_c + \omega_c + \omega_a$	7.02×10^{-38}	1.39×10^{-38}	1.85×10^{-38}	$2.47 \times 10^{-39}(2)$
$\omega_c + \omega_c + \omega_b$	6.64×10^{-39}	5.94×10^{-39}	4.46×10^{-39}	$3.25 \times 10^{-39}(2)$
$\omega_a + \omega_b + \omega_c$	2.64×10^{-38}	7.91×10^{-39}	1.65×10^{-38}	2.39×10^{-39}

 $\omega_a = [4-3]; \omega_b = [5-4]; \omega_c = [6-5]$

(1) = One-Photon Resonance; (2) = Two-Photon Resonance; (3) = Three-Photon Resonance

TABLE 15. TYPE I x ⁽³⁾ CALCULATION RESULTSMOLECULE: [DBr⁷⁹]

ω_s	P(9)	P(10)	P(11)	P(12)
$\omega_a + \omega_a + \omega_a$	2.70×10^{-41}	2.90×10^{-41}	3.11×10^{-41}	3.36×10^{-41}
$\omega_a + \omega_a + \omega_b$	3.19×10^{-41}	3.43×10^{-41}	3.71×10^{-41}	4.03×10^{-41}
$\omega_a + \omega_a + \omega_c$	4.04×10^{-41}	4.39×10^{-41}	4.80×10^{-41}	5.24×10^{-41}
$\omega_b + \omega_b + \omega_b$	4.39×10^{-41}	4.77×10^{-41}	5.22×10^{-41}	5.74×10^{-41}
$\omega_b + \omega_b + \omega_a$	3.74×10^{-41}	4.06×10^{-41}	4.41×10^{-41}	4.82×10^{-41}
$\omega_b + \omega_b + \omega_c$	5.51×10^{-41}	6.05×10^{-41}	6.67×10^{-41}	7.37×10^{-41}
$\omega_c + \omega_c + \omega_c$	8.57×10^{-41}	9.50×10^{-41}	1.06×10^{-40}	1.18×10^{-40}
$\omega_c + \omega_c + \omega_a$	5.94×10^{-41}	6.53×10^{-41}	7.23×10^{-41}	7.96×10^{-41}
$\omega_c + \omega_c + \omega_b$	6.89×10^{-41}	7.61×10^{-41}	8.47×10^{-41}	9.36×10^{-41}
$\omega_a + \omega_b + \omega_c$	4.72×10^{-41}	5.16×10^{-41}	5.67×10^{-41}	6.23×10^{-41}

 $\omega_a = [4-3]$; $\omega_b = [5-4]$; $\omega_c = [6-5]$

(1) = One-Photon Resonance; (2) = Two-Photon Resonance; (3) = Three-Photon Resonance

TABLE 16. TYPE I X⁽³⁾ CALCULATION RESULTS

MOLECULE: [DBr⁸¹]

ω_s	P(9)	P(10)	P(11)	P(12)
$\omega_a + \omega_a + \omega_a$	2.68×10^{-41}	2.87×10^{-41}	3.08×10^{-41}	3.32×10^{-41}
$\omega_a + \omega_a + \omega_b$	3.15×10^{-41}	$3.40 \times 10^{-41}(1)$	3.67×10^{-41}	3.98×10^{-41}
$\omega_a + \omega_a + \omega_c$	3.40×10^{-41}	4.31×10^{-41}	4.71×10^{-41}	5.12×10^{-41}
$\omega_b + \omega_b + \omega_b$	4.34×10^{-41}	$4.72 \times 10^{-41}(1)$	5.15×10^{-41}	5.66×10^{-41}
$\omega_b + \omega_b + \omega_a$	3.70×10^{-41}	$4.01 \times 10^{-41}(1)$	4.35×10^{-41}	4.76×10^{-41}
$\omega_b + \omega_b + \omega_c$	5.39×10^{-41}	$5.93 \times 10^{-41}(1)$	6.54×10^{-41}	7.19×10^{-41}
$\omega_c + \omega_c + \omega_c$	8.20×10^{-41}	9.18×10^{-41}	1.02×10^{-40}	1.12×10^{-40}
$\omega_c + \omega_c + \omega_a$	5.75×10^{-41}	6.36×10^{-41}	7.01×10^{-41}	7.68×10^{-41}
$\omega_c + \omega_c + \omega_b$	6.67×10^{-41}	7.41×10^{-41}	8.20×10^{-41}	9.03×10^{-41}
$\omega_a + \omega_b + \omega_c$	4.63×10^{-41}	5.07×10^{-41}	5.56×10^{-41}	6.08×10^{-41}

$\omega_a = [4-3]$; $\omega_b = [5-4]$; $\omega_c = [6-5]$

(1) = One-Photon Resonance; (2) = Two-Photon Resonance; (3) = Three-Photon Resonance

An analysis of the molecular energy levels shows that the pump frequencies are moderately close to one, two, and three-photon resonances. However, numerous destructive interference effects cancel some of the resonance enhancement terms in the nonlinear susceptibility. Consequently, the values of χ^{THG} and χ^{SFG} fluctuate by as much as an order of magnitude within a small range of pump frequencies. This behavior is evident in the results of the calculations for each of the molecules. As an example, Figure 3 shows the calculated value of χ^{THG} for CO.

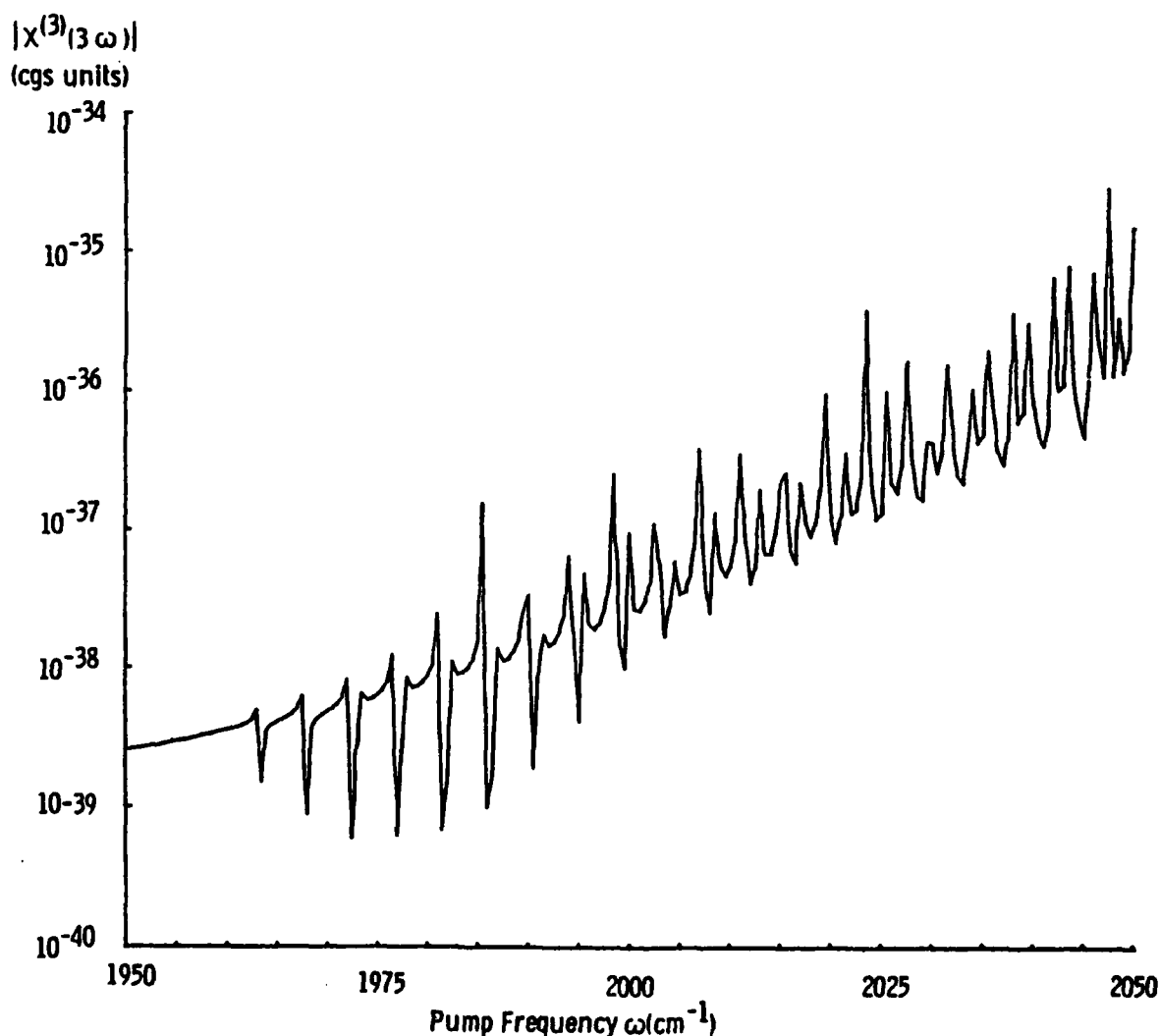


FIGURE 3. NONLINEAR SUSCEPTIBILITY OF CO^{18} FOR THIRD HARMONIC GENERATION

A conversion efficiency estimate based on a χ^{THG} value of 10^{-34} cm⁶/erg with $N = 10^{20}$ cm⁻³, $I = 500$ MW/cm², and $L = 300$ cm shows that nearly 20% efficiency is feasible if phase-matching can be maintained over the interaction length during the entire pulse length. From this analysis, $\chi^{(3)}$ values on the order of 10^{-36} cm⁶/erg suggest efficiencies on the order of 2×10^{-5} . The small conversion efficiencies are the direct result of the small values of the non-linear susceptibilities.

The survey calculations of χ^{THG} were carried out to find the largest two- and three-photon resonance enhancement in each of the type I scheme molecules. Using the optimum pump frequency ranges given in Table 3 as a guide, several known CO laser frequencies²⁸ were chosen to closely match two- or three-photon resonances in DCl, DBr, and NO. The CO laser frequencies did not match the optimum pump frequency ranges of CO¹⁸. Table 17 lists the results of the survey calculations. The χ^{THG} values in the table show significant enhancement for NO and DBr. This suggests that the choice of CO laser output frequencies to match the optimum pump frequency range and the resonances is an important factor in the overall efficiency.

TABLE 17. TYPE I THG SURVEY CALCULATION

CO Laser Frequency		$\chi^{(3)}$ (THG) in cm ⁶ /erg	
ω (cm ⁻¹)	Transition	Molecule	$\chi^{(3)}$
1838.49	P(24) [9-8]	NO	1.41×10^{-35}
1859.80	P(19) [9-8]	NO	1.28×10^{-35}
1846.87	P(16) [10-9]	NO	1.45×10^{-35}
2016.871	P(12) [4-3]	DCl ³⁵	1.52×10^{-37}
2003.154	P(9) [5-4]	DCl ³⁵	0.82×10^{-37}
1991.014	P(12) [5-4]	DCl ³⁷	0.42×10^{-37}
1808.35	P(13) [12-11]	DBr ⁷⁹	1.1×10^{-37}
1809.41	P(19) [11-10]	DBr ⁷⁹	2.1×10^{-37}
1805.29	P(20) [11-10]	DBr ⁸¹	2.1×10^{-36}
1809.10	P(25) [10-9]	DBr ⁸¹	4.6×10^{-37}

3.4.2 Type II Scheme

The references used for the molecular parameters are listed in Table 18. Differential Raman cross section data for HD are not available; however, the similarity of its electronic structure to that of H_2 implies a similar value of $d\sigma/d\Omega$ for both HD and H_2 . Thus, $d\sigma/d\Omega$ values for HD may be scaled from H_2 data using the k^4 dependence of Raman cross section.

TABLE 18. TYPE II SCHEME MOLECULAR PARAMETER REFERENCES

Molecule	Spectroscopic Constants	$(\frac{d\sigma}{d\Omega})_{ }$ and k	Linewidth
H_2	[29]	[30]	[31]
HD	[29]	calculated from [30]	[32]
HF	[33]	[34]	[35]

The Raman cross sections for the 0 and S branches of H_2 and HD were calculated from the depolarization ratio³⁶ and the scattering strength dependence on the rotational quantum number.³⁷ The ratios of the polarized S and 0 branch differential scattering cross sections to that of the Q branch were found to be given by the following relations:

$$\frac{(\frac{d\sigma}{d\Omega})_{||}^{S(J)}}{(\frac{d\sigma}{d\Omega})_{||}^{Q(J)}} = \frac{2(J+2)(2J-1)}{J(2J+1)} \rho_{\lambda}^Q(J) \quad (73)$$

$$\frac{(\frac{d\sigma}{d\Omega})_{||}^{0(J)}}{(\frac{d\sigma}{d\Omega})_{||}^{Q(J)}} = \frac{2(J-1)(2J+3)}{(J+1)(2J+1)} \rho_{\lambda}^Q(J) \quad (74)$$

where $\rho_{\lambda}^Q(J)$ is the Q branch depolarization ratio for linearly polarized incident light.

Experimentally measured values of ρ for H_2 give cross section ratios on the order of 10^{-2} for both S and 0 branches. This implies that $\chi^{(3)}$ values are inherently smaller for the S and 0 branch resonances than those of the Q branch resonance enhancement. This property is indicated in the results of the χ^{THG} calculations given in Table 19.

TABLE 19. TYPE II THG SURVEY CALCULATION

(T = 300 K, P = 1 Atm)

CO Laser Frequency		$ \chi^{(3)} $ (cm ⁶ /erg)	Two-Photon Resonance Molecule Branch (J)
Transition	ω (cm ⁻¹)		
P(19) [12-11]	1784.33	2.0×10^{-38}	H ₂ : O(2)
P(23) [5-4]	1943.99	1.1×10^{-37}	HD: S(0)
P(11) [7-6]	1943.52	1.2×10^{-37}	HD: S(0)
P(10) [4-3]*	2025.07	4.0×10^{-38}	HD: S(1)
P(11) [12-11]	1815.81	1.7×10^{-36}	HD: Q(0)
P(18) [11-10]	1813.50	1.3×10^{-36}	HD: Q(1)
P(19) [11-10]	1809.09	6.6×10^{-37}	HD: Q(2)
P(20) [11-10]	1805.29	2.2×10^{-37}	HD: Q(3)
P(26) [10-9]	1804.76	1.3×10^{-36}	HD: Q(3)
P(14) [12-11]	1804.28	2.4×10^{-36}	HD: Q(3)
P(9) [6-5]*	1977.264	2.4×10^{-39}	HF: Q(3)
P(10) [6-5]*	1973.285	2.7×10^{-39}	HF: Q(4)
P(11) [6-5]*	1969.274	8.8×10^{-40}	HF: Q(5)

* Line selected CO laser frequency

The only line selected CO laser frequency which approaches a two-photon resonance in HD is the P(10) [4-3] transition. However, since the frequency detuning is approximately 1 cm⁻¹ from the S branch resonance χ^{THG} is relatively small. The other lines selected pump frequencies yield smaller χ^{THG} values in HD due to off-resonance conditions. In contrast to HD and H₂, some of the pump frequencies are close to the Q-branch resonances in HF. However, small χ^{THG} values are calculated based on the large linewidth data. Therefore the above results suggest that Q-branch resonances in HD should be considered for optimum $\chi^{(3)}$ resonance enhancement.

3.4.3 Type III Scheme

The molecular parameter references for HCl and DF are listed in Table 20.

TABLE 20. TYPE III SCHEME MOLECULAR PARAMETER REFERENCES

Molecule	Spectroscopic Constants	Transition Dipole Moment	Linewidth
HCl	[38]	[22]	[23]
DF	[39]	[40]	[41]

The results of the χ^{THG} and χ^{SFG} calculations for the line selected CO laser frequencies are summarized in Tables 21 and 22 for HCl and DF, respectively. The values listed in Tables 21 and 22 are in the range of 0.8 to 1.5×10^{-38} cm^6/erg for most of the pump frequency combinations. Based on the conversion efficiency estimate of Section 3.4.1, the type III susceptibilities are predicted to have relatively small efficiencies.

TABLE 21. TYPE III $\chi^{(3)}$ CALCULATION RESULTS
MOLECULE: [HCl³⁵]

ω_s	P(9)	P(10)	P(11)	P(12)
$\omega_a + \omega_a + \omega_a$	7.64×10^{-39}	7.96×10^{-39}	8.30×10^{-39}	8.65×10^{-39}
$\omega_a + \omega_a + \omega_b$	8.36×10^{-39}	8.71×10^{-39}	9.08×10^{-39}	9.48×10^{-39}
$\omega_a + \omega_a + \omega_c$	9.19×10^{-39}	9.59×10^{-39}	1.00×10^{-38}	1.05×10^{-38}
$\omega_b + \omega_b + \omega_b$	9.97×10^{-39}	1.04×10^{-38}	1.09×10^{-38}	1.14×10^{-38}
$\omega_b + \omega_b + \omega_a$	9.14×10^{-39}	9.53×10^{-39}	9.94×10^{-39}	1.04×10^{-38}
$\omega_b + \omega_b + \omega_c$	1.10×10^{-38}	1.15×10^{-38}	1.20×10^{-38}	1.25×10^{-38}
$\omega_c + \omega_c + \omega_c$	1.33×10^{-38}	1.39×10^{-38}	1.46×10^{-38}	1.53×10^{-38}
$\omega_c + \omega_c + \omega_a$	1.11×10^{-38}	1.16×10^{-38}	1.21×10^{-38}	1.27×10^{-38}
$\omega_c + \omega_c + \omega_b$	1.21×10^{-38}	1.26×10^{-38}	1.32×10^{-38}	1.39×10^{-38}
$\omega_a + \omega_b + \omega_c$	1.00×10^{-38}	1.05×10^{-38}	1.10×10^{-38}	1.15×10^{-38}

$\omega_a = [4-3]$; $\omega_b = [5-4]$; $\omega_c = [6-5]$

(1) = One-Photon Resonance; (2) = Two-Photon Resonance; (3) = Three-Photon Resonance

TABLE 22. TYPE III X⁽³⁾ CALCULATION RESULTS

MOLECULE: [DF]

ω_s	P(9)	P(10)	P(11)	P(12)
$\omega_a + \omega_a + \omega_a$	3.64×10^{-39}	3.75×10^{-39}	3.86×10^{-39}	3.98×10^{-39}
$\omega_a + \omega_a + \omega_b$	3.88×10^{-39}	4.00×10^{-39}	4.13×10^{-39}	4.26×10^{-39}
$\omega_a + \omega_a + \omega_c$	4.16×10^{-39}	4.30×10^{-39}	4.44×10^{-39}	4.60×10^{-39}
$\omega_b + \omega_b + \omega_b$	4.43×10^{-39}	4.58×10^{-39}	4.74×10^{-39}	4.91×10^{-39}
$\omega_b + \omega_b + \omega_a$	4.14×10^{-39}	4.28×10^{-39}	4.42×10^{-39}	4.57×10^{-39}
$\omega_b + \omega_b + \omega_c$	4.77×10^{-39}	4.95×10^{-39}	5.14×10^{-39}	5.34×10^{-39}
$\omega_c + \omega_c + \omega_c$	5.61×10^{-39}	5.85×10^{-39}	6.11×10^{-39}	6.41×10^{-39}
$\omega_c + \omega_c + \omega_a$	4.82×10^{-39}	5.00×10^{-39}	5.19×10^{-39}	5.41×10^{-39}
$\omega_c + \omega_c + \omega_b$	5.17×10^{-39}	5.37×10^{-39}	5.59×10^{-39}	5.84×10^{-39}
$\omega_a + \omega_b + \omega_c$	4.46×10^{-39}	4.61×10^{-39}	4.78×10^{-39}	4.95×10^{-39}

$\omega_a = [4-3]$; $\omega_b = [5-4]$; $\omega_c = [6-5]$

(1) = One-Photon Resonance; (2) = Two-Photon Resonance; (3) = Three-Photon Resonance

4.0 EFFICIENCY LIMITATION AND PHASE-MATCHING ANALYSIS

Efficiency limitations in THG and SFG generally arise from the breaking of phase-matching and the competing processes. Breaking of phase-matching can occur through various causes. These include population transfer due to one- and two-photon absorption and intensity dependent refractive index variation caused by quadratic Kerr effect. These time-dependent processes may ultimately limit pulse lengths. Examples of competing processes are stimulated vibrational Raman scattering of the pump fields. Another limitation is imposed by gas breakdown at very high power and energy densities. This section examines the importance of the different efficiency limiting processes. The quantitative analysis yields optimum operating parameters for efficient frequency up-conversion.

The breaking of phase-matching limits conversion efficiency because of reduced effective interaction length for nonlinear coherent processes. For a process involving an interaction length L and a wave vector mismatch Δk , the allowed phase mismatch is given by:⁴²

$$\Delta k L \leq \pi \quad (75)$$

The breaking of phase-matching refers to a condition that violates the above requirement. Since a nonlinear medium is usually chosen to satisfy the phase-matching condition initially, the breaking of phase-matching may arise from dynamic wave vector mismatches caused by refractive index variations in the medium during the conversion process. In the general case of SFG, the phase variation is expressed by:

$$\delta[\Delta k L] = \frac{1}{c} [\omega_s \delta n(\omega_s) - \omega_p \delta n(\omega_p) - \omega_q \delta n(\omega_q) - \omega_r \delta n(\omega_r)] L \quad (76)$$

where $\delta n(\omega_j)$ is the refractive index variation at ω_j . For the special case of THG, the above expression simplifies to:

$$\delta[\Delta k L] = \frac{3\omega}{c} [\delta n(3\omega) - \delta n(\omega)] L \quad (77)$$

In the following sections various linear and nonlinear processes which are responsible for the refractive index variation and the competing effects are discussed in terms of specific efficiency limiting mechanisms.

4.1 Linear Processes

The important linear processes are single-photon absorption at the pump and the generated frequencies, population transfer effects, and thermal defocusing. Since the latter two effects are consequences of pump absorption in the medium, it is essential to choose molecular species which minimize the pump absorption. Therefore, infrared absorption bands of the candidate molecules provide crucial parameters for the assessment of linear efficiency limiting processes.

4.1.1 Absorption Coefficient and Refractive Index at Pump Frequencies

Single-photon absorption of the pump radiation arises from the fundamental transitions in the IR-active molecules. These transitions also determine the refractive indices at frequencies close to them. Both the absorption coefficient and refractive index as a function of pump frequency can be evaluated from the first-order (linear) susceptibility per molecule which is given by⁷

$$\chi^{(1)}(\omega) = -\frac{1}{\hbar} \sum_{a,b} \rho_{aa} |\mu_{ab}|^2 \left[\frac{1}{\omega_{ab} - \omega + i\Gamma_{ab}} + \frac{1}{\omega_{ab} + \omega - i\Gamma_{ab}} \right] \quad (78)$$

The symbols have their usual meanings as used previously in the third-order susceptibility formula. The numerical values of $\chi^{(1)}$ were obtained from the same molecular spectroscopic constants and transition moment data as were used in the calculation of $\chi^{(3)}$ values.

To obtain the numerical values for the absorption coefficient $\alpha(\omega)$ and the refractive index $n(\omega)$, the following relations were used:

$$\alpha(\omega) = \frac{\omega \Gamma}{n(\omega)} \text{Im} [N\chi^{(1)}(\omega)] \quad (79)$$

$$n(\omega) = \left[1 + \text{Re} [N\chi^{(1)}(\omega)] \right]^{1/2} \quad (80)$$

In molecular gases, the real part of $N\chi^{(1)}$ is generally much smaller than unity. Thus, a good approximation of $n(\omega)$ is given by:

$$n(\omega) - 1 \approx \frac{1}{2} \text{Re} [N\chi^{(1)}(\omega)] \quad (81)$$

A computer code for $\chi^{(1)}$ has been developed, and a program listing is given in Appendix B.

The results of the $\alpha(\omega)$ and $n(\omega) - 1$ calculations at STP conditions are plotted in Figures 4 through 6 for the candidate molecules DCl, DBr, and NO, respectively.

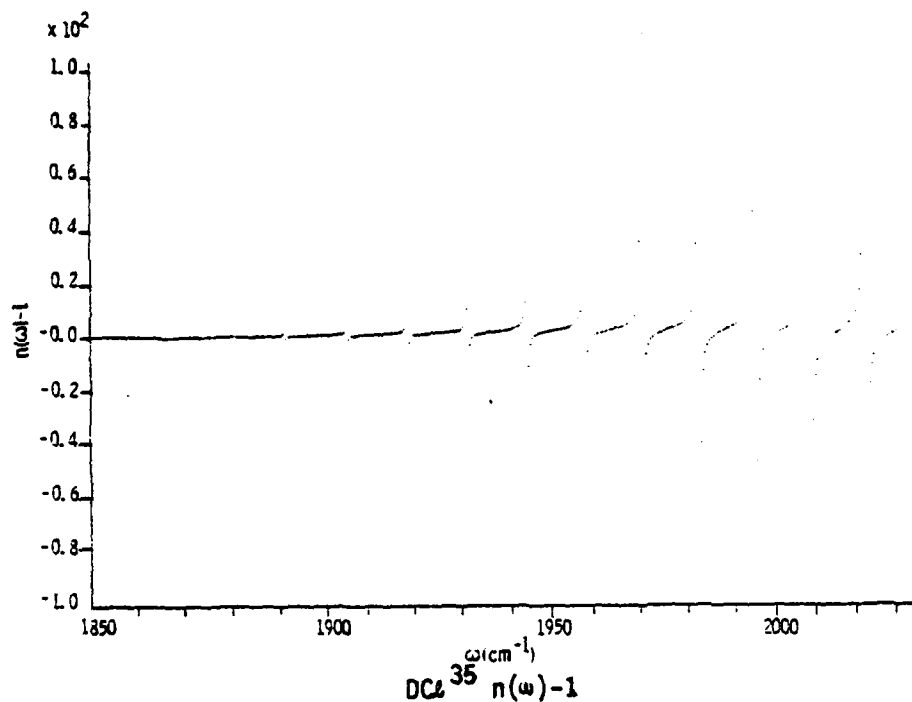


FIGURE 4(a). DCl REFRACTIVE INDEX VS FREQUENCY

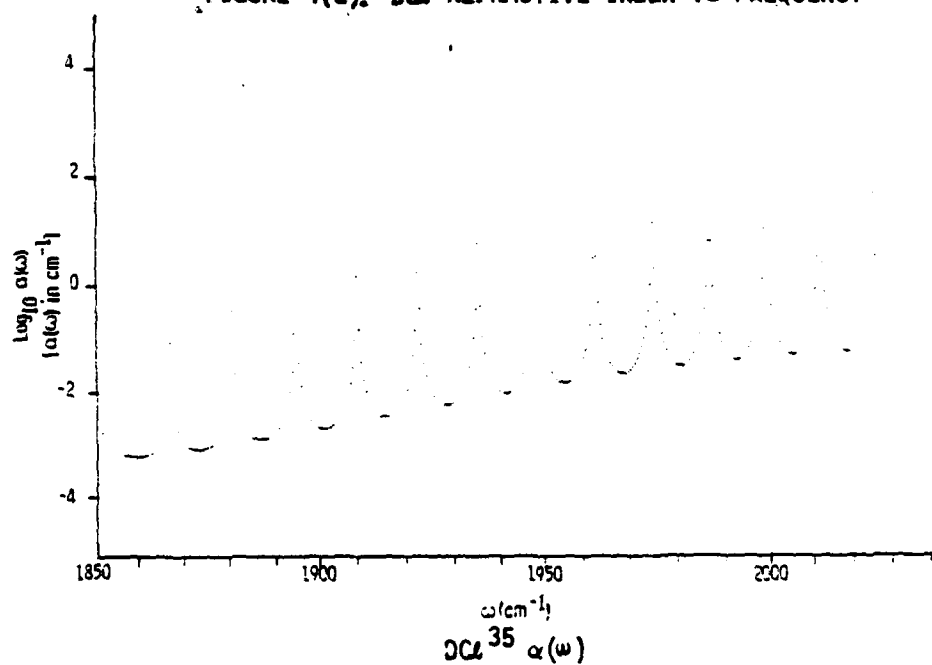


FIGURE 4(b). DCl ABSORPTION COEFFICIENT VS FREQUENCY

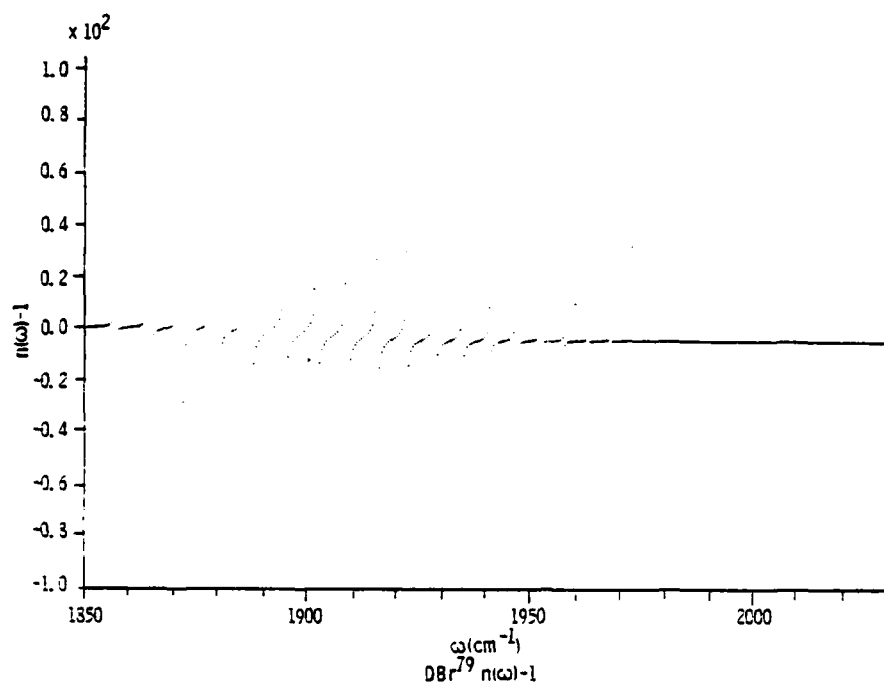


FIGURE 5(a). DBr REFRACTIVE INDEX VS FREQUENCY

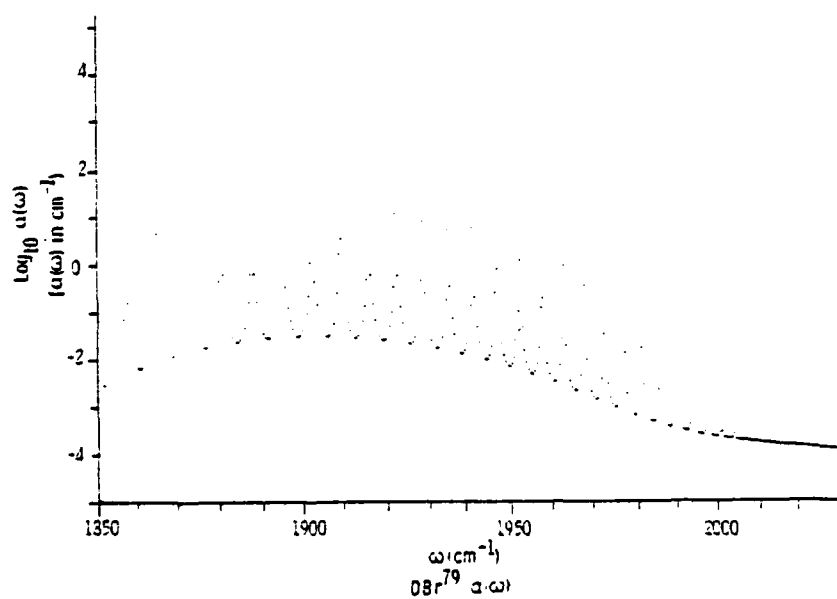


FIGURE 5(b). DBr ABSORPTION COEFFICIENT VS FREQUENCY

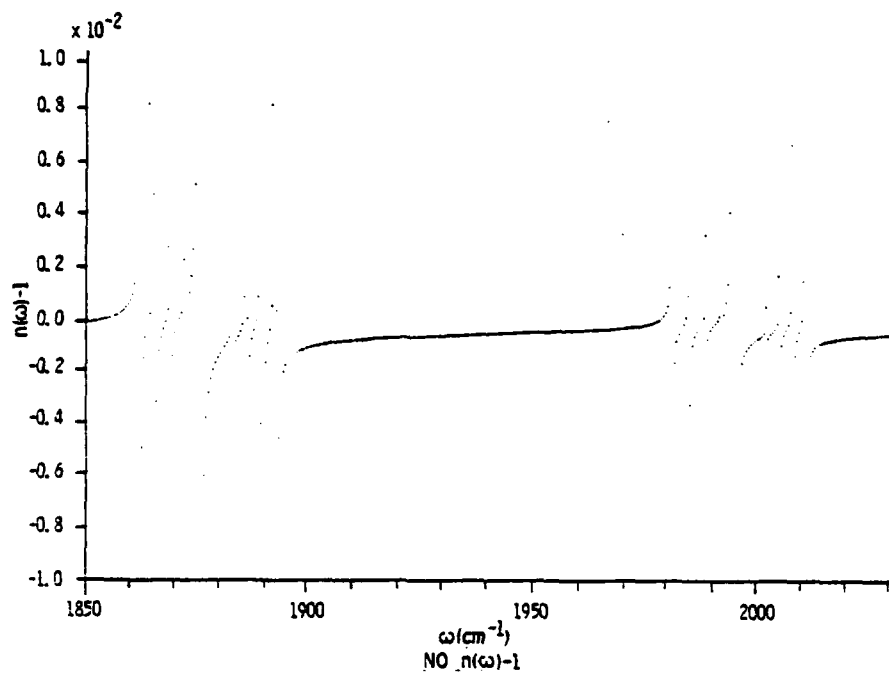


FIGURE 6(a). NO REFRACTIVE INDEX VS FREQUENCY

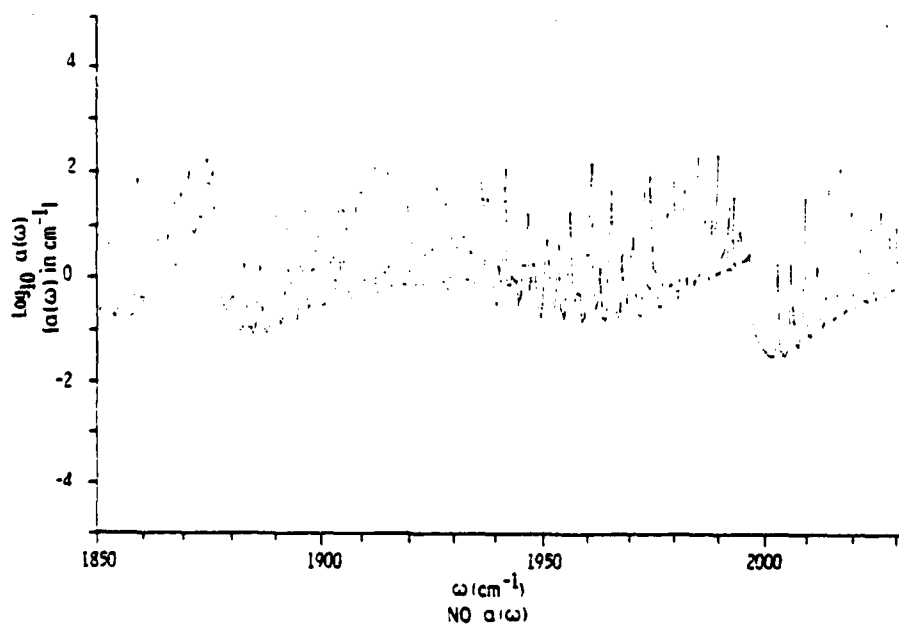


FIGURE 6(b). NO ABSORPTION COEFFICIENT VS FREQUENCY

When significant absorption is present at ω and 3ω , the electric field equations governing THG can be cast in the following form:

$$\frac{dE_3}{dz} = \beta E_1^3 - \frac{1}{2} \alpha_3 E_3 \quad (82a)$$

$$\frac{dE_1}{dz} = \beta E_1^2 - \frac{1}{2} \alpha_1 E_1 \quad (82b)$$

If pump depletion and phase mismatches are considered to be negligible, the generated field amplitude, $E_3(L)$, is given by

$$E_3(L) = \beta (E_1(0))^3 \frac{2}{3\alpha_1 - \alpha_3} \left(e^{-\alpha_3 L/2} - e^{-3\alpha_1 L/2} \right) \quad (83)$$

In the case of strong pump attenuation ($\alpha_1 L \gg 1$) and $\alpha_3 = 0$, the above expression states that the effective interaction length is $(3\alpha_1/2)^{-1}$ which is much less than L . However, if attenuation is small ($\alpha_1 L \ll 1$), an approximate solution for $E_3(L)$ is:

$$E_3(L) \approx \beta (E_1(0))^3 L (1 - 3\alpha_1 L/4) \quad (84)$$

Thus, small attenuation does not significantly reduce the THG efficiency if dynamic phase mismatches are negligible.

4.1.2 Absorption Coefficient and Refractive Index at the Generated Frequencies

Although the generated frequencies are far from the fundamental IR transition bands, they nearly coincide with the overtone transitions in some of the candidate molecules. The calculation of $\alpha(\omega)$ and $n(\omega) - 1$ is straightforward using the $\chi^{(1)}$ computer code. Figures 7 and 8 show the results of the calculations for the first overtone bands of DF and HCl, respectively.

The second overtone bands of the type I scheme molecules are also close to the generated frequencies and are important in the resonance enhancement of $\chi^{(3)}$; however, single-photon absorption at the generated frequencies is exceedingly small (typically $\alpha < 10^{-5} \text{ cm}^{-1}$). Therefore, a model discussed in the previous section, in which $\alpha_3 = 0$ was assumed, is a realistic description of the type I scheme.

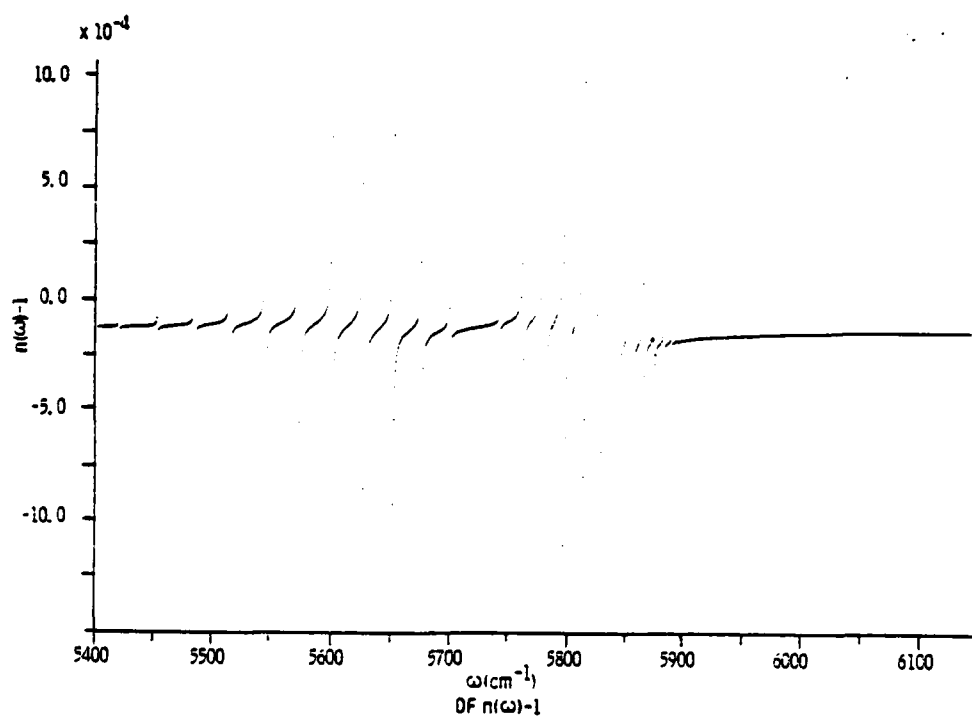


FIGURE 7(a). DF REFRACTIVE INDEX VS FREQUENCY

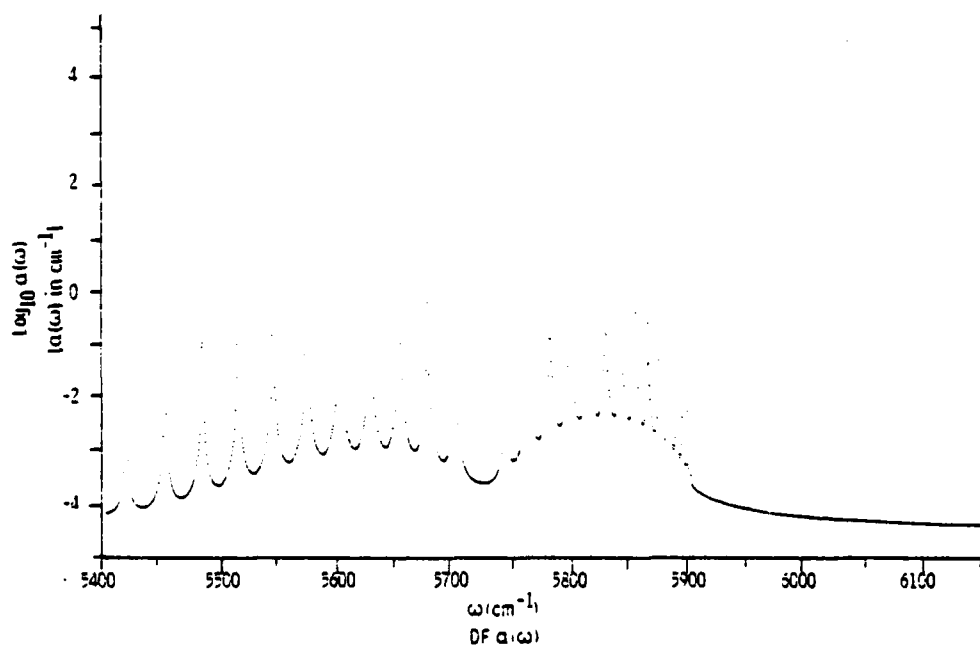


FIGURE 7(b). DF ABSORPTION COEFFICIENT VS FREQUENCY

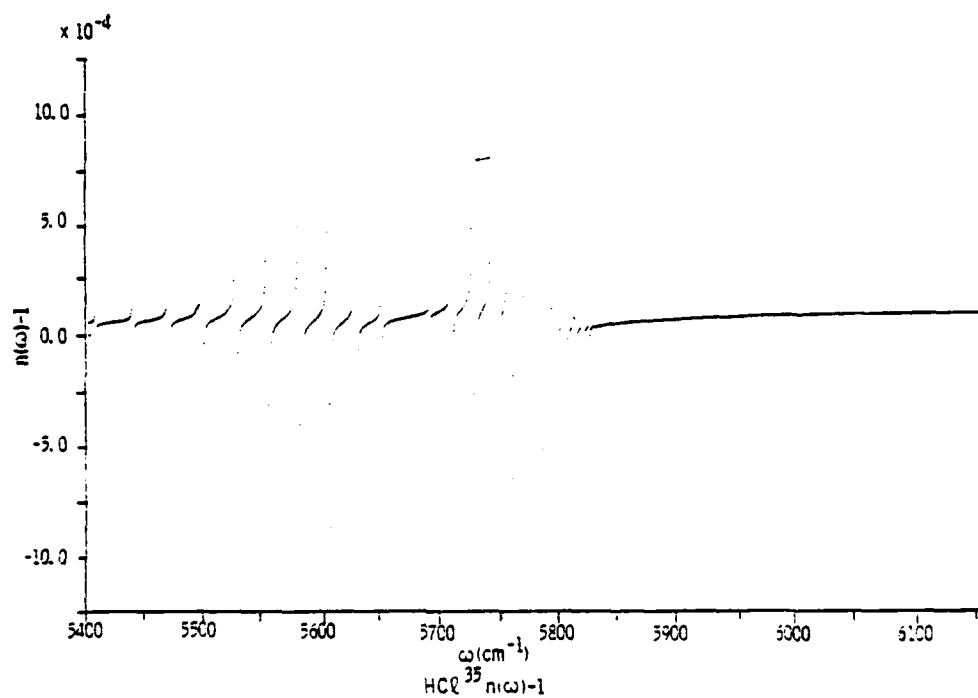


FIGURE 8(a). HCl REFRACTIVE INDEX VS FREQUENCY

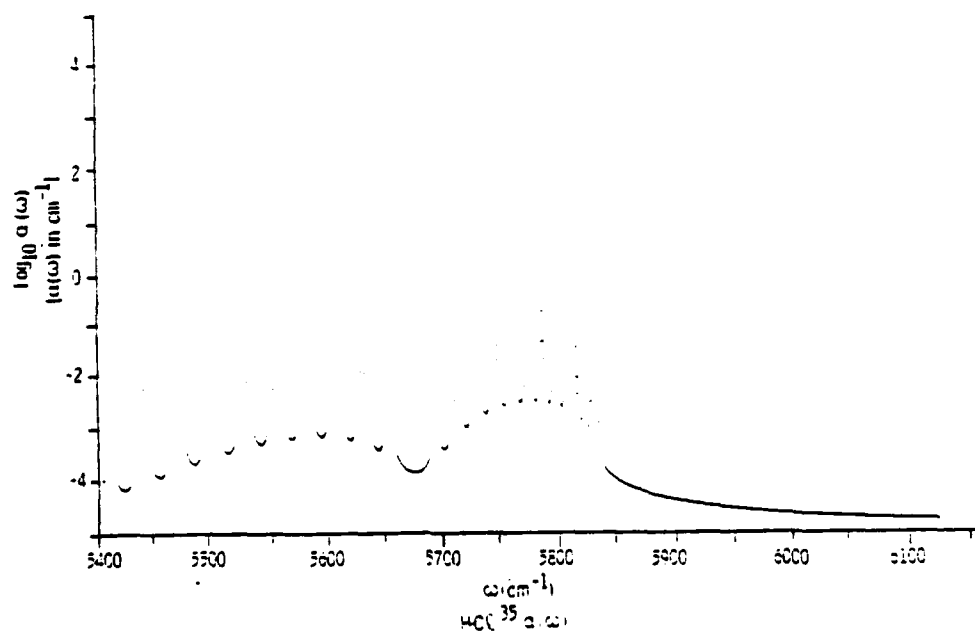


FIGURE 8(b). HCl ABSORPTION COEFFICIENT VS FREQUENCY

In contrast to the type I scheme, absorption in the type III scheme is significant only at the generated frequencies. By setting $\alpha_1 = 0$ in Equation (83), the generated field amplitude becomes

$$E_3(L) = \frac{2\beta}{\alpha_3} (E_1(0))^3 \left(1 - e^{-\alpha_3 L/2}\right) \quad (85)$$

In the strong attenuation limit ($\alpha_3 L \gg 1$), the effective interaction length becomes $(\alpha_3/2)^{-1}$. On the other hand, if $\alpha_3 L \ll 1$, $E_3(L)$ is proportional to $(E_1(0))^3$ and L . From these properties, it is evident that a small attenuation of the generated field is desirable and that the attenuation only slightly reduces the conversion efficiency. These conclusions together with those of the previous section are valid only to the extent in which dynamic phase mismatches can be neglected. It will be shown in the next section, however, that the breaking of the phase-matching condition due to absorption is much more sensitive and critical than pump attenuation in the IR-active candidate molecules.

4.1.3 Population Transfer and Dynamic Phase Mismatch

Whenever ground state molecules absorb pump radiation, a certain fraction of the population is transferred to the first excited vibrational level. Since the fundamental IR transitions determine the refractive indices at the pump frequencies, population transfer perturbs the refractive indices at the pump frequencies. This immediately leads to phase variation through expressions (76) and (77).

Because population transfer is time-dependent, the resulting phase variation is a dynamic process. Although this dynamic phase mismatch can be calculated in principle, such a calculation would require an estimate of population transfer based on the radiative and kinetic properties of the gas, which are beyond the scope of this work. Therefore, a quasi-steady state model was considered for the purpose of illustrating the effects of the dynamic phase mismatch. The basic assumption of this model is that the rotational states of the first excited vibrational state are in thermal equilibrium at the gas temperature. The excited vibrational state population as a whole is considered to be time-dependent in order to allow for pulse length effects and pump intensity fluctuations.

The refractive index variation calculations using the $x^{(1)}$ code were accomplished by specifying a certain relative population transfer value ($\Delta N/N$). For example, in the case of DC2 with $(\Delta N/N) = 10^{-3}$ at STP, different pump frequencies yielded wave vector mismatches from 3.2×10^{-4} to $6.5 \times 10^{-2} \text{ cm}^{-1}$. These values are typical of the type I scheme molecules. For a practical device having an interaction length of 300 cm, the corresponding phase variations are 9.6×10^{-2} to 19.5 radians, thereby indicating that breaking of phase-matching is a serious effect for some pump frequencies and significant for many others. If $(\Delta N/N) = 10^{-2}$ is assumed, most of the pump frequencies would experience severe phase mismatches. This means that population transfer values of as little as 0.1% can lead to significant efficiency reduction and that 1% transfer levels are beyond the tolerance range. Conversely, efficient frequency conversion can be maintained only over a time interval during which population transfer can be held to less than 0.1%.

An estimate for the allowable pulse duration ΔT can be obtained from the following relation:

$$\frac{\Delta N}{N} = \frac{\alpha I \Delta T}{N \hbar \omega} \quad (86)$$

where I is the pump intensity and α is the absorption coefficient. For most of the type I scheme molecules α/N is typically in the range of 10^{-23} cm^2 (off-resonance) to 10^{-19} cm^2 at the peaks of absorption lines. Using the lower limit, the maximum value of ΔT for $I = 0.5 \text{ GW/cm}^2$ is found to be 8×10^{-9} second if $(\Delta N/N)$ is restricted to 10^{-3} . Therefore, at the pump intensities of interest for high conversion efficiencies, the pulse lengths are limited to the nano-second time scale.

4.1.4 Thermal Defocusing

The population transfer may cause thermal defocusing which is a manifestation of refractive index variation across the beam for a nonuniform pump beam cross section. In the case of a gaussian beam profile with an initial beam radius, w_0 , the beam radius changes by a factor of two when the refractive index on the beam axis varies by an amount given by:⁴²

$$\delta n = w_0^2 / 2L^2 \quad (87)$$

where L is the interaction length. If w_0 is taken to be the waist such that $w_0^2 = \lambda b/2\pi$ (b = confocal parameter), then the condition (87) becomes:

$$\delta n = \lambda b/4\pi L^2 \quad (88)$$

For the case of confocal focusing ($b = L$), the numerical value of δn is 1.3×10^{-7} for $L = 300$ cm. From the results of the previous section, $(\Delta N/N) = 10^{-3}$ in DC2 yields δn values in the range of 2.5×10^{-8} to 5.2×10^{-6} . This clearly shows that thermal defocusing has a serious effect on the efficiency due to reduced pump intensities in the nonlinear medium. However, it is also important to note that for large beam cross sections and/or uniform intensity profiles, thermal defocusing effects can be minimized.

4.2 Nonlinear Processes

A number of third-order processes besides THG and SFG may be present at high pump intensities. These include quadratic Kerr effect, two-photon absorption, and stimulated Raman scattering. Other nonlinear processes such as three-photon absorption, gas breakdown, and pump depletion may also affect conversion efficiencies. Quantitative assessment of each of these intensity-dependent processes is discussed in the following sections.

4.2.1 Two-Photon Absorption

In the type I and II resonance enhancement schemes, small two-photon detunings are used to obtain large $\chi^{(3)}$ values. Because of such near resonances, the probability of two-photon absorption (TPA) can be very significant. As in the single-photon absorption case, two-photon absorption can reduce conversion efficiency due to pump attenuation, dynamic phase mismatch, and thermal defocusing. Thus, it is clear that a compromise between large $\chi^{(3)}$ enhancement and two-photon absorption should be considered.

For relatively small TPA, the attenuation parameter, $a^{(2)}_L$, is defined by

$$a^{(2)}_L \approx 1 - I_p(L)/I_p(0) \quad (89)$$

In the case of self-absorption, the attenuation parameter at the pump frequency, ω_p , is given by:

$$a^{(2)}_L = \frac{3}{2} \omega_p \tau_p^2 [NL I_p(0)] [\chi_p^{TPA}(\omega_p)] \quad (90a)$$

where
$$\chi_p^{TPA}(\omega_p) = \text{Im } \chi_p^{(3)}(\omega_p, -\omega_p, \omega_p) \quad (90b)$$

If photons of unequal frequencies cause TPA, the induced absorption at ω is characterized by:

$$a^{(2)}_L = 3 \omega_p \eta^2 \sum_j [NL I_j(0)] [\chi_p^{TPA}(\omega_j)] \quad (91a)$$

where
$$\chi_p^{TPA}(\omega_j) = \text{Im } \chi_p^{(3)}(\omega_p, -\omega_j, \omega_j) \text{ for } j \neq p \quad (91b)$$

A numerical estimate for $a^{(2)}_L$ at typical operating conditions can be obtained by assuming $\omega_p = 3.772 \times 10^{14}$ rad/sec (i.e., 2000 cm^{-1}), $N = 10^{26} \text{ m}^{-3}$, $L = 1 \text{ m}$, and $I_p(0) = 5 \times 10^{12} \text{ W/m}^2$. A representative value for (two-photon resonant) χ_p^{TPA} is $10^{-34} \text{ cm}^6/\text{erg}$ which is equivalent to $1.235 \times 10^{-59} \text{ MKS}$. With these parameters, $a^{(2)}_L$ is equal to 0.498, or nearly half of the pump radiation is absorbed. Therefore, two-photon absorption is a significant efficiency limiting process if χ_p^{TPA} values are on the order of $10^{-34} \text{ cm}^6/\text{erg}$. For the CO laser frequencies, calculations show that χ_p^{TPA} values approach this magnitude only in the type II scheme.

4.2.2 Quadratic Kerr Effect

Another process intimately related to TPA is quadratic Kerr effect which causes intensity dependent refractive index variations through the real part of $\chi_p^{(3)}(\omega_p, -\omega_p, \omega_p)$. The principal effect of this process involves phase shifts along the direction of propagation, which can cause breaking of phase-matching. For a nonuniform beam intensity, the refractive index variations also lead to beam divergence (Kerr defocusing). However, since beam uniformity can be controlled to a certain extent, the Kerr phase shifts are inherently more important.

The definition of the Kerr phase shift at the pump frequency is given by

$$(\Delta kL)_{\text{Kerr}} = \frac{3}{4} \omega_p \eta^2 [NL I_p] [\chi_p^{\text{Kerr}}(\omega_p)] \quad (92a)$$

where
$$\chi_p^{\text{Kerr}}(\omega_p) = \text{Re } \chi_p^{(3)}(\omega_p, -\omega_p, \omega_p) \quad (92b)$$

In the presence of other pump frequencies, the Kerr phase shift at ω_i is defined by

$$(\Delta k L)_{\text{Kerr}} = \frac{3}{2} \omega_i \eta^2 \sum_j [NL I_j] [\chi_i^{\text{Kerr}}(\omega_j)] \quad (93a)$$

where
$$\chi_i^{\text{Kerr}}(\omega_j) = \text{Re } \chi^{(3)}(\omega_i, -\omega_j, \omega_j) \quad i \neq j \quad (93b)$$

The above expression also describes the Kerr phase shift at the generated frequencies, ω_s , when ω_s is substituted for ω_i . In the case of SFG, all phase shifts due to various frequency combinations must be summed using (93a, b).

Since the quadratic Kerr effect vanishes (aside from small nonresonant contributions) at the exact two-photon resonance, the Kerr phase shifts can be made negligible, in principle, by an appropriate choice of pump frequencies. However, for CO frequency tripling, the two-photon detunings are generally non-zero. Thus, considerable phase shifts may be encountered. For example, if the operating conditions for the TPA calculation in the previous section are assumed and if the value of the Kerr nonlinearity at the pump frequency is assumed to be $5 \times 10^{-35} \text{ cm}^6/\text{erg}$ (i.e., peak of χ^{Kerr} when $\chi^{\text{TPA}} = 10^{-34} \text{ cm}^6/\text{erg}$ on resonance), the resulting phase shift is 0.125 radian. While this shift is smaller than π , the predicted phase-matched efficiency is only 4.7% (neglecting pump attenuation) if the magnitude of χ^{THG} were equal to χ^{Kerr} . This suggests that a large ratio of $|\chi^{\text{THG}}|/|\chi^{\text{Kerr}}|$ is desirable in order to maximize the THG efficiency without the Kerr induced phase mismatches.

In the type I resonance enhancement scheme, χ^{Kerr} can be calculated with the $\chi^{(3)}$ code. For the line selected CO laser frequencies $|\chi_p^{\text{Kerr}}(\omega_p)|$ values are typically two orders of magnitude larger than $|\chi^{\text{THG}}|$. In contrast $|\chi_s^{\text{Kerr}}(\omega_p)|$ values are an order of magnitude smaller than $|\chi^{\text{THG}}|$. These observations indicate that the Kerr induced phase mismatches at the pump frequencies are likely to limit the THG efficiencies in the type I scheme.

The role of the Kerr induced phase mismatches in the type II scheme is important due to the fact that all the third order processes are related through a common two-photon resonance enhancement. For example, if the detuning is large with respect to the linewidth, $|\chi^{\text{Kerr}}|$ is equal to $|\chi^{\text{THG}}|/3$. On the other hand, at

exact two-photon resonance ($\Delta\omega = 0$), χ^{Kerr} vanishes and $|\chi^{\text{THG}}|$ is equal to $3 \times |\chi^{\text{TPA}}|$. At intermediate detunings, both the Kerr phase shift and TPA pump attenuation must be considered together. Such a treatment⁴³ has shown that high efficiencies are possible with phase shifts close to $\pi/2$ while holding TPA losses to about 20%. Although the $\chi^{(3)}$ calculations for the type II scheme indicate phase shifts much smaller than $\pi/2$ at the CO laser pump frequencies due to relatively large detunings, analysis shows that if a near two-photon resonance can be achieved on a Raman-active Q-branch transition, the desired phase shifts are feasible. This point will be discussed further in connection with multiline SFG in HD.

In the type III resonance enhancement scheme, quadratic Kerr effect at the pump and the generated frequencies can be expected to be small. This is one of the advantageous features of the scheme when it was considered initially. A further analysis has shown that the Kerr effect introduces a level shift⁴⁴ of the three-photon resonance according to

$$\delta\omega \sim - \frac{|\mu|^2 \eta I_p}{\hbar^2 \Omega} \quad (94)$$

where Ω is the vibronic transition frequency and μ is the associated matrix between the vibronic state and the $v = 2$ level of the ground electronic state. In principle, all such transitions must be included in calculating the level shift, but approximation based on a single strong transition yields an order of magnitude estimate of 10^{-2} cm^{-1} at the typical operating conditions. Since this is a small shift relative to the transition linewidth, resonance enhancement is not affected appreciably. Also, the Kerr induced phase mismatch can be estimated using the following relations:

$$(\Delta k L)_{\text{Kerr}} = \frac{3\omega_p \Delta n L}{n} \quad (95a)$$

with

$$\Delta n \sim - \frac{N |\mu_{20}|^2 \delta\omega}{\hbar (\Delta\omega)^2} \quad (95b)$$

where μ_{20} represents the first overtone transition matrix element and $\Delta\omega$ is the detuning which is assumed to be large compared to the linewidth. Substituting representative parameters of the type III molecules into the above expressions yields a phase shift of 0.03 radian if $\delta\omega = 10^{-2} \text{ cm}^{-1}$ and $\Delta\omega = 1 \text{ cm}^{-1}$ ($1.886 \times 10^{11} \text{ rad/sec}$) are used. Thus, breaking of the phase-matching condition due to quadratic Kerr effect is not believed to be a serious limitation in the type III scheme.

4.2.3 Stimulated Raman Scattering

Stimulated Raman scattering (SRS) in molecular gases may involve vibrational and/or rotational Raman transitions. In the vibrational SRS process IR frequencies up-converted via THG or SFG become the "pump" radiation. In the rotational SRS process, both the pump and the up-converted radiation can act as source terms for amplifying the respective Stokes radiation. In either SRS processes, the THG and SFG efficiencies will be limited through a competition of frequency conversion processes.

A key parameter, which indicates when the SRS processes become important, is the stimulated Raman gain coefficient g_s . This parameter is defined by:⁴⁵

$$g_s = \frac{4 \Delta N \lambda_s^2}{\gamma_R} \left(\frac{I_p}{\hbar \omega_p} \right) \left(\frac{d\sigma}{d\Omega} \right)_\parallel^p \quad (96)$$

where

- ΔN = population density difference
- λ_s = Stokes radiation wavelength
- γ_R = Raman transition linewidth (FWHM) in rad/sec
- I_p = pump intensity
- ω_p = pump frequency in rad/sec
- $\left(\frac{d\sigma}{d\Omega} \right)_\parallel^p$ = differential Raman scattering cross section for the pump radiation

The empirical values of the various parameters are generally available, but the cross section data are usually measured for the Stokes radiation in the visible region,^{30,34} These data can be scaled to the IR frequencies by making use of the ω_s^4 dependence of $(d\sigma/d\Omega)^s$ and the relationship

$$\left(\frac{d\sigma}{d\Omega} \right)_\parallel^p = \left(\frac{d\sigma}{d\Omega} \right)_\parallel^s \left(\frac{\omega_p}{\omega_s} \right) \quad (97)$$

Substituting the expression (97) into (96), one obtains

$$g_s = \frac{16 \pi^2 \Delta N c^2 \omega_s}{\hbar \gamma_R} \left[\omega_s^{-4} \left(\frac{d\sigma}{d\Omega} \right)_\parallel^s \right] I_p \quad (98)$$

where the quantity inside the brackets is nearly invariant at Stokes frequencies in the visible and IR regions. Thus, by evaluating the invariant quantity from visible Raman scattering data, Raman gain coefficients can be calculated for the IR region. Table 23 lists the results of the calculations based on a ΔN value of 1 amagat ($2.69 \times 10^{25} \text{ m}^{-3}$) for the vibrational SRS gain at an intensity of 1 GW/cm^2 (10^{13} W/m^2). In these calculations the pump frequency is assumed to be 6000 cm^{-1} . Since not all cross section data were available, g_s estimates for the deuterated molecules (i.e., HD, DC₂, DBr, and DF) were scaled from those of the normal species by the ratio of the Stokes frequencies.

The threshold gain for Raman oscillation is usually considered to be $g_s L = 30$. For practical device lengths, the g_s values in Table 23 indicate that vibrational SRS oscillation can be regarded as a small effect in all the molecules except for H₂. The hydrogen gas is a special case in which g_s increases with higher pressures (up to 20 amagats). For example, at 8 amagats, the linewidth is the same as that at 1 amagat,³¹ thereby increasing the g_s value by a factor of 8.

Another effect of vibrational SRS is Raman amplification of the pump radiation by the generated radiation. By amplifying the pump radiation the generated radiation transfers the up-converted power back into the pump radiation. This process acts as a stabilizing mechanism to establish a steady-state efficiency condition. An analysis of this THG/SRS interaction shows that a characteristic parameter is given by:⁴³

$$\kappa = \left| \frac{\chi_{\text{THG}}}{6\chi_{\text{SRS}}} \right|^2 \left[1 + \left(\frac{\Delta\omega}{\gamma_R} \right)^2 \right] \quad (99)$$

When the value of κ is close to or larger than unity, the SRS process is not important; efficiency will be limited by other processes. However, if $\kappa \ll 1$, then the efficiency limit is equal to the value of κ . For the type I scheme molecules, $\chi^{(3)}$ code calculations yield $|\chi_{\text{SRS}}|$ values which are an order of magnitude smaller than $|\chi_{\text{THG}}|$. This indicates that vibrational Raman amplification in the type I scheme is not a significant limiting process. In contrast, $\kappa = 0.25$ on resonance ($\Delta\omega = 0$) in the type II scheme, which suggests that vibrational Raman amplification is an important factor governing the maximum THG efficiency.

TABLE 23. VIBRATIONAL RAMAN GAIN COEFFICIENTS

Molecule	Raman Data ($\lambda_p = 488.0 \text{ nm}$) @ STP					IR SRS Gain	
	$\omega_s (\text{cm}^{-1})$	$(d\sigma/d\Omega)_R^S (\text{cm}^2)$	$\omega_R (\text{cm}^{-1})$	$\gamma_R (\text{cm}^{-1})$	$\gamma_R (\text{cm}^{-1})$	$\omega_s (\text{cm}^{-1})$	$g_s (\text{m}^{-1})$
[Transition]							
CO [Q]	18346.8	3.3×10^{-31}	2145	0.0877		3855	0.37
NO [Q]	18614.8	8.9×10^{-32}	1877	0.057		4123	0.15
HBr [Q]	17933.8	2.3×10^{-30}	2558	0.13		3442	1.7
HCl [Q]	17605.8	1.4×10^{-30}	2886	0.248		3114	0.53
HF [Q]	16529.8	4.9×10^{-31}	3962	0.5		2038	0.077
H ₂ [Q(1)]	16336.8	5.3×10^{-31}	4155	0.014		1845	2.8
HD [Q(1)]	-	-	3628.2	0.05		2372	1.0
DF [Q]	-	-	2904	0.466		3096	0.13
DCl [Q]	-	-	2091	0.248		3909	0.67
DBr [Q]	-	-	1839	0.13		4161	2.1

Rotational Raman scattering is a third-order process that does not share any of the resonance enhancement paths used in the THG and SFG processes. As such, the rotational SRS process represents a potential competing loss mechanism for the pump and the generated radiation. As in the vibrational SRS case, a key parameter in the rotational SRS is the Raman gain coefficient. Expression (98) is still a valid formula for calculating g_s , but ΔN must be defined in terms of an actual population difference because of much smaller Raman shifts in the rotational case. A formula for ΔN as a function of the rotational quantum number of the initial state is given by

$$\Delta N_J = N(f_J - f_{J+2}) \quad (100)$$

where N = total number density
 f_J = fraction of molecules in the initial state
 f_{J+2} = fraction of molecules in the final state

Under equilibrium conditions at a temperature T , the population distribution can be expressed by:

$$f_{J'} = \frac{2J' + 1}{Q} e^{-E(J')/kT} \quad (101)$$

where $Q \approx kT/hc B_0$ (rotational partition function)

and $E(J') \approx hc B_0 J' (J' + 1)$

It is evident from the above formulas that population differences become smaller with smaller values of B_0 . For example, $J = 6 \rightarrow J = 8$ S(6) transition in CO at room temperature has a calculated value of $\Delta N_{J=6}/N = 1.41 \times 10^{-3}$. Since the rotational Raman cross sections are roughly comparable to the vibrational Raman cross sections,³⁰ the g_s values for the rotational SRS are smaller than the vibrational Raman gains by the $\Delta N/N$ ratio. A survey of the candidate molecules shows that only H_2 has sufficiently large rotational Raman shifts to make $\Delta N/N$ ratios close to those of the vibrational Raman shifts.

Recent experimental demonstrations^{46,47} of rotational SRS in H_2 ($S_0(0)$) using CO_2 laser radiation indicate that rotational Raman shifting can be a very

efficient IR frequency conversion process. Based on the information given in these experiments, the rotational Raman gain coefficient is predicted to be in the range of 11 to 20 m^{-1} at a CO laser pump (single-line) intensity of 1 GW/cm^2 . The predicted value of g_s implies efficient rotational Raman shifting for interaction lengths in excess of 3 m. Furthermore, the H_2 ($S_0(1)$) transition may also be important at room temperature with a g_s value comparable to that of the $S_0(0)$ transition.

Although H_2 presents a potentially serious efficiency limitation due to rotational SRS, other type II molecules (HD and HF) appear to have a lesser problem. This is because of smaller ΔN values and larger Raman linewidths in HD and HF compared to that of H_2 , both of which reduce the g_s values sufficiently to prevent Raman oscillation.

4.2.4 Three-Photon Absorption

Three-photon absorption (ThPA) is a nonlinear process governed by a fifth-order susceptibility. Because ThPA is a higher-order effect its presence is negligible unless exceptionally small frequency detunings or high pump intensities are employed. Thus, the only resonance enhancement scheme amenable to ThPA is the type I scheme with near-resonant detunings at one-, two-, and three-photon resonances.

In the near-resonant case, three-photon transition probability per unit time can be written as⁴⁸

$$W(\text{ThPA}) = \frac{\pi g_L(3\omega) \eta^3 I^3}{256 \hbar^6 n^3} \left(\frac{\mu_{32} \mu_{21} \mu_{10}}{\Delta\omega_1 \Delta\omega_2} \right)^2 \quad (102)$$

where $g_L(3\omega)$ is the ThPA line shape function and all other parameters have their usual meanings. This expression can be compared with two-photon transition probability per unit time as given by:⁴⁸

$$W(\text{TPA}) = \frac{\pi g_L(2\omega) \eta^2 I^2}{32 \hbar^4 n^2} \left(\frac{\mu_{21} \mu_{10}}{\Delta\omega_1} \right)^2 \quad (103)$$

If the two-photon detuning is substantially larger than the linewidth, $g_L(2\omega)$ can be approximated by $\Gamma_2/\pi\Delta\omega_2^2$. Similarly, $g_L(3\omega)$ is approximately equal

to $\Gamma_3/\pi\Delta\omega_3^2$ when $\Delta\omega_3^2 \gg \Gamma_3^2$. With these approximations, the ratio of the transition probabilities may be expressed as:

$$\frac{W(\text{ThPA})}{W(\text{TPA})} = \frac{\Gamma_3}{\Gamma_2} \left(\frac{\mu_{32}}{\Delta\omega_3} \right)^2 \frac{\eta I}{8n\hbar^2} \quad (104)$$

For most type I molecules, the Γ_3/Γ_2 ratio is close to unity and $|\mu_{32}|$ is on the order of 0.1 debye. Using $I = 1 \text{ GW/cm}^2$ (10^{13} W/m^2) and $\Delta\omega_3 = 1 \text{ cm}^{-1}$ ($1.886 \times 10^{11} \text{ rad/sec}$), expression (104) yields a ratio of 0.13. Since three-photon detunings in the type I molecules are generally larger than 1 cm^{-1} for various combinations of CO laser frequencies, the above ratio indicates that ThPA effects are an order of magnitude smaller than those of TPA.

4.2.5 Gas Breakdown

Laser induced gas breakdown is a well known phenomenon with high peak power laser beams and is a major consideration in the analysis of efficiency limitations. Since beam propagation is severely affected when gas breakdown occurs, the critical intensity at which the breakdown is initiated sets the upper limit on the operating intensities for a frequency converter.

A literature survey showed that laser induced gas breakdown data are not available for the case of CO laser radiation interacting with the particular THG candidate molecular gases. Most of the experimentally observed breakdown intensities in the IR are reported for the $10 \mu\text{m}$ radiation. For example, at 3 atmospheres of H_2 the reported experimental conditions⁴⁶ imply a breakdown power density of 2.8 GW/cm^2 at $10 \mu\text{m}$. The corresponding breakdown energy density would be 196 J/cm^2 . If the quadratic frequency dependence of breakdown intensity⁴⁹ is assumed, the $10 \mu\text{m}$ radiation data suggest a value of 11 GW/cm^2 for the $5 \mu\text{m}$ radiation provided all other parameters are unchanged. However, since semi-empirical models^{49,50} of gas breakdown predict different behavior for short and long laser pulse lengths, estimates using scaling arguments based on $10 \mu\text{m}$ data should be regarded as a rough indication. Therefore, breakdown intensities based on the presently available information may be reasonably expected to be in the range of 1 to 10 GW/cm^2 . These intensity limits in turn imply minimum values of χ^{THG} for efficient conversion. At the lower limit, $|\chi^{\text{THG}}|$ values in excess of $10^{-34} \text{ cm}^6/\text{erg}^1$ are necessary, which establishes a criterion for selecting particular candidate molecules.

4.2.6 Pump Depletion

Efficiency limitation analysis so far has been presented with the assumption that pump radiation does not change appreciably in order to illustrate various limitations. In reality, frequency conversion processes do involve pump depletion by definition, but an analytical treatment becomes complex because of nonlinear coupled differential equations governing the generation and depletion processes. In general, these equations do not have closed form solutions and therefore require numerical methods for analyzing the effects of pump depletion. However, rather than computing various numerical solutions encompassing all aspects of interacting processes, a simple model including only the THG and pump depletion processes has been analyzed. This approach has an advantage of yielding an analytical solution to aid in understanding the efficiency when there is substantial pump depletion. The equations of this model, neglecting phase mismatches, can be cast in the following form:

$$\frac{dE_3}{dz} = \beta E_1^3 \quad (105)$$

$$\frac{dE_1}{dz} = -\beta E_1^2 E_3 \quad (106)$$

$$\text{where } \beta = \frac{i \omega_3 \eta_N \chi^{\text{THG}}}{8 \eta_3}.$$

Combining the Equations (105) and (106) yields the statement of energy conservation

$$E_1^2(0) - E_1^2(Z) = E_3^2(Z) \quad (107)$$

Substitution of this relation into (105) and a direct integration gives the conversion efficiency ϵ :

$$\begin{aligned} \epsilon &= \frac{E_3(L)^2}{E_1(0)^2} \\ &= \frac{\eta_0}{1 + \eta_0} \end{aligned} \quad (108)$$

where

$$\eta_0 = (\beta E_1^2(0) L)^2 \propto |\chi^{\text{THG}}|^2 (NIL)^2$$

For small pump intensities, $\eta_0 \ll 1$, and the efficiency is approximately given by the value of η_0 , which is exactly the efficiency one would obtain by integrating (105) assuming no pump depletion. Hence, the efficiency figures

calculated without pump depletion are still useful in predicting the actual efficiencies provided that expression (108) is used. The relation (108) also shows that efficiencies below 10% can be calculated quite accurately without including pump depletion effects.

At very high pump intensities for which $\eta_0 > 1$, THG conversion efficiency is no longer increasing quadratically with pump intensity. Thus, pump depletion leads to an efficiency saturation behavior as described by (108). Because SFG and THG are basically related processes, similar saturation effects can be expected for SFG efficiencies.

4.3 Optimum Scheme







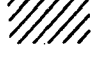

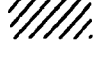
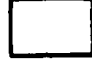









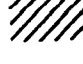
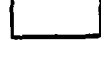












The discussions of various efficiency limiting processes and the calculations of key parameters in the previous sections can be summarized qualitatively as shown in Table 24. When a particular process causes a substantial decrease (e.g. more than 10%) in the actual efficiency relative to the predicted efficiency in the absence of the process, that process is considered to be significant. If the effect leads to efficiency losses on the order of a percent for some candidate molecules of a given enhancement scheme, then the limiting process is considered moderate. Processes which are predicted to produce less than one percent changes in the conversion efficiency are regarded as small, and those with no measurable consequences are considered negligible. The table aids in illustrating the essential efficiency limiting characteristics for each of the three resonance enhancement schemes. Based on these characteristics, the following observations can be made:

In the type I resonance enhancement scheme, pump absorption leading to dynamic phase mismatches is found to be the primary efficiency limiting process. Since this scheme requires near-resonant conditions at one-, two-, and three-photon detunings, the pump absorption is always present and inherently restricts the application of the type I scheme to short pump pulses.

The type II scheme avoids dynamic phase mismatch caused by pump absorption. Other competing nonlinear processes become significant at the high pump intensities required for efficient conversion, however. Although two-photon absorption, quadratic Kerr effect, and stimulated Raman scattering ultimately

TABLE 24. EFFICIENCY LIMITATION ANALYSIS

SUMMARY

PROCESS	RESONANCE ENHANCEMENT SCHEME		
	TYPE I	TYPE II	TYPE III
NONLINEAR EFFECTS:			
● Two-Photon Absorption			
● Quadratic Kerr Effect			
● Stimulated Raman Scattering (Vibrational)			
● Stimulated Raman Scattering (Rotational)			
● Three-Photon Absorption			
● Gas Breakdown			
● Saturation			
LINEAR EFFECTS:			
● Absorption Loss at Pump Frequency			
● Absorption Loss at Sum Frequency			
● Population Transfer-Induced Phase Mismatch			
● Thermal Defocusing			

 Negligible
  Small
  Moderate
  Significant

limit the efficiency, near unity THG and SFG conversion efficiencies are predicted under optimum conditions. The parameters that govern these conditions are the two-photon resonance frequency and the values of Kerr-induced phase shifts.

The type III scheme analysis and the $\chi^{(3)}$ calculations show that relatively small conversion efficiencies can be expected. The principal efficiency limitation in this scheme is optical gas breakdown at high pump intensities. The high pump intensities are necessary to compensate for the relatively small nonlinear susceptibilities calculated for candidate molecules of this scheme.

In view of the efficiency limiting properties of the three enhancement schemes, the type II scheme provides a most promising technique for up-converting CO laser frequencies. In particular, H_2 and HD have an added advantage of extremely low dispersion in the infrared region. The refractive indices for H_2 can be calculated from a Sellmeier formula,⁵¹ and the calculated THG and SFG coherence length (distance at which $\Delta kL = \pi$) at 1 amagat is approximately 300 cm. This value is not very sensitive to the range of the line-selected CO laser frequencies, which permits simultaneous phase-matching for various combinations of pump frequencies. Since H_2 and HD are essentially identical in their electronic properties, dispersion properties can be expected to be similar. Thus, both H_2 and HD appear to be most suited for multiline THG or SFG.

5.0 MULTILINE THG AND SFG ANALYSIS

The CO laser output consists of several frequencies, as elucidated in Section 3.4. Thus, efficient THG and SFG processes for a number of lines are required. The phase-matching requirement for various frequency combinations is an important consideration in multifrequency THG and SFG. For example, it is desirable to phase-match all of the CO laser lines referred to in Section 3.4 for THG in a given gas mixture. The THG and SFG conversion efficiencies of the various frequency combinations may differ from one particular set to another because of the frequency dependence of the nonlinear susceptibility. Therefore, a scheme in which $\chi^{(3)}$ is near optimum and relatively insensitive to changes in the pump frequencies is needed. In the following section, calculations on candidate molecules for each of the three resonance enhancement schemes are discussed in relation to the criteria outlined above. Accordingly, an appropriate scheme for SFG is suggested.

5.1 Efficient THG and SFG Optimization

Efficient THG and SFG of the line selected CO laser frequencies requires optimization of the nonlinear susceptibility and phase-matching properties and suppression of the efficiency limiting processes. The nonlinear susceptibility calculations and the efficiency limitation analysis show that the type II resonance enhancement scheme allows efficient multiline frequency up-conversion under appropriate conditions in H₂ or HD. These molecules have extremely small dispersion and absorption in the infrared and have relatively high peak values of $\chi^{(3)}$ on resonance. The $\chi^{(3)}$ frequency dependence also allows SFG for a number of different pump frequencies when one or more pairs of frequencies are two-photon resonant.

One important factor to consider in the type II scheme is the effect of competing nonlinear processes. In particular, stimulated rotational Raman scattering can be a dominant frequency conversion process under certain conditions. Several reports of efficient Raman shifting of CO₂ laser radiation in hydrogen indicate the significance of this competing effect.^{46,47}

Two important aspects of stimulated Raman scattering (SRS) should be noted. First, SRS represents a loss mechanism for the pump radiation and thereby decreases the THG and SFG efficiency. Second, frequencies shifted by SRS may

participate further in other nonlinear processes including induced two-photon absorption and sum frequency generation.

A survey calculation of the Raman-shifted multiline CO frequencies in H_2 and HD shows that induced TPA and SFG may indeed occur. Analysis of the χ^{SFG} values for these frequencies indicates that susceptibilities in the neighborhood of $10^{-34} \text{ cm}^6/\text{erg}$ are possible with certain combinations of the pump and the shifted frequencies. Figure 9 shows the normalized $|\chi^{SFG}|$ as a function of two-photon resonance frequency detuning for HD Q(1) transition at various gas densities. Figure 10 illustrates the corresponding curves for the normalized $|\chi^{SFG}|$ as a function of gas density at certain detunings. The scale factor for the actual value of $|\chi^{SFG}|$ is $3.14 \times 10^{-34} \text{ cm}^6/\text{erg}$. Figure 11 shows the normalized χ^{Kerr} and χ^{TPA} as a function of frequency detuning, which are obtained from the real and imaginary parts according to the equations in Table 9.

The actual frequency detunings ($\Delta\omega_0$) obtainable for HD resonances from the certain combinations of the pump and the Raman shifted frequencies in H_2 (354.381 cm^{-1} shift²⁹) are in the range of 0.2 to 1 cm^{-1} . For example, P(11) and P(12) of [5-4] give $\Delta\omega_0 = 0.328 \text{ cm}^{-1}$ for the HD Q(0) resonance, and P(9) and P(13) of [4-3] yield $\Delta\omega_0 = 1.012 \text{ cm}^{-1}$ for the HD Q(1) resonance. P(11) [6-5] and P(12) [4-3] also approach the Q(0) resonance with $\Delta\omega_0 = 0.291 \text{ cm}^{-1}$. These detunings lead to χ^{SFG} values of $10^{-34} \text{ cm}^6/\text{erg}$. This suggests that efficient SFG may occur if phase-matching requirements can be satisfied.

5.2 Two-Step Frequency Conversion

The results of the multiline THG and SFG analysis suggest that an efficient multiline CO laser frequency up-converter may be possible with the use of a Raman shifting as an intermediate step. The Raman shifting in H_2 converts a part of the total pump radiation into coherent radiation near $6 \mu\text{m}$. The frequencies of the remaining pump radiation and the shifted frequencies add to yield the two-photon resonances in HD. This two-step process is schematically illustrated in Figure 12. The pump and the shifted frequencies are represented by $\{\omega\}$ and $\{\omega'\}$, respectively. The generated sum frequencies are of the form $\omega_s = 2\omega + \omega'$ or $2\omega' + \omega$ and are denoted by $\{\omega_s\}$.

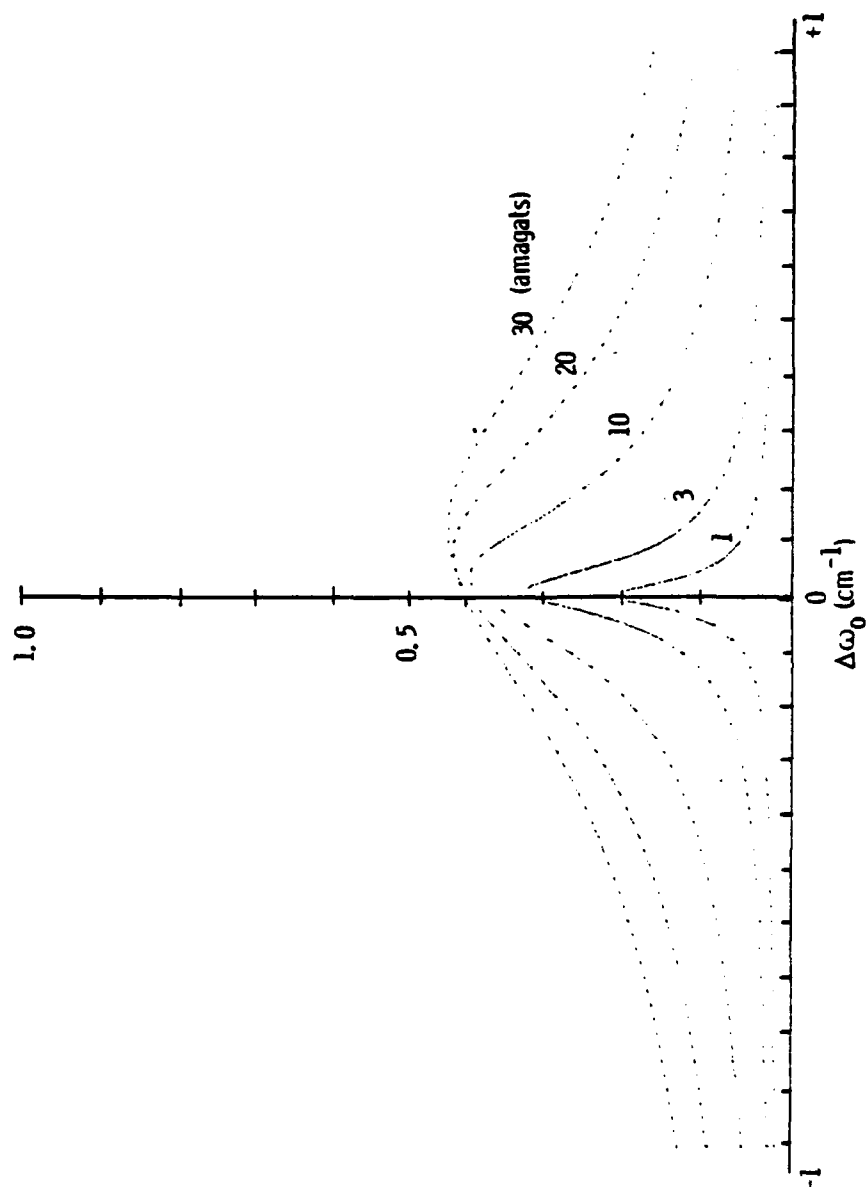


FIGURE 9. NORMALIZED $|\chi^{SFG}|$ VS HD Q(1) TWO-PHOTON RESONANCE FREQUENCY DETUNING

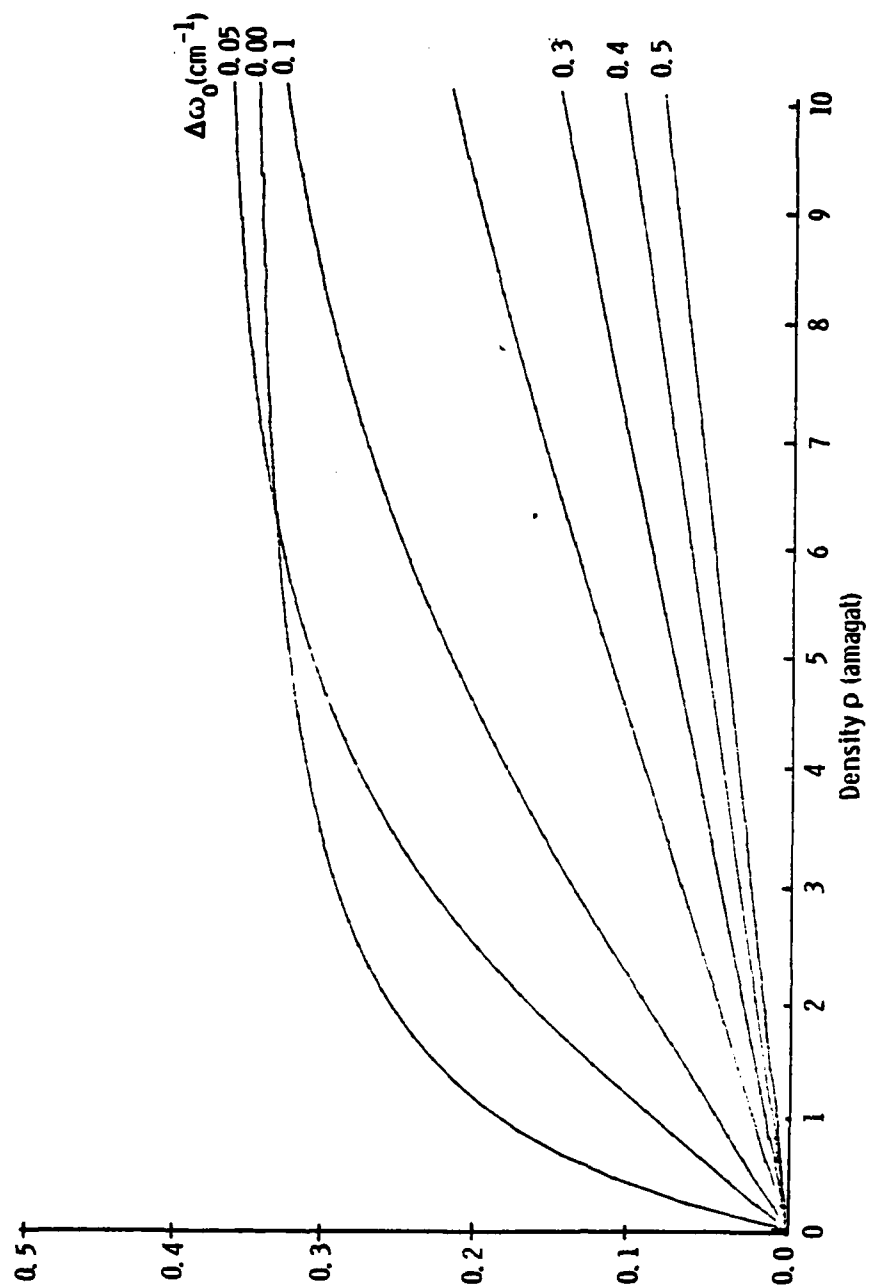


FIGURE 10. NORMALIZED $|x^{SFG}|$ VS DENSITY

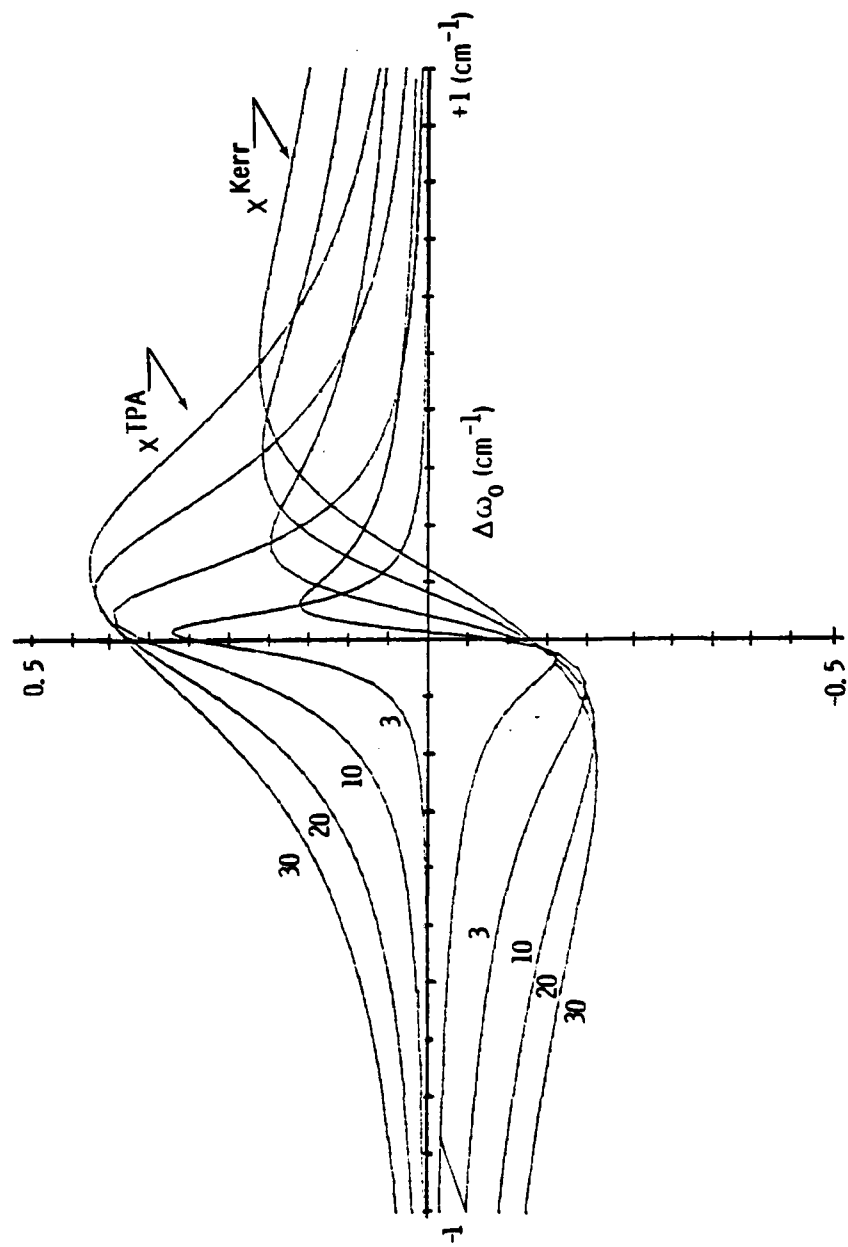
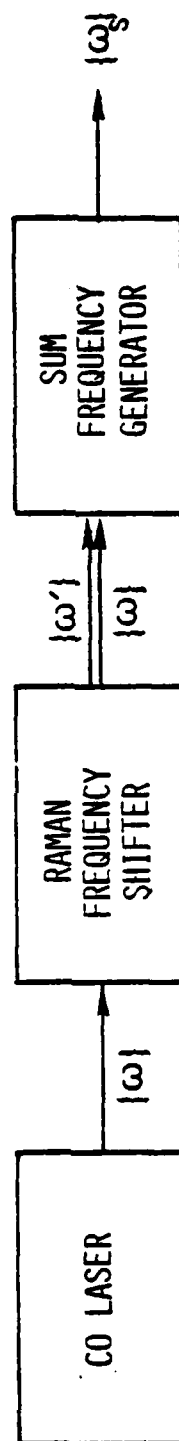


FIGURE 11. NORMALIZED χ_{Kerr} AND χ_{TPA} VS HD Q(1) TWO-PHOTON RESONANCE FREQUENCY DETUNING



$$\omega_S = 2\omega + \omega' \text{ AND } 2\omega' + \omega$$

FIGURE 12. SCHEMATIC OF TWO-STEP CO LASER SUM FREQUENCY GENERATION

6.0 EXPERIMENTAL PROGRAM

The results of this study indicate that frequency up-conversion according to the type II resonance enhancement scheme in HD may be potentially efficient and warrants further investigation. Experimental data are needed to verify theoretical predictions presented in this report. Of particular interest is the frequency dependence of the conversion efficiency and of the phase-matching properties of HD. This may be used to determine the optimum parameters of the nonlinear medium for multifrequency CO laser frequency up-conversion.

6.1 Approach

The third-order susceptibility calculations and efficiency limitation analysis indicate that two-photon resonantly enhanced sum frequency generation in HD is the most promising approach to up-convert multiline CO laser frequencies. In order to verify this feasibility, an experimental investigation of SFG in HD is suggested. The investigation should consist of first setting up an experimental facility to generate tunable and fixed IR frequencies in the 5-6 μm region and then performing parametric SFG experiments using the generated frequencies. These IR frequencies are relevant to the two-step frequency conversion process described in Section 5.2.

6.2 Experimental Facility

An IR source facility based on a Nd:YAG laser system operating at ten pulses per second would be a suitable choice because of high data acquisition rate. Figure 13 shows a block diagram of the experimental setup including a fixed and a tunable IR source. The fixed IR frequency at 6.2 μm can be obtained by vibrational Raman frequency shifting of the Nd:YAG laser output in H_2 and HD. Figure 14 shows a schematic layout of the fixed IR source. The tunable IR frequency can be generated by difference frequency mixing⁵² of the second harmonic of the Nd:YAG laser output and a tunable dye laser output near 0.596 μm . Alternatively, a dye output at 0.690 μm may be Raman shifted three times in H_2 to yield a tunable IR output. Figure 15 shows the two possible configurations of the tunable IR source. The tunable IR frequency is near 2015 cm^{-1} (4.96 μm) so that the sum of the tunable and the fixed IR frequencies matches the two-photon Q-branch resonances in HD. The operating conditions of the IR source facility are summarized in Table 25.

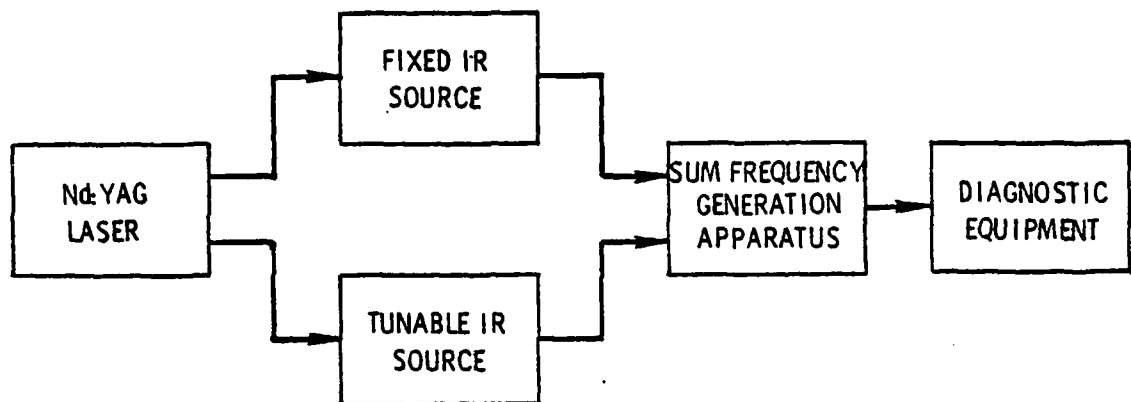


FIGURE 13 SUM FREQUENCY GENERATION EXPERIMENT BLOCK DIAGRAM

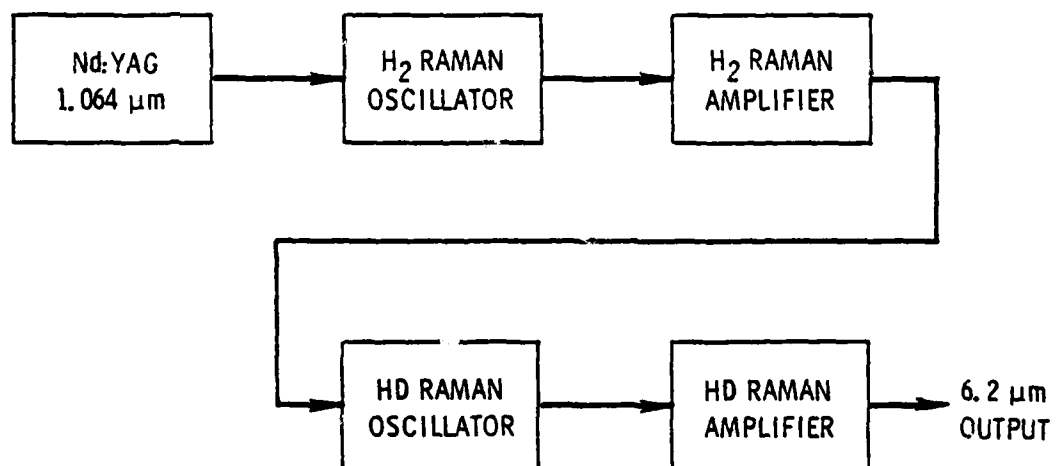


FIGURE 14. FIXED IR SOURCE BLOCK DIAGRAM

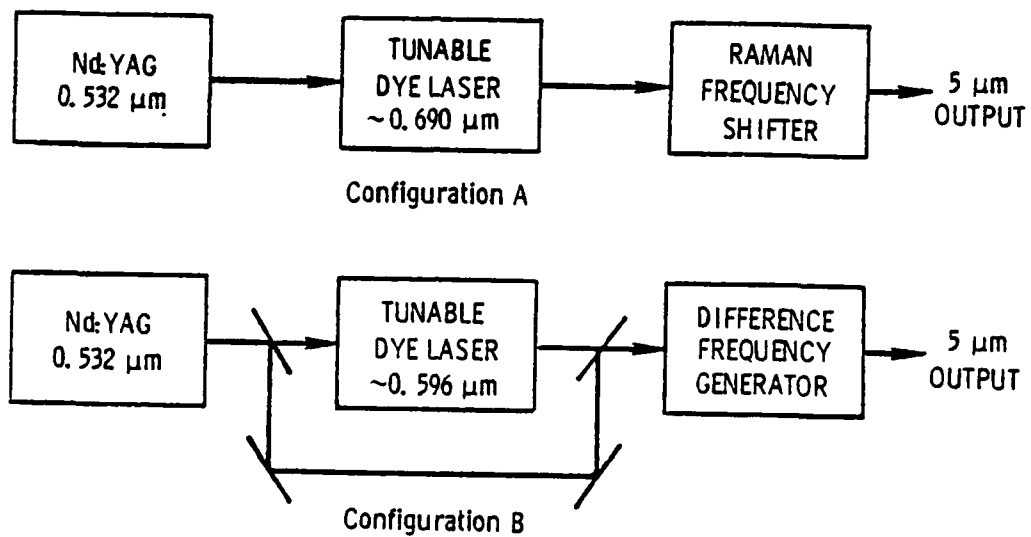


FIGURE 15. TUNABLE IR SOURCE BLOCK DIAGRAM

TABLE 25. COHERENT IR SOURCE FACILITY

FIXED IR SOURCE

Pump Laser:	Nd:YAG 1.064 μm , 10 pps, 50 MW peak power
Frequency Converter:	Vibrational Raman shifting in H_2 and HD (7783.4 cm^{-1})
IR Output:	~ 5 MW peak power at 6.2 μm

TUNABLE IR SOURCE

Pump Laser:	Nd:YAG Second Harmonic 0.532 μm , 10 pps, 20 MW peak power
Frequency Tuning:	Dye laser oscillator/amplifier ~ 7 MW peak power output at 0.59 μm
Frequency Conversion:	Difference frequency mixing of 0.532 μm and 0.596 μm in LiIO_3
IR Output:	~ 0.02 MW peak power at 4.96 μm

An apparatus for the SFG experiment is shown in Figure 16. It incorporates a cell consisting of a tube filled with several atmospheres of HD at 293 K, two calcium fluoride windows (to seal the ends of the tube) which transmit the pump and the generated radiation, and a gas handling system consisting of valves, gauges, and a vacuum system that controls the cell pressure.

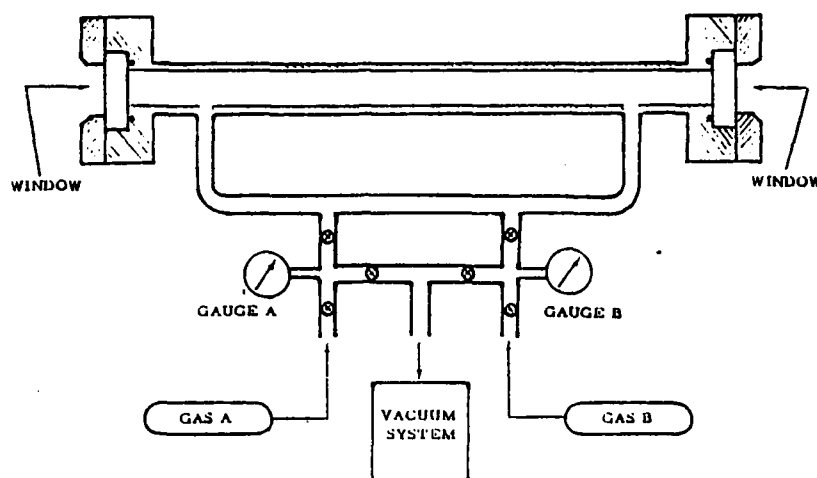


FIGURE 16. SCHEMATIC OF EXPERIMENTAL APPARATUS

6.3 Parametric Study

The parametric study should include conversion efficiency measurements as a function of two-photon resonance frequency detuning, SFG gas pressure, and pump source intensity. From these measurements the SFG nonlinear susceptibilities and the phase-matching properties of the nonlinear medium can be compared with the calculated values.

7.0 CONCLUSION

Detailed analysis and calculations on the feasibility of efficient CO laser frequency tripling have been completed. The results of this study indicate that direct frequency tripling of multiline CO laser output leads to small conversion efficiencies. These efficiencies are primarily dictated by the small nonlinear susceptibilities and the efficiency limiting processes of the molecules surveyed. However, the analysis of the three resonance enhancement schemes has yielded a potentially efficient sum frequency generation scheme in hydrogen molecules if the pump frequencies can satisfy the two-photon resonance condition.

Of the three resonance enhancement schemes investigated, the two-photon resonance (type II) scheme has been found to meet the requirements for efficient multiline frequency up-conversion of the CO laser frequencies. Various efficiency limiting processes found in the two other schemes are minimized in this scheme, and high SFG conversion efficiencies are predicted for a number of pump frequency combinations.

Unfortunately, the efficient CO laser lines do not yield frequency combinations that directly satisfy the strong resonance conditions in H₂ or HD. However, from the analysis of stimulated rotational Raman scattering as a competing efficiency limiting process, the Raman shift in H₂ has been found to generate frequencies which lead to HD two-photon resonances when combined with the original pump frequencies. Because Raman shifting has been demonstrated to be an efficient conversion process, this resonance coincidence provides a method of frequency up-conversion using an intermediate frequency shifting stage to optimize the sum frequency generation efficiencies. With such a two-step conversion process, output wavelengths in the 1.77 and 1.90 μm regions can be obtained.

In order to verify the feasibility of efficient sum frequency generation in HD, and experimental investigation of third-order susceptibility is recommended for future study. The measurement of SFG susceptibilities and phase-matching properties of HD should yield useful parameters for evaluating this molecular medium as a potentially efficient frequency up-converter.

8.0 REFERENCES

1. S. R. J. Brueck and H. Kildal, Appl. Phys. Lett. 33, 928 (1978).
2. S. R. J. Brueck and H. Kildal, Opt. Lett. 2, 33 (1978).
3. H. Kildal, IEEE J. Quant. Electron QE-13, 109 (1977).
4. M. H. Kang, V. T. Nguyen, T. Y. Chang, T. C. Damen, and E. G. Burkhardt, Appl. Phys. Lett. 33, 303 (1978).
5. C. L. Pan, C. Y. She, W. M. Fairbank, Jr., and K. W. Billman, IEEE J. Quant. Electron QE-13, 763 (1977).
6. M. J. Pellin and J. T. Yardley, Appl. Phys. Lett. 29, 304 (1976).
7. P. N. Butcher, Nonlinear Optical Phenomena, Bulletin 200, Engineering Experiment Station, Ohio State University, Columbus, Ohio (1965).
8. G. Herzberg, Molecular Spectra and Molecular Structure: I. Spectra of Diatomic Molecules, Second Edition, (Van Nostrand Reinhold Co., New York, 1950) p. 208.
9. D. B. Keck and C. D. Hause, J. Mol. Spectrosc. 26, 163 (1968).
10. M. Rotenberg, N. Metropolis, R. Bivin, and J. K. Wooten, Jr., "The 3-j and 6-j Symbols," Technology Press, Massachusetts Institute of Technology, Cambridge, Mass. (1959).
11. C. H. Townes and A. L. Schawlow, Microwave Spectroscopy, (McGraw Hill Book Co. Inc., 1955), p. 74.
12. Placzek, The Rayleigh and Raman Scattering, translated from Handbuch der Radiologie, Edited by Erich Marx, Leipzig, Akademische Verlagsgesellschaft VI, 2, (1934) pp. 209-374, UCRL Trans. No. 526(L) by Ann Werbin (1959).
13. R. H. Pantell and H. E. Puthoff, Fundamentals of Quantum Electronics, (Wiley, New York, 1969), pp. 241-242.
14. V. E. Merchant and N. R. Isenor, IEEE J. Quant. Electron. QE-12, 603 (1976).
15. D. Chen, K. Rao, and R. McDowell, J. Mol. Spectry. 61, 71 (1976)
16. J. P. Bouanich, J. Quant. Spectrosc. Radiat. Transfer 17, 636 (1977).
17. J. Bonamy and D. Robert, J. Quant. Spectrosc. Radiat. Transfer 16, 185 (1976).

18. A. Henry, M. F. LeMoal, Ph. Cardinet, and A. Valentin, *J. Mol. Spectry.* 70, 18 (1978).
19. F. P. Billingsley, *J. Mol. Spectry.* 61, 53 (1976).
20. L. L. Abels and J. H. Shaw, *J. Mol. Spectry.* 20, 11 (1966).
21. B. Rosen, *Spectroscopic Data Relative to Diatomic Molecules*, (Pergamon, New York, 1970).
22. F. G. Smith, *J. Quant. Spectrosc. Radiat. Transfer* 13, 717 (1973).
23. A. Rosenberg, A. Lightman, and A. Ben-Rouven, *J. Quant. Spectrosc. Radiat. Transfer* 12, 219 (1972).
24. A. Faqt, D. van Lerberghe, G. Guelachvili, C. Amoit, P. Bernage, and P. Niay, *Mol. Phys.* 32, 955 (1976).
25. R. N. Stocker and A. Goldman, *J. Quant. Spectrosc. Radiat. Transfer* 16, 335 (1976).
26. H. J. Babrov, *J. Chem. Phys.* 40, 831 (1964).
27. G. Herzberg, *Op. Cit.*, pp. 141-144.
28. "Molecular Lasers," *Laser Handbook*, Chemical Rubber Co., pp. 307-310.
29. B. P. Stoicheff, *Can. J. Phys.* 35, 730 (1957).
30. W. R. Fenner, H. A. Hyatt, J. M. Kellam, S.P.S. Porto, *J.O.S.A.* 63, 73 (1973).
31. M. A. Henesian, L. Kulevskii, R. L. Byer, and R. L. Herbst, (Abstract) *Opt. Commun.* 18, 225 (1976).
32. T. Witkowitz and A. D. May, *Can. J. Phys.* 54, 575 (1976).
33. D. V. Webb and K. N. Rao, *J. Mol. Spectry.* 28, 121 (1968).
34. J. M. Cherlow, H. A. Hyatt, S.P.S. Porto, *J. Chem. Phys.* 63, 3996 (1975).
35. R. E. Meredith, *J. Quant. Spectrosc. Radiat. Transfer* 12, 485 (1972).
36. W. Holzer, Y. LeDuff, and K. Altmann, *J. Chem. Phys.* 58, 642 (1973).
37. K. Altmann and G. Strey, *J. Mol. Spectry.* 44, 571 (1972).
38. D. H. Rank, B. S. Rao, and T. A. Wiggins, *J. Mol. Spectry.* 17, 122 (1965).

39. Calculated from Reference 21 and isotope shift.
40. R. N. Sileo and T. A. Cool, J. Chem. Phys. 65, 117 (1976).
41. F. G. Smith and R. E. Meredith, J. Quant. Spectrosc. Radiat. Transfer 14, 385 (1974).
42. R. B. Miles and S. E. Harris, IEEE J. Quant. Electron. QE-9, 470 (1973).
43. E. A. Stappaerts, IEEE J. Quant. Electron QE-15, 110 (1979).
44. E. A. Stappaerts, Phys. Rev. A 11, 1664 (1975).
45. N. Bloembergen, Am. J. Phys. 35, 989 (1967).
46. R. L. Byer and W. R. Trutna, Opt. Lett. 3, 144 (1978).
47. P. Rabinowitz, A. Stein, R. Brickman, and A. Kaldor, Opt. Lett. 3, 147 (1978).
48. R. H. Pantell and H. E. Puthoff, Op. Cit., pp. 141-142.
49. D. C. Smith, J. Appl. Phys. 41, 4501 (1970).
50. C. C. Wang and L. I. Davis, Phys. Rev. Lett. 26, 822 (1971).
51. M. Karplus, J. Chem. Phys. 41, 880 (1964).
52. D. W. Meltzer and L. S. Goldberg, Opt. Commun. 5, 209 (1972).

APPENDIX A: $\chi^{(3)}$ CODE

Program Structure and Performance

The program consists of loops over the vibrational and rotational quantum numbers. Inside these nested loops, subroutines are called and the following steps are performed:

- (1) Calculation of rotational and vibrational terms, and partition functions
- (2) Calculation of rotational populations and all transition frequencies allowed by selection rules
- (3) Calculation of the frequency denominator which occurs in the nested sum over states
- (4) Inclusion of all permutations of the three input frequencies

Several subroutines are called in the course of the program. The structure and function of each of these is relatively simple, and, therefore, will only be described briefly. Subroutine FREQ calculates the frequency denominator and sets up the indices to be printed when a resonance is encountered. Subroutine SUMO provides the contributions to the sum over states of the total angular momentum projected along the molecular axis (OMEGA) when the molecular ground state is spatially degenerate (LAMBDA is not zero).

Matrix elements involving anharmonic oscillator eigenfunctions which are required for inclusion of an upper electronic level in the $\chi^{(3)}$ calculation are calculated in the subroutine LMENTS. The sum over state of the total angular momentum projected along the molecular axis for a spatially degenerate upper electronic level is performed in the subroutine TUMO. Finally, the frequency denominators which involve more than one electronic level are evaluated in subroutine GREQ.

The data items to be input, specified in READ statements at the beginning of the main program, consist of alphanumeric symbols, indicators, spectroscopic constants, and transition moments. The spectroscopic constants may be found in the literature. All input variables should be expressed in cgs units unless otherwise specified. In addition, the program presets all unspecified variables to zero.

In the program, the input variables have been assigned the following names:

LABEL is an alphanumeric array which stores the name of the molecule for which the calculation is performed

NV is the number of vibrational levels used in the calculation

NJ is the number of rotational levels used in the calculation

WE, WEXE, WEYE, WEZE are the familiar vibrational constants: ω_e , $\omega_e x_e$, $\omega_e y_e$, $\omega_e z_e$, respectively

BE, ALPHA, GAMMA, DE, BETA are the usual rotational constants: B_e , α_e , γ_e , D_e , β_e , respectively

AE, DELTA are additional rotational constants which must be specified only if the ground electronic state is spatially degenerate

OMEGAE is the energy of an upper electronic state; this is set to zero if it is desired to only include the ground electronic state in the calculation

MGE is a real array which stores the electronic transition moments

U(5,5) is a real array which stores the dipole moments for vibrational transitions between states labeled N and M (in Debye)

FWHM is a real array which stores the linewidths for vibrational and rotational transitions

TEMP is the temperature of the system being modeled

WSIZE is the size of the interval about the input pump frequencies inside of which the program will indicate that a resonance has been approached.

IWRITE is an integer flag such that if it is set equal to one the program prints out the individual excitation path contributions or if it is set equal to two the program calculates only the contribution from the $v_a = 0$, $v_b = 3$, $v_c = 2$, $v_d = 1$ excitation path

IPOINT is an integer flag such that if it is set equal to one the program calculates results for frequency tripling for pump frequencies ranging from WQ to WP with a step size of WR

WP, WQ, WR these are the pump frequencies (in cm^{-1}). The program terminates when all three are set to zero

There are also several COMMON variables used in the program. SIZE, AE, DELTA, WE, WEXE are also input variables and have been described. Some other COMMON variables are listed and described below:

NA, NB,
NC, ND are the indices for the appropriate vibrational levels

RA, RB
RC, RD are the indices for the appropriate rotational levels

FABCD(20) is the frequency denominator

EAB, EAC, EAD are the imaginary half-widths

W(2,5,50) is a real array which stores the calculated energy levels

CA(5,50)
CB(5,50) are the intermediate coupling coefficients ($\Lambda \neq 0$)

RS(2,3,50) is a real array which stores the calculated intermediate coupling coefficients ($\Lambda \neq 0$)

X(5,2,3) is a real array containing the anharmonic oscillator matrix elements (when an upper electronic state is included in the calculation)

OMEGAA, OMEGAB
OMEGAC, OMEGAD are the projections of the total angular moments on the molecular axis ($\Lambda \neq 0$)

The output consists of various blocks listing the following:

- (1) All input data
- (3) Single path contributions of the susceptibility (if IWRITE = 1)
- (4) The sum frequency, the real part of $\chi^{(3)}$, the imaginary part of $\chi^{(3)}$, and the modulus of $\chi^{(3)}$

A complete calculation for one molecule, considering up to 4 vibrational levels and 30 rotational levels takes less than 26 seconds on a CDC 6600, yielding results for 10 sets of pump frequencies.

Program Listing

74/14 00PT=2 UU

FTN 4,6-433R

11/22/78 11.36.27

```

PROGRAM CHITHRE (INPUT,OUTPUT,TAPE5=INPUT,TAPE6=OUTPUT,DEBUG=OUTPUT
5)
THIS PROGRAM CALCULATES THIRD ORDER SUSCEPTIBILITIES FROM SPECTRO-
SCOPIC DATA

INPUTS

LAMBDA(I), I=1,4 (8A10)
NV, NJ (215)
NV = NUMBER OF VIBRATIONAL LEVELS USED IN THIS CALCULATION
NJ = NUMBER OF ROTATIONAL LEVELS USED IN THIS CALCULATION

WE, WEXE, WEYE, WEZE (4E15.8)
THESE ARE THE VIBRATIONAL CONSTANTS (IN RECIPROCAL CM)

AE, ALPHA, GAMMA, DE, DELTA (5E15.8)
THESE ARE THE ROTATIONAL CONSTANTS (IN RECIPROCAL CM)

DE, DELTA (2E15.8)
ADDITIONAL ROTATIONAL CONSTANTS FOR LAMBDA NE 0 CASE
WHEN BOTH AE AND DELTA ARE SET TO ZERO, PROGRAM ASSUMES LAMBDA = 0

OMEGA E: MUE(I), I=1,3 (4E15.8)
OMEGA E = ELECTRONIC ENERGY: ZERO IF ONLY GROUND STATE IS INCLUDED
MUE(I) = THE ELECTRONIC TRANSITION MOMENTS

FOR EACH VIBRATIONAL LEVEL, N---
J(M,N), M=1,NV (5E15.8)
J(M,N) = DIPOLE MOMENTS FOR VIBRATIONAL TRANSITIONS N TO M
(IN DEBYE)

FWHM(L), L=1,4V (5E15.8)
L INCLUDING (IN RECIPROCAL CM)---
L=1, ROTATIONAL
L=2, U T, 1 VIBRATIONAL
L=3, U T, 2 VIBRATIONAL
ETC.

```

87

CHITHRE 74/74 OPT=2 UO

FTN 4.6+433H

11/22/78 11.36.27

```

      READ(5,105) WE, WEXE, WEYE, WEZE
105 FORMAT(5E15.8)
      WRITE(6,106)
106 FORMAT(1/5X,*, VIBRATIONAL CONSTANTS:*, 6X,*, WE*, 12X,*, WEXE*, 11X,*, WEYE*,
      E, 11X,*, WEZE*, 12X,*, (IN RECIPROCAL CM)* )
      WRITE(6,107) WE, WEXE, WEYE, WEZE
107 FORMAT(25X, 5E15.8)
      READ(5,108) BE, ALPHA, GAMMA, DE, HETA
      WRITE(6,108)
108 FORMAT(1/5X,*, ROTATIONAL CONSTANTS:*, 7X,*, BE*, 12X,*, ALPHA*, 10X,
      E,*, GAMMA*, 11X,*, DE*, 12X,*, HETA*, 12X,*, (IN RECIPROCAL CM)* )
      WRITE(6,109) BE, ALPHA, GAMMA, DE, HETA
      READ(5,109) AE, DELTA
      WRITE(6,109)
109 FORMAT(1/5X,*, ROTATIONAL CONSTANTS:*, 7X,*, AE*, 12X,*, DELTA*, 11X,
      E,*, (IN RECIPROCAL CM)* )
      WRITE(6,109) AE, DELTA
      READ(5,109) OMEGAE, (MGE(I), I=1,3)
      IF (OMEGAE.EQ.0.) GO TO 200
      WRITE(6,109)
109 FORMAT(1/5X,*, ELECTRONIC STATE:*, 9X,*, ENERGY*, 9X,*, MGE(1)*, 9X,
      E,*, MGE(2)*, 9X,*, MGE(3)* )
      WRITE(6,109) OMEGAE, (MGE(I), I=1,3)
200 CONTINUE
      WRITE(6,109)
109 FORMAT(1H1, //, 5X,*, VIBRATIONAL TRANSITION MOMENTS (IN DEBYE)*, //,
      E, 22X,*, 00*, 14X,*, 1*, 14X,*, 2*, 14X,*, 3*, 14X,*, 4* )
      DO 10 L=1, NV
      READ(5,109) (U(M,N), M=1, NV)
      NN=N-1
      WRITE(6,110) NN, (U(M,N), M=1, NV)
110 FORMAT(1/5X, 15, 5X, 5E15.8)
      10 CONTINUE
      READ(5,109) (FWHM(L), L=1, NV)
      WRITE(6,111)
111 FORMAT(1H1, //, 5X,*, LINEWIDTHS: ROTATIONAL*, 6X,*, 0 TO 1*, 9X,*, 0 TO
      E, 2*, 9X,*, 0 TO 3*, 9X,*, 0 TO 4*, 9X,*, (IN RECIPROCAL CM)* )
      WRITE(6,112) (FWHM(L), L=1, NV)
112 FORMAT(15X, 4E15.8)
C   CALCULATE INTERMEDIATE CONSTANTS FOR THE ENERGY LEVELS
      WE=2.*DE*(12.*HE*2-ALPHA*WE)/(3.*WE*2)
      DO 20 L=1, NV
      V=L-1
      Y=V*0.5
      R(L)=BE-ALPHA*Y+GAMMA*Y*2
      D(L)=DE-HETA*Y
      G(L)=WE*Y-WEXE*Y*2+WEYE*Y*3+WEZE*Y*4
      IF (AE.FU.0..AND).DELTA.FU.0.) GO TO 20
      A(L)=AE-DELTA*Y
      LAMBDA(L)=A(L)/B(L)
      ASC[P(L)=A(L)-2.*D(L)-2.*R(L)*R(L)/A(L)
      NV(1,1)=B(L)+D(L)+R(L)*(1/LAMBDA(L)+2./LAMBDA(L)**2)
      NV(1,2)=B(L)+D(L)+R(L)*(1/LAMBDA(L)+2./LAMBDA(L)**2)
      NV(1,1)=B(L)+D(L)*(1/LAMBDA(L)**3+4./LAMBDA(L)**4)
      NV(1,2)=B(L)+D(L)*(1/LAMBDA(L)**3+4./LAMBDA(L)**4)
      NV(1,1)=HL-H(L)*(2./LAMBDA(L)**5+20./LAMBDA(L)**6)
      NV(1,2)=HL-H(L)*(2./LAMBDA(L)**5+20./LAMBDA(L)**6)

```

CHITHRE 116
CHITHRE 117
CHITHRE 118
CHITHRE 119
CHITHRE 120
CHITHRE 121
CHITHRE 122
CHITHRE 123
CHITHRE 124
CHITHRE 125
CHITHRE 126
CHITHRE 127
CHITHRE 128
CHITHRE 129
CHITHRE 130
CHITHRE 131
CHITHRE 132
CHITHRE 133
CHITHRE 134
CHITHRE 135
CHITHRE 136
CHITHRE 137
CHITHRE 138
CHITHRE 139
CHITHRE 140
CHITHRE 141
CHITHRE 142
CHITHRE 143
CHITHRE 144
CHITHRE 145
CHITHRE 146
CHITHRE 147
CHITHRE 148
CHITHRE 149
CHITHRE 150
CHITHRE 151
CHITHRE 152
CHITHRE 153
CHITHRE 154
CHITHRE 155
CHITHRE 156
CHITHRE 157
CHITHRE 158
CHITHRE 159
CHITHRE 160
CHITHRE 161
CHITHRE 162
CHITHRE 163
CHITHRE 164
CHITHRE 165
CHITHRE 166
CHITHRE 167
CHITHRE 168
CHITHRE 169
CHITHRE 170
CHITHRE 171
CHITHRE 172

AD-A080 810

NORTHROP RESEARCH AND TECHNOLOGY CENTER PALOS VERDES --ETC F/6 20/5
INVESTIGATION OF EFFICIENT CO LASER FREQUENCY TRIPLING. (U)

SEP 79 H KOMINE, E A STAPPAERTS, A S BERWER F29601-78-C-0068

UNCLASSIFIED

NRTC79-13R

AFWL-TR-79-71

NL

2 2

2 2

2 2

2 2

2 2

2 2

2 2

2 2

2 2

2 2

2 2

2 2

2 2

2 2

2 2

2 2

2 2

2 2

2 2

2 2

2 2

2 2

2 2

2 2

2 2

2 2

2 2

2 2

2 2

2 2

2 2

2 2

2 2

2 2

2 2

2 2

2 2

2 2

2 2

2 2

2 2

2 2

2 2

2 2

2 2

2 2

2 2

2 2

2 2

2 2

2 2

2 2

2 2

2 2

2 2

2 2

2 2

2 2

2 2

2 2

2 2

2 2

2 2

2 2

2 2

2 2

2 2

END

DATE

FILED

3 80

100

CHITHRE 74/74 OPT=2 UU

FTN 4.6+433H

11/22/78 11.36.27

```

20 CONTINUE
C   CALCULATE <X**1> WHEN INCLUDING AN ELECTRONIC STATE
   IF (OMEGA.EQ.0.) CALL LMENTS
C
   NUP=NJ+2
C   ITOP IS THE NUMBER OF OMEGA VALUES IN THE CALCULATION
   ITOP=2
   IF (AE.EQ.0. AND DELTA.EQ.0.) ITOP=1
   DO 500 J=1,NUP
   IF (AE.EQ.0. AND DELTA.EQ.0.) GO TO 400
C   CALCULATE THE REDUCED MATRIX ELEMENTS FOR LAMBDA NE 0, RS(I,K,J)
C   I = 1 FOR OMEGA OF 1/2
C   I = 2 FOR OMEGA OF 3/2
C   K = 1 FOR RX LY RY
C   K = 2 FOR RX EY RY
C   K = 3 FOR RX GY RY
C   J = THE INDEX FOR X-ST ROTATIONAL LEVEL
C
   P=2*J-1
   R=R/2.
   RS(1,1,J)=SQRT(((R+1.)*2-0.5*0.5)/(R+1.))
   IF (R.EQ.0.) GO TO 340
   RS(2,1,J)=SQRT(((R+1.)*2-1.5*1.5)/(R+1.))
   GO TO 350
340 RS(2,1,J)=0.
350 RS(1,2,J)=SQRT(0.5*0.5*(2.*R+1.)/(R*(R+1.)))
   RS(2,2,J)=SQRT(1.5*1.5*(2.*R+1.)/(R*(R+1.)))
   RS(1,3,J)=SQRT((R*R-0.5*0.5)/R)
   IF (R.LT.1.) GO TO 390
   RS(2,3,J)=SQRT((R*R-1.5*1.5)/R)
   GO TO 400
390 RS(2,3,J)=0.
400 CONTINUE
C
   DO 500 N=1,NV
   IF (AE.EQ.0. AND DELTA.EQ.0.) GO TO 300
C   CONSTRUCT THE INTERMEDIATE COUPLING COEFFICIENTS FOR LAMBDA NE 0
C
   X=SQRT(LAMBDA(N)*(LAMBDA(N)-4.)*4.*(R+0.5)**2)
   CA(N,J)=SQRT((X-2.*LAMBDA(N))/(2.*X))
   IF (J.EQ.1) GO TO 245
   CH(N,J)=SQRT((X+2.-LAMBDA(N))/(2.*X))
   GO TO 300
245 CH(N,J)=0.
300 CONTINUE
C
   DO 500 I=1,ITOP
C   CALCULATE THE ENERGY LEVELS
C
   IF (AE.EQ.0. AND DELTA.EQ.0.) GO TO 205
   G(1,N,J) = G(N) - D(N) + (-1.)*I*ASCRIP(N)/2. +
     EV(N,1)*(R+0.5)**2 - DV(N,1)*(R+0.5)**4 + HV(N,1)*(R+0.5)**6
   GO TO 500
205 P=J-1

```

```

CHITHRE 173
CHITHRE 174
CHITHRE 175
CHITHRE 176
CHITHRE 177
CHITHRE 178
CHITHRE 179
CHITHRE 180
CHITHRE 181
CHITHRE 182
CHITHRE 183
CHITHRE 184
CHITHRE 185
CHITHRE 186
CHITHRE 187
CHITHRE 188
CHITHRE 189
CHITHRE 190
CHITHRE 191
CHITHRE 192
CHITHRE 193
CHITHRE 194
CHITHRE 195
CHITHRE 196
CHITHRE 197
CHITHRE 198
CHITHRE 199
CHITHRE 200
CHITHRE 201
CHITHRE 202
CHITHRE 203
CHITHRE 204
CHITHRE 205
CHITHRE 206
CHITHRE 207
CHITHRE 208
CHITHRE 209
CHITHRE 210
CHITHRE 211
CHITHRE 212
CHITHRE 213
CHITHRE 214
CHITHRE 215
CHITHRE 216
CHITHRE 217
CHITHRE 218
CHITHRE 219
CHITHRE 220
CHITHRE 221
CHITHRE 222
CHITHRE 223
CHITHRE 224
CHITHRE 225
CHITHRE 226
CHITHRE 227
CHITHRE 228
CHITHRE 229

```

CHITHRE 74/74 OPT=2 UO

FTN 4.6+433B

11/22/78 11.36.27

```

      W(I,N,J) = G(I) * H(N)*R*(R+1.) - D(N)*(R*(R+1.))*2 *
      EHE*(R*(R+1.))*3
500 CONTINUE
C
      READ(5,105)TEMP,WSIZE
      WRITE(6,115)TEMP
113 FORMAT(//.5X.*TEMPERATURE FOR THIS CALCULATION IS *.E15.8.* KELV*)
      READ(5,105)IWRITE,IPOINT
      IF(IWRITE.NE.2) GO TO 21
      IF(OMEGA.E.NE.0.) GO TO 21
      WRITE(6,124)
122 FORMAT(//.5X.*THE RESONANCE APPROXIMATION HAS BEEN APPLIED IN THIS
      = CALCULATION*./)
C
      CALCULATE THE PARTITION FUNCTION
21 IF(AE.EQ.0..AND)DELTA.EQ.0.) GO TO 22
      ESHIFT=ASCHIP(1)*4.*BV(1,2)-16.*DV(1,2)*64.*HV(1,2)-BV(1,1)*
      EDV(1,1)-HV(1,1)
      Q=2. * (1.*EXP(-ESHIFT/(6.9503E-01*TEMP)))*6.9503E-01*TEMP/B(1)*
      EXP(-15.*B(1)/(6.9503E-01*TEMP*4.))
      GO TO 23
22 CONTINUE
      Q=6.9503E-01*TEMP/B(1)
23 CONTINUE
C
      READ IN WP, WQ, WR: TERMINATE THE PROGRAM IF THEY ARE ALL ZERO
25 READ(5,105)WP,WQ,WR
      IF(WP.EQ.0..AND)WQ.EQ.0..AND)WR.EQ.0) GO TO 1000
      NUM=0
      IF(IPOINT.NE.1) GO TO 55
      WMAX = WP
      WMIN = WQ
      WSIZE = ABS(WR)
      IF(WMAX.LT.WMIN) WSIZE=-WSIZE
      NUM=(WMAX-WMIN)/WSIZE
55 CONTINUE
      WRITE(6,120)WSIZE
126 FORMAT(//.5X.*RESONANCES WITHIN A RANGE OF *.E15.8.* /CM CENTERED
      ABOUT EACH OF THE PUMP FREQUENCIES ARE INDICATED BY THE PROGRAM*)
      NUM=NUM+1
      DO 2000 ITER=1,NUM
      IF(IPOINT.NE.1) GO TO 65
      WP=WMIN+(ITER-1)*WSIZE
      WQ=WP
      WR=WP
65 WRITE(6,114)WP,WQ,WR
114 FORMAT(////.5X.*THE PUMP FREQUENCIES ARE*.3(SX,E15.8))
C
      PERMUTE THE PUMP FREQUENCIES
C
C
C
      NFP IS THE NUMBER OF FREQUENCY PERMUTATIONS
      NFP=1
      IF(WP.NE.WQ)NFP=NFP+1
      IF(WP.NE.WR)NFP=NFP+1
      IF(WQ.NE.WR)NFP=NFP+1
      IF(NFP.GT.3)NFP=NFP+2
C
      PM IS THE NUMBER OF TIMES EACH PERMUTATION APPEARS
      PM=NFP
      IF(IWRITE.NE.1) GO TO 45

```

CHITHRE 230
 CHITHRE 231
 CHITHRE 232
 CHITHRE 233
 CHITHRE 234
 CHITHRE 235
 CHITHRE 236
 CHITHRE 237
 CHITHRE 238
 CHITHRE 239
 CHITHRE 240
 CHITHRE 241
 CHITHRE 242
 CHITHRE 243
 CHITHRE 244
 CHITHRE 245
 CHITHRE 246
 CHITHRE 247
 CHITHRE 248
 CHITHRE 249
 CHITHRE 250
 CHITHRE 251
 CHITHRE 252
 CHITHRE 253
 CHITHRE 254
 CHITHRE 255
 CHITHRE 256
 CHITHRE 257
 CHITHRE 258
 CHITHRE 259
 CHITHRE 260
 CHITHRE 261
 CHITHRE 262
 CHITHRE 263
 CHITHRE 264
 CHITHRE 265
 CHITHRE 266
 CHITHRE 267
 CHITHRE 268
 CHITHRE 269
 CHITHRE 270
 CHITHRE 271
 CHITHRE 272
 CHITHRE 273
 CHITHRE 274
 CHITHRE 275
 CHITHRE 276
 CHITHRE 277
 CHITHRE 278
 CHITHRE 279
 CHITHRE 280
 CHITHRE 281
 CHITHRE 282
 CHITHRE 283
 CHITHRE 284
 CHITHRE 285
 CHITHRE 286

CHITHRE 74/14 OPT=2 UU

FTN 4.6.433B

11/22/78 11.36.27

```

      WRITE(6,119)
119  FORMAT(//,5X,*,SINGLE PATH CONTRIBUTIONS TO THE SUSCEPTIBILITY*)
      WRITE(6,117)
117  FORMAT(//,25X,*,VB*,13X,*,VC*,13X,*,VD*,13X,*,VECH[3*,18X,*,MCH[3*,18X,
      =*ABCH[3*,/])
C
C      BEGIN THE SUM OVER VIBRATIONAL LEVELS
C
      45  CH[3]=(0.,0.)
      IF (OMEGA.L.NE.0.) GO TO 7
      IF (WRITE.NE.2) GO TO 7
C      PICK OUT SINGLE PATH FOR RESONANCE APPROXIMATION
      NBLO=4
      NBHI=4
      NCLO=3
      NCHI=3
      NDLO=2
      NDHI=2
      GO TO 4
C
      7  NBLN=1
      NBHI=NV
      NCLO=1
      NCHI=NV
      NDLO=1
      NDHI=NV
      A CONTINUE
      DO 60 NB=NBLO,NBHI
      IF (OMEGA.EQ.0) GO TO 34
      IF (NB.EQ.3) GO TO 19
      IF (NB.EQ.4) GO TO 29
      GO TO 39
      19  NCHI=NV+1
      NDHI=NV+1
      GO TO 39
      29  NCHI=NV
      NDHI=NV
      39  CONTINUE
      DO 70 NC=NCLO,NCHI
      DO 80 ND=NDLO,NDHI
      IF (NC.EQ.(NV+1).AND.ND.EQ.(NV+1)) GO TO 80
      SUMV(VB,NC,ND)=(0.,0.)
C
C      BEGIN THE SUM OVER FREQUENCY PERMUTATIONS
C
      DO 90 N=1,NFP
      GO TO (1,2,3,4,5,6),N
      1  W1=WP
      W2=WJ
      W3=WR
      GO TO 30
      2  W1=WJ
      W2=WR
      W3=WP
      GO TO 30
      3  W1=WR
      W2=WP

```

```

CHITHRE 287
CHITHRE 288
CHITHRE 289
CHITHRE 290
CHITHRE 291
CHITHRE 292
CHITHRE 293
CHITHRE 294
CHITHRE 295
CHITHRE 296
CHITHRE 297
CHITHRE 298
CHITHRE 299
CHITHRE 300
CHITHRE 301
CHITHRE 302
CHITHRE 303
CHITHRE 304
CHITHRE 305
CHITHRE 306
CHITHRE 307
CHITHRE 308
CHITHRE 309
CHITHRE 310
CHITHRE 311
CHITHRE 312
CHITHRE 313
CHITHRE 314
CHITHRE 315
CHITHRE 316
CHITHRE 317
CHITHRE 318
CHITHRE 319
CHITHRE 320
CHITHRE 321
CHITHRE 322
CHITHRE 323
CHITHRE 324
CHITHRE 325
CHITHRE 326
CHITHRE 327
CHITHRE 328
CHITHRE 329
CHITHRE 330
CHITHRE 331
CHITHRE 332
CHITHRE 333
CHITHRE 334
CHITHRE 335
CHITHRE 336
CHITHRE 337
CHITHRE 338
CHITHRE 339
CHITHRE 340
CHITHRE 341
CHITHRE 342
CHITHRE 343

```

CHITHRE 74/74 OPT=2 UO

FTN 4.6+4338

11/22/78 11.36.27

```

      WJ=WQ
      GU TO 30
4     W1=WP
      WC=WR
      WJ=WQ
      GU TO 30
5     W1=WQ
      W2=WP
      WJ=WP
      GU TO 30
6     W1=WR
      W2=WQ
      WJ=WP
      GU TO 30
30    NA=1
C     CALCULATE IMAGINARY HALFWIDTHS
      EAD=(0.,0.5)*FWHM(NB)
      EAC=(0.,0.5)*FWHM(NC)
      EAD=(0.,0.5)*FWHM(ND)
      IF(NC.EQ.(NV+1).OR.ND.EQ.(NV+1)) GO TO 3000
C     TAKE THE PRODUCT OF THE DIPOLE MATRIX ELEMENTS
      PV=1/(NA*NB)*U(NB,NC)*U(NC,ND)*1/(ND,NA)
C     BEGIN THE SUM OVER ROTATIONAL LEVELS
      SUMJ=(0.,0.)
      IF(LA.EQ.0..AND.DELTA.EQ.0.) GO TO 1060
C     ASSIGN VALUES OF VIBRATIONAL LEVEL INDICES TO BE PASSED TO SUMO
      MA=NA
      MB=NB
      MC=NC
      MU=ND
      DO 1050 J=1,NJ
C     R IS THE ACTUAL ROTATIONAL QUANTUM NUMBER
      R=2*J-1
      R=R/2.
      SA=R
      DO 1035 K=1,14
      PK(K)=0.
      F(K,1)=(0.,0.)
1075  F(K,2)=(0.,0.)
C
C     SUM OVER ROTATIONAL LEVELS BY PATHS
C
      IF(R-1.5) 1015,1012,1011
1011  KN=1
      SH=R-1.
      SC=R-2.
      SU=R-1.
      PK(1)=2./(15.*(2.*R-1.))
      CALL SHMO
1012  KN=2
      SH=R-1.
      SC=R
      SU=R-1.
      PK(2)=(4.*R*(R+1.)/(15.*R*(2.*R-1.)*(2.*R+1.))
      CALL SHMO
      KN=1
      SH=U+1.

```

```

CHITHRE 344
CHITHRE 345
CHITHRE 346
CHITHRE 347
CHITHRE 348
CHITHRE 349
CHITHRE 350
CHITHRE 351
CHITHRE 352
CHITHRE 353
CHITHRE 354
CHITHRE 355
CHITHRE 356
CHITHRE 357
CHITHRE 358
CHITHRE 359
CHITHRE 360
CHITHRE 361
CHITHRE 362
CHITHRE 363
CHITHRE 364
CHITHRE 365
CHITHRE 366
CHITHRE 367
CHITHRE 368
CHITHRE 369
CHITHRE 370
CHITHRE 371
CHITHRE 372
CHITHRE 373
CHITHRE 374
CHITHRE 375
CHITHRE 376
CHITHRE 377
CHITHRE 378
CHITHRE 379
CHITHRE 380
CHITHRE 381
CHITHRE 382
CHITHRE 383
CHITHRE 384
CHITHRE 385
CHITHRE 386
CHITHRE 387
CHITHRE 388
CHITHRE 389
CHITHRE 390
CHITHRE 391
CHITHRE 392
CHITHRE 393
CHITHRE 394
CHITHRE 395
CHITHRE 396
CHITHRE 397
CHITHRE 398
CHITHRE 399
CHITHRE 400

```

CHITHRE 74/74 OPT=2 UU

FTN 4.6+433H

11/22/78 11.36.27

```

SC=0
SU=R-1.
PR(3)=2./(15.*(2.*R+1.))
CALL SUMO
KN=4
SU=R-1.
SC=0
SU=R+1.
PR(4)=PR(3)
CALL SUMO
KN=7
SU=R
SC=0
SU=R-1.
PR(7)=(R-1.)/(15.*R*(2.*R+1.))
CALL SUMO
KN=9
SU=R
SC=R-1.
SU=0
PR(9)=PR(7)
CALL SUMO
KN=11
SU=R-1.
SC=R
SU=R
PR(11)=PR(7)
CALL SUMO
KN=13
SU=R-1.
SC=R-1.
SU=R-1.
PR(13)=(R+1.)/(15.*R*(2.*R-1.))
CALL SUMO
KN=15
SU=R
SC=R-1.
SU=R-1.
PR(15)=SQR(((R+1.)*(R-1.)/(R*R*(2.*R+1.)*(2.*R-1.)))/15.
CALL SUMO
KN=17
SU=R-1.
SC=R-1.
SU=R
PR(17)=PR(15)
CALL SUMO
1015 KN=5
SU=R+1.
SC=0
SU=R+1.
PR(5)=(4.*R*R*R.*R+5.)/(15.*(R+1.)*(2.*R+1.)*(2.*R+3.))
CALL SUMO
KN=6
SU=R+1.
SC=R+2.
SU=R+1.
PR(6)=2./(15.*(2.*R+3.))

```

```

CHITHRE 401
CHITHRE 402
CHITHRE 403
CHITHRE 404
CHITHRE 405
CHITHRE 406
CHITHRE 407
CHITHRE 408
CHITHRE 409
CHITHRE 410
CHITHRE 411
CHITHRE 412
CHITHRE 413
CHITHRE 414
CHITHRE 415
CHITHRE 416
CHITHRE 417
CHITHRE 418
CHITHRE 419
CHITHRE 420
CHITHRE 421
CHITHRE 422
CHITHRE 423
CHITHRE 424
CHITHRE 425
CHITHRE 426
CHITHRE 427
CHITHRE 428
CHITHRE 429
CHITHRE 430
CHITHRE 431
CHITHRE 432
CHITHRE 433
CHITHRE 434
CHITHRE 435
CHITHRE 436
CHITHRE 437
CHITHRE 438
CHITHRE 439
CHITHRE 440
CHITHRE 441
CHITHRE 442
CHITHRE 443
CHITHRE 444
CHITHRE 445
CHITHRE 446
CHITHRE 447
CHITHRE 448
CHITHRE 449
CHITHRE 450
CHITHRE 451
CHITHRE 452
CHITHRE 453
CHITHRE 454
CHITHRE 455
CHITHRE 456
CHITHRE 457

```

CHITHRE 74/74 NPT=2 UO

FTN 4.6+4338

11/22/78 11.36.27

```

CALL SUMO
KN=8
SH=R
SC=R
SU=R+1.
PR(8)=(R+2.)/(15.*(R+1.)*(2.*R+1.))
CALL SUMO
KN=10
SH=R
SC=R+1.
SU=R
PR(10)=PR(8)
CALL SUMO
KN=12
SH=R+1.
SC=R
SU=R
PR(12)=PR(8)
CALL SUMO
KN=14
SH=R+1.
SC=R+1.
SU=R+1.
PR(14)=R/(15.*(R+1.)*(2.*R+3.))
CALL SUMO
KN=16
SH=R
SC=R+1.
SU=R+1.
PR(16)=SUMT(R*(R+2.)/(R+1.)*(R+1.)*(2.*R+1.)*(2.*R+3.))/15.
CALL SUMO
KN=18
SH=R+1.
SC=R+1.
SU=R
PR(18)=PR(16)
CALL SUMO
KN=19
SH=R
SC=R
SU=R
PR(19)=(3.*R+0.3.*R-1.)/(15.*R*(R+1.)*(2.*R+1.))
CALL SUMO
C
C      BEGIN SUM OVER PATHS
C
PR(12)=PR(8)
DO 1040 K=1,19
SUML(2)=(0.,0.)
SUML(1)=(0.,0.)
SUML(1)=SUML(1)+PR(K)*F(K,1)
IF(R.EQ.0.0) GO TO 1040
SUML(2)=SUML(2)+PR(K)*F(K,2)
1040 CONTINUE
NK=(R+0.5)*2
F=HV(1,1)*NK-HV(1,1)*RH*2+HV(1,1)*RH*3-HV(1,1)*DV(1,1)-HV(1,1)
DIS=EXP(-E/(6.9503E-01*TEMP))/O

```

```

CHITHRE 458
CHITHRE 459
CHITHRE 460
CHITHRE 461
CHITHRE 462
CHITHRE 463
CHITHRE 464
CHITHRE 465
CHITHRE 466
CHITHRE 467
CHITHRE 468
CHITHRE 469
CHITHRE 470
CHITHRE 471
CHITHRE 472
CHITHRE 473
CHITHRE 474
CHITHRE 475
CHITHRE 476
CHITHRE 477
CHITHRE 478
CHITHRE 479
CHITHRE 480
CHITHRE 481
CHITHRE 482
CHITHRE 483
CHITHRE 484
CHITHRE 485
CHITHRE 486
CHITHRE 487
CHITHRE 488
CHITHRE 489
CHITHRE 490
CHITHRE 491
CHITHRE 492
CHITHRE 493
CHITHRE 494
CHITHRE 495
CHITHRE 496
CHITHRE 497
CHITHRE 498
CHITHRE 499
CHITHRE 500
CHITHRE 501
CHITHRE 502
CHITHRE 503
CHITHRE 504
CHITHRE 505
CHITHRE 506
CHITHRE 507
CHITHRE 508
CHITHRE 509
CHITHRE 510
CHITHRE 511
CHITHRE 512
CHITHRE 513
CHITHRE 514

```


CHITHRE 74/74 OPT=2 UO

FTN 4.6+4338

11/22/78 11.36.27

```

SUMJ=SUMJ+SUML(1)*DIS
IF (R.EQ.0.5) GO TO 1050
E=BV(1,2)*MH-DV(1,2)*RH**2+HV(1,2)*RR**3+ASCRIP(1)-HV(1,1)*DV(1,1)
E=HV(1,1)
DIS=EXP(-E/(6.450JE-01*TEMP))/Q
SUMJ=SUMJ+SUML(2)*DIS
1050 CONTINUE
GO TO 1111
1060 CONTINUE
DO 50 J=1,NJ
C  K IS THE ACTUAL ROTATIONAL QUANTUM NUMBER
  K=J-1
  RA=R
  DO 35 K=1,0
    PH(K)=0.
  35 FAUCD(K)=(0.,0.)
C
C  SUM OVER THE ROTATIONAL LEVELS BY PATHS
C
  IF(W-1.)15,12,11
11 K=1
  PH=R-1.
  RC=R-2.
  RU=R-1.
  PM(1)=2.*K*(R-1.)/(15.*(2.*R-1.)*(2.*R+1.))
  CALL FREQ
12 K=2
  PH=R-1.
  RC=R
  RU=R-1.
  PM(2)=2.*K*(R+1.)/(15.*(2.*R-1.)*(2.*R+1.)*2)
  CALL FREQ
  K=3
  PH=R+1.
  RC=R
  RU=R-1.
  PM(3)=2.*K*(R+1.)/(15.*(2.*R+1.)*2)
  CALL FREQ
  K=4
  PH=R-1.
  RC=R
  RU=R+1.
  PM(4)=2.*K*(R+1.)/(15.*(2.*R+1.)*2)
  CALL FREQ
15 K=5
  PH=R+1.
  RC=R
  RU=R+1.
  PM(5)=(K+1.)*(4.*R**2+8.*R+5)/(15.*(2.*R+3.)*(2.*R+1.)*2)
  CALL FREQ
  K=6
  PH=R+1.
  RC=R+2.
  RU=R+1.
  PM(6)=2.*K*(R+1.)*(R+2.)/(15.*(2.*R+3.)*(2.*R+1.))
  CALL FREQ
C

```

```

CHITHRE 515
CHITHRE 516
CHITHRE 517
CHITHRE 518
CHITHRE 519
CHITHRE 520
CHITHRE 521
CHITHRE 522
CHITHRE 523
CHITHRE 524
CHITHRE 525
CHITHRE 526
CHITHRE 527
CHITHRE 528
CHITHRE 529
CHITHRE 530
CHITHRE 531
CHITHRE 532
CHITHRE 533
CHITHRE 534
CHITHRE 535
CHITHRE 536
CHITHRE 537
CHITHRE 538
CHITHRE 539
CHITHRE 540
CHITHRE 541
CHITHRE 542
CHITHRE 543
CHITHRE 544
CHITHRE 545
CHITHRE 546
CHITHRE 547
CHITHRE 548
CHITHRE 549
CHITHRE 550
CHITHRE 551
CHITHRE 552
CHITHRE 553
CHITHRE 554
CHITHRE 555
CHITHRE 556
CHITHRE 557
CHITHRE 558
CHITHRE 559
CHITHRE 560
CHITHRE 561
CHITHRE 562
CHITHRE 563
CHITHRE 564
CHITHRE 565
CHITHRE 566
CHITHRE 567
CHITHRE 568
CHITHRE 569
CHITHRE 570
CHITHRE 571

```

CHITHRE 74/74 OPT=2 UO

FTN 4.6+4338

11/22/78 11.36.27

```

C BEGIN THE SUM OVER PATHS
C
  SUMK=(0.+0.)
  DO 40 K=1.6
    SUMK=SUMK+PR(K)*FAHCD(K)
    PR=PR*(R+1.)
    E=B(1)*RR-U(1)*RR**2+ME*RR**3
    DIS=(2.*R+1.)*EXP(-E/(6.9503E-01*TEMP))/Q
    SUMJ=SUMJ+SUMK*DIS
  GO TO 1111
3000 INDEX=1
  IF (NC.EQ.NV+1) INDEX=2
  DV=J*(NA+NB)/OMEGA E
C BEGIN THE SUM OVER ROTATIONAL LEVELS
  SUMJ=(0.+0.)
  DO 2050 J=1,NJ
C R IS THE ACTUAL ROTATIONAL QUANTUM NUMBER
  R=J-1
  TA=R
  DO 2035 K=1.6
    PR(K)=0.
    G(K,1)=(0.+0.)
2035 G(K,2)=(0.+0.)
C
C SUM OVER ROTATIONAL LEVELS BY PATHS
C
  IF (P.LT.1) GO TO 2015
  KM=1
  TB=P+1.
  TC=P
  TD=R+1.
  PR(1)=2./(15.*(2.*R+1.))
  CALL T1MU
2015 KM=2
  TB=P+1.
  TC=P
  TD=R+1.
  PR(2)=(4.*R*R+R+5.)/(15.*(R+1.)*(2.*R+1)*(2.*R+3.))
  CALL T1MU
  KM=3
  TB=P+1.
  TC=P+2.
  TD=P+1.
  PR(3)=2./(15.*(2.*P+3.))
  CALL T1MU
  KM=4
  TB=P+1.
  TC=P
  TD=R
  PR(4)=-(R+2.)/(15.*(R+1.)*(2.*R+1.))
  CALL T1MU
  KM=5
  TB=P+1.
  TC=P+1.
  TD=P+1.
  PR(5)=R/(15.*(R+1.)*(2.*P+3.))
  CALL T1MU

```

```

CHITHRE 572
CHITHRE 573
CHITHRE 574
CHITHRE 575
CHITHRE 576
CHITHRE 577
CHITHRE 578
CHITHRE 579
CHITHRE 580
CHITHRE 581
CHITHRE 582
CHITHRE 583
CHITHRE 584
CHITHRE 585
CHITHRE 586
CHITHRE 587
CHITHRE 588
CHITHRE 589
CHITHRE 590
CHITHRE 591
CHITHRE 592
CHITHRE 593
CHITHRE 594
CHITHRE 595
CHITHRE 596
CHITHRE 597
CHITHRE 598
CHITHRE 599
CHITHRE 600
CHITHRE 601
CHITHRE 602
CHITHRE 603
CHITHRE 604
CHITHRE 605
CHITHRE 606
CHITHRE 607
CHITHRE 608
CHITHRE 609
CHITHRE 610
CHITHRE 611
CHITHRE 612
CHITHRE 613
CHITHRE 614
CHITHRE 615
CHITHRE 616
CHITHRE 617
CHITHRE 618
CHITHRE 619
CHITHRE 620
CHITHRE 621
CHITHRE 622
CHITHRE 623
CHITHRE 624
CHITHRE 625
CHITHRE 626
CHITHRE 627
CHITHRE 628

```

CHITHRE 74/14 OPT=2 UU

FTN 4.6+433B

11/22/78 11.16.27

```

      KM=A
      TU=1.
      TC=1.
      TD=1.
      PR(n)=-SUMT(R*(H+2.)/(H+1.)*(H+1.)*(2.*R+1.)*(2.*R+3.))/15.
      CALL TUMU
C
C      BEGIN THE SUM OVER PATHS
C
      TUML=(0.+0.)
      DO 2040 K=1,6
2040  TUML=TUML+PR(K)*G(K,INDEX)
      PR=PR*(K+1.)
      E=0(1)*RR-U(1)*RR**2*HE*RR**3
      DIS=(2.*K+1.)*EXP(-E/(6.9503E-01*TFMP))/Q
2050  SUMJ=SUMJ+TUML*DIS
      NA=NC
      IF (INDEX.EQ.2) NX=ND
      UU=MGE(1)*MGE(1)*X(NX,INDEX,1) + (MGE(1)*MGE(2)*MGE(2)*MGE(1))
      ==X(NX,INDEX,2) + (MGE(1)*MGE(3)*MGE(2)*MGE(2)*MGE(3)*MGE(1))
      ==X(NX,INDEX,3)
      PV=PV+UU
1111 CONTINUE
C      END THE SUM OVER ROTATIONAL LEVELS
      SUMV(NR,NC,ND)=SUMV(NB,NC,ND)+SUMJ*PV
90 CONTINUE
C
C      END THE SUM OVER FREQUENCY PERMUTATIONS
C
      SUMV(NR,NC,ND)=PM*(-2.13E-26)*SUMV(NB,NC,ND)
      IF (IWRITE.NE.1) GO TO 100
      NDA=NB-1
      NCA=NC-1
      NUA=ND-1
      MODSUMV=CAUS(SUMV(NB,NC,ND))
      WRITE(6,110) NHA,NCA,NDA,SUMV(NB,NC,ND),MODSUMV
110  FORMAT(22A,15,10X,15,10X,15,8X,E15.8,8X,E15.8,8X,E15.8)
100  CH13=CH13+SUMV(NB,NC,ND)
80 CONTINUE
70 CONTINUE
60 CONTINUE
C
C      END THE SUM OVER VIBRATIONAL LEVELS FOR A GIVEN PERMUTATION OF THE
C      PUMP FREQUENCIES
C
C
C      OUTPUT THE RESULTS
C
      WS=IP+QU+WK
      MODCHI=CAUS(CH13)
      WRITE(6,115) WS,CH13,MODCHI
115  FORMAT(15X,*,FOR THE SUM FREQUENCY *,E15.8,/,5X, *,THIRD ORDER SUS
      ACCEPTIBILITY HAS RE PART *,E15.8,*, CM6/ERG *,/,5X, *,THIRD ORDER SUS
      ACCEPTIBILITY HAS IM PART *,E15.8,*, CM6/ERG *,/,5X, *,THIRD ORDER SUS
      ACCEPTIBILITY HAS MODULUS *,E15.8,*, CM6/ERG *)
2000 CONTINUE
      GO TO 25

```

```

CHITHRE 629
CHITHRE 630
CHITHRE 631
CHITHRE 632
CHITHRE 633
CHITHRE 634
CHITHRE 635
CHITHRE 636
CHITHRE 637
CHITHRE 638
CHITHRE 639
CHITHRE 640
CHITHRE 641
CHITHRE 642
CHITHRE 643
CHITHRE 644
CHITHRE 645
CHITHRE 646
CHITHRE 647
CHITHRE 648
CHITHRE 649
CHITHRE 650
CHITHRE 651
CHITHRE 652
CHITHRE 653
CHITHRE 654
CHITHRE 655
CHITHRE 656
CHITHRE 657
CHITHRE 658
CHITHRE 659
CHITHRE 660
CHITHRE 661
CHITHRE 662
CHITHRE 663
CHITHRE 664
CHITHRE 665
CHITHRE 666
CHITHRE 667
CHITHRE 668
CHITHRE 669
CHITHRE 670
CHITHRE 671
CHITHRE 672
CHITHRE 673
CHITHRE 674
CHITHRE 675
CHITHRE 676
CHITHRE 677
CHITHRE 678
CHITHRE 679
CHITHRE 680
CHITHRE 681
CHITHRE 682
CHITHRE 683
CHITHRE 684
CHITHRE 685

```

CHITHRE 74/74 OPT=2 UD

FTN 4.6+433B

11/22/78 11.36.27

1000 WRITE(6,116)
116 FORMAT(////.5X,*THAT'S ALL FOLKS*)
STOP
END

CHITHRE 686
CHITHRE 687
CHITHRE 688
CHITHRE 689

FREQ 74/74 OPT=2 UU

FTN 4.6+433B

11/22/78 11.36.27

	SUBROUTINE FREQ	FREQ	2
C		FREQ	3
C	THIS SUBROUTINE CALCULATES THE FREQUENCY DENOMINATOR FABCD	FREQ	4
C		FREQ	5
	INTEGER OMEGAA,OMEGAB,OMEGAC,OMEGAD	FREQ	6
	COMPLEX FABCD(20),EAB,EAC,EAD,FD1,FD2,FD3,FD4,FD5,FD6,GABCD(20)	FREQ	7
	COMMON/CFREQ/ NA,NB,NC,ND,RA,RR,RC,RD,W1,W2,W3,K,W(2,5,50),	FREQ	8
	EABCD(20),EAB,EAC,EAD,WSIZE,AE,DELTA	FREQ	9
	COMMON/DSUMU/L,OMEGAA,OMEGAB,OMEGAC,OMEGAD,GABCD(20),SA,SB,SC,SD	FREQ	10
CS	DEBIG	FREQ	11
CS	ARRAYS	FREQ	12
CS	GUIN5	FREQ	13
	IF(AE.EQ.0..AND.DELTA.EQ.0.) GO TO 5	FREQ	14
C		FREQ	15
C	CALCULATE ENERGY LEVEL DIFFERENCES	FREQ	16
C		FREQ	17
	JA=SA*0.5	FREQ	18
	JB=SB*0.5	FREQ	19
	JC=SC*0.5	FREQ	20
	JD=SD*0.5	FREQ	21
	WAB=W(OMEGAA,NA,JA)-W(OMEGAB,NB,JB)	FREQ	22
	WAC=W(OMEGAA,NA,JA)-W(OMEGAC,NC,JC)	FREQ	23
	WAD=W(OMEGAA,NA,JA)-W(OMEGAD,ND,JD)	FREQ	24
	GO TO 7	FREQ	25
5	JA=RA*1.	FREQ	26
	JB=RB*1.	FREQ	27
	JC=RC*1.	FREQ	28
	JD=RD*1.	FREQ	29
	WAB=W(1,NA,JA)-W(1,NB,JB)	FREQ	30
	WAC=W(1,NA,JA)-W(1,NC,JC)	FREQ	31
	WAD=W(1,NA,JA)-W(1,ND,JD)	FREQ	32
7	CONTINUE	FREQ	33
C		FREQ	34
C	SET UP INDICES TO BE PRINTED WHEN A RESONANCE IS ENCOUNTERED	FREQ	35
C		FREQ	36
	NAX=NA-1	FREQ	37
	NBX=NB-1	FREQ	38
	NXC=NC-1	FREQ	39
	NXD=ND-1	FREQ	40
	IF(AE.EQ.0..AND.DELTA.EQ.0.) GO TO 10	FREQ	41
	IA=2.*SA	FREQ	42
	IB=2.*SB	FREQ	43
	IC=2.*SC	FREQ	44
	ID=2.*SD	FREQ	45
	KA=2*OMEGAA-1	FREQ	46
	KB=2*OMEGAB-1	FREQ	47
	KC=2*OMEGAC-1	FREQ	48
	KD=2*OMEGAD-1	FREQ	49
	GO TO 17	FREQ	50
10	CONTINUE	FREQ	51
	IA=4A	FREQ	52
	IB=4B	FREQ	53
	IC=4C	FREQ	54
	ID=4D	FREQ	55
17	CONTINUE	FREQ	56
C		FREQ	57
	FUM=1000.	FREQ	58

FREQ 74/74 OPT=2 UO

FTN 4.6+4338

11/22/78 11.36.27

```

F01=WAB+EAB+W1+W2+W3
F02=WAD-EAD-W1-W2-W3
WSIZE3=WSIZE*3./2.
IF (ABS(REAL(F01)).LE.WSIZE3) FDR=REAL(F01)
IF (FDR.NE.1000.) GO TO 410
11 IF (ABS(REAL(F02)).LE.WSIZE3) FDR=REAL(F02)
IF (FDR.NE.1000.) GO TO 420
1 F03=WAC+EAC+W2+W3
F04=WAC-EAC-W1-W2
WSIZE2=WSIZE*2./2.
IF (ABS(REAL(F03)).LE.WSIZE2) FDR=REAL(F03)
IF (FDR.NE.1000.) GO TO 510
12 IF (ABS(REAL(F04)).LE.WSIZE2) FDR=REAL(F04)
IF (FDR.NE.1000.) GO TO 520
2 F05=WAB+EAB+W3
F06=WAB-EAB-W1
WSIZE1=WSIZE*1./2.
IF (ABS(REAL(F05)).LE.WSIZE1) FDR=REAL(F05)
IF (FDR.NE.1000.) GO TO 610
13 IF (ABS(REAL(F06)).LE.WSIZE1) FDR=REAL(F06)
IF (FDR.NE.1000.) GO TO 620
3 IF (AE.F0.U..AND.DELTA.EQ.0.) GO TO 23
GABCD(L)=(1/F01+1/F06)/(F03*F05)+(1/F02+1/F05)/(F04*F06)
GO TO 33
23 GABCD(K)=(1/F01+1/F06)/(F03*F05)+(1/F02+1/F05)/(F04*F06)
77 CONTINUE
RETURN
C
C WRITE STATEMENTS USED WHEN A RESONANCE IS ENCOUNTERED FOLLOW
C
410 IF (AE.F0.U..AND.DELTA.EQ.0.) GO TO 41
WRITE(6,140) NAX,NHX,NCX,NDX,IA,IB,IC,ID,KA,KB,KC,KD,FDR
140 FORMAT(/,5X,'THREE PHOTON RESONANCE: VA=*,15.5X,* VB=*,15.5X,*
* VC=*,15.5X,* VD=*,15./,29X,* JA=*,13./,2*.5X,* JB=*,13./,2*.
* JC=*,13./,2*.5X,* JD=*,13./,2*./,29X,* KA=*,13./,2*.5X,*
* KB=*,13./,2*.5X,* KC=*,13./,2*.5X,* KD=*,13./,2*.5X,* DW=*,
E15.8)
FUR=1000.
GO TO 11
420 IF (AE.F0.U..AND.DELTA.EQ.0.) GO TO 42
WRITE(6,140) NAX,NHX,NCX,NDX,IA,IB,IC,ID,KA,KB,KC,KD,FDR
FUR=1000.
GO TO 1
510 IF (AE.F0.U..AND.DELTA.EQ.0.) GO TO 51
WRITE(6,150) NAX,NHX,NCX,NDX,IA,IB,IC,ID,KA,KB,KC,KD,FDR
150 FORMAT(/,5X,'TWO PHOTON RESONANCE: VA=*,15.5X,* VB=*,15.5X,*
* VC=*,15.5X,* VD=*,15./,27X,* JA=*,13./,2*.5X,* JB=*,13./,2*.
* JC=*,13./,2*.5X,* JD=*,13./,2*./,27X,* KA=*,13./,2*.5X,*
* KB=*,13./,2*.5X,* KC=*,13./,2*.5X,* KD=*,13./,2*.5X,* DW=*,
E15.8)
FUR=1000.
GO TO 12
520 IF (AE.F0.U..AND.DELTA.EQ.0.) GO TO 52
WRITE(6,150) NAX,NHX,NCX,NDX,IA,IB,IC,ID,KA,KB,KC,KD,FDR
FUR=1000.
GO TO 2
610 IF (AE.F0.U..AND.DELTA.EQ.0.) GO TO 61

```

```

FREQ 59
FREQ 60
FREQ 61
FREQ 62
FREQ 63
FREQ 64
FREQ 65
FREQ 66
FREQ 67
FREQ 68
FREQ 69
FREQ 70
FREQ 71
FREQ 72
FREQ 73
FREQ 74
FREQ 75
FREQ 76
FREQ 77
FREQ 78
FREQ 79
FREQ 80
FREQ 81
FREQ 82
FREQ 83
FREQ 84
FREQ 85
FREQ 86
FREQ 87
FREQ 88
FREQ 89
FREQ 90
FREQ 91
FREQ 92
FREQ 93
FREQ 94
FREQ 95
FREQ 96
FREQ 97
FREQ 98
FREQ 99
FREQ 100
FREQ 101
FREQ 102
FREQ 103
FREQ 104
FREQ 105
FREQ 106
FREQ 107
FREQ 108
FREQ 109
FREQ 110
FREQ 111
FREQ 112
FREQ 113
FREQ 114
FREQ 115

```

FREQ

74/14

OPT=2 UU

FTN 4.6+433H

11/22/78 11.36.27

```

WRITE(6,100) NAX,NBX,NCX,NDX,IA,IB,IC,ID,KA,KB,KC,KD,FDR      FREQ      116
100 FUMMAT(1/.5X, *ONE PHOTON RESONANCE: VA= *.15,5X,* VB= *.15,5X, FREQ      117
   * VC= *.15,5X,* VD= *.15,/.27X,* JA= *.13,*/2*,5X,* JB= *.13,*/2*, FREQ      118
   * JC= *.13,*/2*,5X,* JU= *.13,*/2*,*/27X,* KA= *.13,*/2*,5X, FREQ      119
   * KB= *.13,*/2*,5X,* KC= *.13,*/2*,5X,* KD= *.13,*/2*,5X,* DW= *, FREQ      120
   *E15.8) FREQ      121
FUM=1000. FREQ      122
GO TO 13 FREQ      123
620 IF(XAE.EQ.0..AND.DELTA.EQ.0.) GO TO 62 FREQ      124
WRITE(6,100) NAX,NBX,NCX,NDX,IA,IB,IC,ID,KA,KB,KC,KD,FDR FREQ      125
FUM=1000. FREQ      126
GO TO 3 FREQ      127
41 WRITE(6,14) NAX,NBX,NCX,NDX,IA,IB,IC,ID,FDR FREQ      128
14 FUMMAT(1/.5X, *THREE PHOTON RESONANCE: VA= *.15,5X,* VB= *.15,5X, FREQ      129
   * VC= *.15,5X,* VD= *.15,/.29X,* JA= *.15,5X,* JB= *.15,5X,* JC= * FREQ      130
   * JD= *.15,5X,* JU= *.15,5X,* DW= *.E15.8) FREQ      131
FUM=1000. FREQ      132
GO TO 11 FREQ      133
42 WRITE(6,14) NAX,NBX,NCX,NDX,IA,IB,IC,ID,FDR FREQ      134
FUM=1000. FREQ      135
GO TO 1 FREQ      136
51 WRITE(6,15) NAX,NBX,NCX,NDX,IA,IB,IC,ID,FDR FREQ      137
15 FUMMAT(1/.5X, *TWO PHOTON RESONANCE: VA= *.15,5X,* VB= *.15,5X, FREQ      138
   * VC= *.15,5X,* VD= *.15,/.27X,* JA= *.15,5X,* JB= *.15,5X,* JC= * FREQ      139
   * JD= *.15,5X,* JU= *.15,5X,* DW= *.E15.8) FREQ      140
FUM=1000. FREQ      141
GO TO 12 FREQ      142
52 WRITE(6,15) NAX,NBX,NCX,NDX,IA,IB,IC,ID,FDR FREQ      143
FUM=1000. FREQ      144
GO TO 2 FREQ      145
61 WRITE(6,16) NAX,NBX,NCX,NDX,IA,IB,IC,ID,FDR FREQ      146
16 FUMMAT(1/.5X, *ONE PHOTON RESONANCE: VA= *.15,5X,* VB= *.15,5X, FREQ      147
   * VC= *.15,5X,* VD= *.15,/.27X,* JA= *.15,5X,* JB= *.15,5X,* JC= * FREQ      148
   * JD= *.15,5X,* JU= *.15,5X,* DW= *.E15.8) FREQ      149
FUM=1000. FREQ      150
GO TO 13 FREQ      151
62 WRITE(6,16) NAX,NBX,NCX,NDX,IA,IB,IC,ID,FDR FREQ      152
FUM=1000. FREQ      153
GO TO 3 FREQ      154
END FREQ      155

```

SUMO 14/14 OPT=2 UU

FTN 4.6-433B

11/22/78 11.36.27

	SUBROUTINE SUMO	SUMO	2
C		SUMO	3
C	THIS SUBROUTINE CALCULATES THE CONTRIBUTIONS TO THE OMEGA SUM	SUMO	4
C	OVER PATHS	SUMO	5
C		SUMO	6
	COMPLEX F=BCD(20),F(20,2)	SUMO	7
	DIMENSION K1(4),K2(4),PHI1(4),PHI2(4),PHI3(4),PHI(20)	SUMO	8
	COMMON/CSUM0/NA,NB,NC,ND,RA,RB,RC,RD,F(20,2),K,CA(5,50),CB(5,50),	SUMO	9
	ERR(2,3,50)	SUMO	10
	COMMON/DSUM0/L,IA,IB,IC,ID,FABCD(20),SA,SB,SC,SD	SUMO	11
CS	DEBUG	SUMO	12
CS	ARRAYS	SUMO	13
CS	GUTS	SUMO	14
C		SUMO	15
C	DEFINE ROTATIONAL LEVEL INDICES TO BE PASSED TO FREQ	SUMO	16
C		SUMO	17
	SA=RA	SUMO	18
	SB=RB	SUMO	19
	SC=RC	SUMO	20
	SD=RD	SUMO	21
C		SUMO	22
	JA=PA+0.5	SUMO	23
	JB=PB+0.5	SUMO	24
	JC=PC+0.5	SUMO	25
	JD=PD+0.5	SUMO	26
C		SUMO	27
C	SUM THE REDUCED MATRIX ELEMENTS	SUMO	28
C		SUMO	29
	IF (RA=RB) 11,12,13	SUMO	30
11	R1(1)=RR(1,1,JA)	SUMO	31
	R2(1)=RR(2,1,JA)	SUMO	32
	GO TO 20	SUMO	33
12	R1(1)=RR(1,2,JA)	SUMO	34
	R2(1)=RR(2,2,JA)	SUMO	35
	GO TO 20	SUMO	36
13	R1(1)=RR(1,3,JA)	SUMO	37
	R2(1)=RR(2,3,JA)	SUMO	38
C		SUMO	39
20	IF (RB=RC) 21,22,23	SUMO	40
21	R1(2)=RR(1,1,JB)	SUMO	41
	R2(2)=RR(2,1,JB)	SUMO	42
	GO TO 30	SUMO	43
22	R1(2)=RR(1,2,JB)	SUMO	44
	R2(2)=RR(2,2,JB)	SUMO	45
	GO TO 30	SUMO	46
23	R1(2)=RR(1,3,JB)	SUMO	47
	R2(2)=RR(2,3,JB)	SUMO	48
C		SUMO	49
30	IF (PC=RD) 31,32,33	SUMO	50
31	R1(3)=RR(1,1,JC)	SUMO	51
	R2(3)=RR(2,1,JC)	SUMO	52
	GO TO 40	SUMO	53
32	R1(3)=RR(1,2,JC)	SUMO	54
	R2(3)=RR(2,2,JC)	SUMO	55
	GO TO 40	SUMO	56
33	R1(3)=RR(1,3,JC)	SUMO	57
	R2(3)=RR(2,3,JC)	SUMO	58

SUM0 74/74 OPT=2 UO

FTN 4.6+4338

11/22/78 11.36.27

```

C
40 IF(PD-RA) *1,42,43
41 R1(4)=PR(1+1,JD)
   R2(4)=PR(2+1,JD)
   GO TO 50
42 R1(4)=PR(1+2,JD)
   R2(4)=PR(2+2,JD)
   GO TO 50
43 R1(4)=PR(1+3,JD)
   R2(4)=PR(2+3,JD)
50 CONTINUE

C
C DETERMINE THE PHIS
C
PHI1(1)=CA(NA,JA)*CA(NB,JB)*R1(1)*CB(NA,JA)*CB(NB,JB)*R2(1)
PHI1(2)=CA(NB,JB)*CA(NC,JC)*R1(2)*CB(NB,JB)*CB(NC,JC)*R2(2)
PHI1(3)=CA(NC,JC)*CA(ND,JD)*R1(3)*CB(NC,JC)*CB(ND,JD)*R2(3)
PHI1(4)=CA(ND,JD)*CA(NA,JA)*R1(4)*CB(ND,JD)*CB(NA,JA)*R2(4)

C
PHI2(1)=CA(NA,JA)*CA(NB,JB)*R2(1)*CB(NA,JA)*CB(NB,JB)*R1(1)
PHI2(2)=CA(NB,JB)*CA(NC,JC)*R2(2)*CB(NB,JB)*CB(NC,JC)*R1(2)
PHI2(3)=CA(NC,JC)*CA(ND,JD)*R2(3)*CB(NC,JC)*CB(ND,JD)*R1(3)
PHI2(4)=CA(ND,JD)*CA(NA,JA)*R2(4)*CB(ND,JD)*CB(NA,JA)*R1(4)

C
PHI3(1)=CA(NA,JA)*CB(NB,JB)*R1(1)-CB(NA,JA)*CA(NB,JB)*R2(1)
PHI3(2)=CA(NB,JB)*CB(NC,JC)*R1(2)-CB(NB,JB)*CA(NC,JC)*R2(2)
PHI3(3)=CA(NC,JC)*CB(ND,JD)*R1(3)-CB(NC,JC)*CA(ND,JD)*R2(3)
PHI3(4)=CA(ND,JD)*CB(NA,JA)*R1(4)-CB(ND,JD)*CA(NA,JA)*R2(4)

C
C SUM OVER OMEGA BY PATHS FOR OMEGA EQ 0.5
C
IA=1

C
L=1
IB=1
IC=1
ID=1
PHI(1)=PHI1(1)*PHI1(2)*PHI1(3)*PHI1(4)
CALL FREQ
L=2
IB=1
IC=1
ID=2
PHI(2)=PHI1(1)*PHI1(2)*PHI3(3)*PHI3(4)
CALL FREQ
L=3
IB=1
IC=2
ID=1
PHI(3)=PHI1(1)*PHI3(2)*PHI3(3)*PHI1(4)
CALL FREQ
L=4
IB=1
IC=2
ID=2
PHI(4)=PHI1(1)*PHI3(2)*PHI2(3)*PHI3(4)
CALL FREQ

```

```

SUM0 59
SUM0 60
SUM0 61
SUM0 62
SUM0 63
SUM0 64
SUM0 65
SUM0 66
SUM0 67
SUM0 68
SUM0 69
SUM0 70
SUM0 71
SUM0 72
SUM0 73
SUM0 74
SUM0 75
SUM0 76
SUM0 77
SUM0 78
SUM0 79
SUM0 80
SUM0 81
SUM0 82
SUM0 83
SUM0 84
SUM0 85
SUM0 86
SUM0 87
SUM0 88
SUM0 89
SUM0 90
SUM0 91
SUM0 92
SUM0 93
SUM0 94
SUM0 95
SUM0 96
SUM0 97
SUM0 98
SUM0 99
SUM0 100
SUM0 101
SUM0 102
SUM0 103
SUM0 104
SUM0 105
SUM0 106
SUM0 107
SUM0 108
SUM0 109
SUM0 110
SUM0 111
SUM0 112
SUM0 113
SUM0 114
SUM0 115

```

SUM0 74/74 OPT=2 UU

FTN 4.6+4JH

11/22/78 11.36.27

```

L=5
IH=2
IC=1
IU=1
PHI(5)=PHI(1)*PHI(2)*PHI(3)*PHI(4)
CALL FREQ
L=6
IH=2
IC=1
IU=2
PHI(6)=PHI(1)*PHI(2)*PHI(3)*PHI(4)
CALL FREQ
L=7
IH=2
IC=2
IU=1
PHI(7)=PHI(1)*PHI(2)*PHI(3)*PHI(4)
CALL FREQ
L=8
IH=2
IC=2
IU=2
PHI(8)=PHI(1)*PHI(2)*PHI(3)*PHI(4)
CALL FREQ
C
C BEGIN SUM OVER PATHS
C
F(K,1)=(0.,0.)
DO 60 L=1,8
60 F(K,1) = F(K,1) + PHI(L)*FABCD(L)
IF (RA.EQ.0.5) GO TO 80
C
C SUM OVER OMEGA BY PATHS FOR OMEGA EQ 1.5
C
IA=2
C
L=1
IH=2
IC=2
IU=2
PHI(1)=PHI(1)*PHI(2)*PHI(3)*PHI(4)
CALL FREQ
L=2
IH=2
IC=2
IU=1
PHI(2)=PHI(1)*PHI(2)*PHI(3)*PHI(4)
CALL FREQ
L=3
IH=2
IC=1
IU=2
PHI(3)=PHI(1)*PHI(2)*PHI(3)*PHI(4)
CALL FREQ
L=4
IH=2
IC=1
IU=1

```

```

SUM0 116
SUM0 117
SUM0 118
SUM0 119
SUM0 120
SUM0 121
SUM0 122
SUM0 123
SUM0 124
SUM0 125
SUM0 126
SUM0 127
SUM0 128
SUM0 129
SUM0 130
SUM0 131
SUM0 132
SUM0 133
SUM0 134
SUM0 135
SUM0 136
SUM0 137
SUM0 138
SUM0 139
SUM0 140
SUM0 141
SUM0 142
SUM0 143
SUM0 144
SUM0 145
SUM0 146
SUM0 147
SUM0 148
SUM0 149
SUM0 150
SUM0 151
SUM0 152
SUM0 153
SUM0 154
SUM0 155
SUM0 156
SUM0 157
SUM0 158
SUM0 159
SUM0 160
SUM0 161
SUM0 162
SUM0 163
SUM0 164
SUM0 165
SUM0 166
SUM0 167
SUM0 168
SUM0 169
SUM0 170
SUM0 171
SUM0 172

```

SUM0 74/74 OPT=2 U0

FTN 4.6+433H

11/22/78 11.36.27

```

IU=1
PHI(4)=PHI2(1)*PHI3(2)*PHI1(3)*PHI3(4)
CALL FREQ
L=5
IU=1
IC=2
IU=2
PHI(5)=PHI3(1)*PHI3(2)*PHI2(3)*PHI2(4)
CALL FREQ
L=6
IH=1
IC=2
IU=1
PHI(6)=PHI3(1)*PHI3(2)*PHI3(3)*PHI3(4)
CALL FREQ
L=7
IH=1
IC=1
ID=2
PHI(7)=PHI3(1)*PHI1(2)*PHI3(3)*PHI2(4)
CALL FREQ
L=8
IU=1
IC=1
ID=1
PHI(8)=PHI3(1)*PHI1(2)*PHI1(3)*PHI3(4)
CALL FREQ

```

```

SUM0 173
SUM0 174
SUM0 175
SUM0 176
SUM0 177
SUM0 178
SUM0 179
SUM0 180
SUM0 181
SUM0 182
SUM0 183
SUM0 184
SUM0 185
SUM0 186
SUM0 187
SUM0 188
SUM0 189
SUM0 190
SUM0 191
SUM0 192
SUM0 193
SUM0 194
SUM0 195
SUM0 196
SUM0 197
SUM0 198
SUM0 199
SUM0 200
SUM0 201
SUM0 202
SUM0 203
SUM0 204
SUM0 205
SUM0 206
SUM0 207
SUM0 208

```

C
C
C

```

      BEGIN SUM OVER PATHS
      F(K,2)=(0.+0.)
      DO 70 L=1,8
70    F(K,2) = F(K,2) + PHI(L)*FABCD(L)
      AD CONTINUE
      RETURN
      END

```

LMFNTS 74/74 OPT=2 UU

FTN 4.6-438

11/22/78 11.36.27

```

SUBROUTINE LMENTS
COMMON/LMCOM/WE,WEXE,X(5*2*3)
REAL N(5)

C THIS SUBROUTINE CALCULATES THE EXPECTATION VALUE OF X**I FOR
C ANHARMONIC OSCILLATOR EIGENFUNCTIONS; THE RESULTS ARE STORED IN
C X(K,I,CASE,I+1)
C WHERE
C <J>X**I+K> J=0 FOR CASE 1
C J=2 FOR CASE 2
C K=0,1,2,3,4
C I=0,1,2

EPSIL=-2.*SQRT(WEXE/(15.*WE))

C DETERMINE THE NORMALIZATION CONSTANTS
C
DO 10 IK=1,5
R=IK-1
10 N(IK)=SQRT((1+EPSIL**2.*((5.*R+7.)*(2.*R+7.)*12.*(2.*R+1.)*
ESQRT(R*(K+1.)))/72.)

C DETERMINE THE MATRIX ELEMENTS
C
X(1,1,1)=1.
X(2,1,1)=-EPSIL*(SQRT(2.)*1.)/2./N(1)/N(2)
X(3,1,1)=-EPSIL**2.*(21.*2.*SQRT(6.))/24./N(1)/N(3)
X(4,1,1)=-EPSIL*(SQRT(3.)*1.)/6./N(1)/N(4)
X(5,1,1)=-EPSIL**2.*SQRT(6.)*(5.*SQRT(5.))/12./N(1)/N(5)
X(1,2,1)=-EPSIL**2.*(21.*2.*SQRT(6.))/24./N(1)/N(3)
X(2,2,1)=-EPSIL*(SQRT(2.)*1.-SQRT(3.))/2./N(2)/N(3)
X(3,2,1)=1.
X(4,2,1)=-EPSIL*(SQRT(2.)*SQRT(3.)*SQRT(6.))/2./N(4)/N(3)
X(5,2,1)=-EPSIL**2.*(121.*6.*SQRT(70.))/24./N(5)/N(3)
X(1,1,2)=-EPSIL*3./2./N(1)/N(1)
X(2,1,2)=(1./SQRT(2.)*EPSIL**2.*(7.*SQRT(2.))/12.)/N(1)/N(2)
X(3,1,2)=-EPSIL*3.*(SQRT(2.)*1.)/4./N(1)/N(3)
X(4,1,2)=EPSIL**2.*(39.*2.*SQRT(3.))/8./N(1)/N(4)
X(5,1,2)=-EPSIL*SQRT(6.)/12./N(1)/N(5)
X(1,2,2)=-EPSIL*3.*(SQRT(2.)*1.)/4./N(1)/N(3)
X(2,2,2)=(1.*EPSIL**2.*(17.*SQRT(2.)*74.*209.*SQRT(2./3.)*14.*
ESQRT(3.))/48.)/N(2)/N(3)
X(3,2,2)=-EPSIL*5.*SQRT(3.)/2./N(3)/N(3)
X(4,2,2)=(SQRT(3./2.)*EPSIL**2.*(27.*SQRT(2.)*19.*SQRT(3.)*304.*
E14.*SQRT(6.))/12.)/N(4)/N(3)
X(5,2,2)=-EPSIL*(34.*6.*SQRT(6.)*23.*SQRT(3.))/N(5)/N(3)
X(1,1,3)=(1./2.*EPSIL**2.*181./72.)/N(1)/N(1)
X(2,1,3)=-EPSIL*(3.*SQRT(2.)*2.)/2./N(1)/N(2)
X(3,1,3)=(SQRT(2.)/2.*EPSIL**2.*13.*(9.*13.*SQRT(6.))/72.)/
E/N(1)/N(3)
X(4,1,3)=-EPSIL*(8.*SQRT(3.)*7.)/6./N(1)/N(4)
X(5,1,3)=-EPSIL**2.*SQRT(6.)*(103.*10.*SQRT(5.))/48./N(1)/N(5)
X(1,2,3)=(SQRT(2.)/2.*EPSIL**2.*13.*(9.*3.*SQRT(6.))/72.)/
E/N(1)/N(3)
X(2,2,3)=-EPSIL*(SQRT(3.)*3.*SQRT(2.)*1.)/N(2)/N(3)
X(3,2,3)=15./2.*EPSIL**2.*(41.*SQRT(6.)*170.)/48./N(3)/N(3)
X(4,2,3)=-EPSIL*(12.*SQRT(3.)*9.*SQRT(2.)*2.*SQRT(6.))/2./N(4)/N(3)

```

LMENTS 2
LMENTS 3
LMENTS 4
LMENTS 5
LMENTS 6
LMENTS 7
LMENTS 8
LMENTS 9
LMENTS 10
LMENTS 11
LMENTS 12
LMENTS 13
LMENTS 14
LMENTS 15
LMENTS 16
LMENTS 17
LMENTS 18
LMENTS 19
LMENTS 20
LMENTS 21
LMENTS 22
LMENTS 23
LMENTS 24
LMENTS 25
LMENTS 26
LMENTS 27
LMENTS 28
LMENTS 29
LMENTS 30
LMENTS 31
LMENTS 32
LMENTS 33
LMENTS 34
LMENTS 35
LMENTS 36
LMENTS 37
LMENTS 38
LMENTS 39
LMENTS 40
LMENTS 41
LMENTS 42
LMENTS 43
LMENTS 44
LMENTS 45
LMENTS 46
LMENTS 47
LMENTS 48
LMENTS 49
LMENTS 50
LMENTS 51
LMENTS 52
LMENTS 53
LMENTS 54
LMENTS 55
LMENTS 56
LMENTS 57
LMENTS 58

LMENTS 74/74 OPT=2 UO

FTN 4.6+4338

11/22/78 11.36.27

X(5.2.1)=(SQRT(3.1)*EPSIL**2.*(329..42.*SQRT(10.)*63.*SQRT(4.)*
E363.*SQRT(5.1)/24.1/N(5)/N(3)
RETURN
END

LMENTS 59
LMENTS 60
LMENTS 61
LMENTS 62

TUMU 74/74 OP(=2 UU

FTN 4.6.433H

11/22/78 11.36.27

```

SUBROUTINE TUMU
  COMPLEX ADD(6,2),G(6,2)
  COMMON/CTUMU/RA,RB,RC,RD,K,G(6,2),INDEX
  COMMON/UTUMU/TA,TB,TC,TD,IK,ABCD(6,2),INDEX
  C
  C   DEFINE ROTATIONAL LEVEL INDICES TO BE PASSED TO GREU
  C
  TA=RA
  TB=RB
  TC=RC
  TD=RD
  C
  IK=K
  C
  INDEX=INDEX
  C
  JA=RA+1
  JB=RB+1
  JC=RC+1
  JD=RD+1
  C
  IF (INDEX.EQ.2) GO TO 10
  GO TO (1,2,3,4,5,6),K
  1 G(1,1)=RA*(RA+1.)/4.
  GO TO 7
  2 G(2,1)=RA*(RA+1.)/4.
  GO TO 7
  3 G(3,1)=(RA+1.)*(RA+3.)/4.
  GO TO 7
  4 G(4,1)=0.
  GO TO 7
  5 G(5,1)=(RA+1.)*(2.*RA+3.)/4.
  GO TO 7
  6 G(6,1)=0.
  7 CONTINUE
  CALL GREU
  G(K,1)=G(K,1)*ABCD(K,1)
  GO TO 20
  C
  10 CONTINUE
  GO TO (11,12,13,14,15,16),K
  11 G(1,2)=(RA+3.)*(RA+1.)/4.
  GO TO 17
  12 G(2,2)=(RA+1.)*(RA+2.)/4.
  GO TO 17
  13 G(3,2)=(RA+1.)*(RA+2.)/4.
  GO TO 17
  14 G(4,2)=(2.*RA+1.)*(RA+1.)/4.
  GO TO 17
  15 G(5,2)=0.
  GO TO 7
  16 G(6,2)=0.
  17 CONTINUE
  CALL GREU
  G(K,2)=G(K,2)*ABCD(K,2)
  20 CONTINUE
  RETURN

```

TUMU	2
TUMU	3
TUMU	4
TUMU	5
TUMU	6
TUMU	7
TUMU	8
TUMU	9
TUMU	10
TUMU	11
TUMU	12
TUMU	13
TUMU	14
TUMU	15
TUMU	16
TUMU	17
TUMU	18
TUMU	19
TUMU	20
TUMU	21
TUMU	22
TUMU	23
TUMU	24
TUMU	25
TUMU	6
TUMU	27
TUMU	28
TUMU	29
TUMU	30
TUMU	31
TUMU	32
TUMU	33
TUMU	34
TUMU	35
TUMU	36
TUMU	37
TUMU	38
TUMU	39
TUMU	40
TUMU	41
TUMU	42
TUMU	43
TUMU	44
TUMU	45
TUMU	46
TUMU	47
TUMU	48
TUMU	49
TUMU	50
TUMU	51
TUMU	52
TUMU	53
TUMU	54
TUMU	55
TUMU	56
TUMU	57
TUMU	58

TUMD 74/74 OPT=2 UO

FTN 4.6+433R

11/22/78 11.36.27

END

TUMD 59

GREQ 74/74 OPT=2 UO

FTN 4.6+4338

11/22/78 11.36.27

	SUBROUTINE GREQ	GREQ	2
C		GREQ	3
C	THIS SUBROUTINE CALCULATES THE ELECTRONIC FREQUENCY DENOMINATOR	GREQ	4
C		GREQ	5
	COMPLEX ABCD(4,2),EAB,EAC,EAD	GREQ	6
	COMMON/CFREQ/ NA,NB,NC,ND,NA,RR,RC,RD,W1,W2,W3,K,W(2,5,50),	GREQ	7
	EFAHCD(20),EAB,EAC,EAD,WSIZE,AE,DELTA	GREQ	8
	COMMON/UTUMU/TA,TB,TC,TD,IK,ABCD(6,2),INDEX	GREQ	9
C		GREQ	10
C	CALCULATE ENERGY LEVEL DIFFERENCES AND FREQUENCY DENOMINATORS	GREQ	11
C		GREQ	12
	JA=PA+1.	GREQ	13
	JB=PB+1.	GREQ	14
	JC=PC+1.	GREQ	15
	JD=PD+1.	GREQ	16
	WAB=W(1,NA,JA)-W(1,NB,JB)	GREQ	17
	IF (INDEX.EQ.2) GO TO 10	GREQ	18
	WAC=W(1,NA,JA)-W(1,NC,JC)	GREQ	19
	ABCD(1K+1)=1./(WAC+EAC+W2+W3)/(WAB+W3+EAB)	GREQ	20
	GO TO 20	GREQ	21
10	WAD=W(1,NA,JA)-W(1,ND,JD)	GREQ	22
	AUCD(1K+2)=1./(WAD+EAD+W3)/(WAB+W3+EAB)	GREQ	23
20	CONTINUE	GREQ	24
	RETURN	GREQ	25
	END	GREQ	26

Sample Run

CALCULATION OF THE THIRD ORDER SUSCEPTIBILITY
HCL THIRD ORDER SUSCEPTIBILITY SCAN

THIS CALCULATION USES 4 VIBRATIONAL LEVELS AND 30 ROTATIONAL LEVELS

VIBRATIONAL CONSTANTS:	WE	WEXE	WEYE	WEZE	(IN RECIPROCAL CM)
	.29969403E-04	.52818500E-02	.22430000E-00	.12100000E-01	
ROTATIONAL CONSTANTS:	BE	ALPHA	GAMMA	DE	BETA (IN RECIPROCAL CM)
	.10593416E-02	.30718100E-00	.17724000E-02	.53193600E-03	.75100000E-05
ROTATIONAL CONSTANTS:	AE	DELTA	(IN RECIPROCAL CM)		
	0.	0.			
ELECTRONIC STATE:	ENERGY	MGE(1)	MGE(2)	MGE(3)	
	.80000000E-05	.60000000E-01	.71200000E-00	-.77500000E-01	

VIBRATIONAL TRANSITION MOMENTS (IN DEBYE)

	0	1	2	3	4
0	.11084700E+01	.71200000E-01	-.77500000E-02	-.51500000E-03	
1	.71200000E-01	.11084700E+01	.99320000E-01	-.14300000E-01	
2	-.77500000E-02	.99320000E-01	.11670000E+01	.11930000E-01	
3	-.51500000E-03	-.14300000E-01	.11930000E-01	.11950000E-01	

LINEWIDTHS: ROTATIONAL 0 TO 1 0 TO 2 0 TO 3 0 TO 4 (IN RECIPROCAL CM)
 .2250000E+00 .2400000E+00 .2150000E+00 .2050000E+00

TEMPERATURE FOR THIS CALCULATION IS .3000000E+03 KELV

RESONANCES WITHIN A RANGE OF .1000000E+00 /CM CENTERED ABOUT EACH OF THE PUMP FREQUENCIES ARE INDICATED BY THE PROGRAM

THE PUMP FREQUENCIES ARE .20250680E+04 .20250680E+04 .20250680E+04

FOR THE SUM FREQUENCY .6075200E+04
 THIRD ORDER SUSCEPTIBILITY HAS RE PART -.7961330E-38 CM6/ERG
 THIRD ORDER SUSCEPTIBILITY HAS IM PART .3986172E-42 CM6/ERG
 THIRD ORDER SUSCEPTIBILITY HAS MODULUS .7961330E-38 CM6/ERG

RESONANCES WITHIN A RANGE OF .1000000E+00 /CM CENTERED ABOUT EACH OF THE PUMP FREQUENCIES ARE INDICATED BY THE PROGRAM

THE PUMP FREQUENCIES ARE .20250680E+04 .20250680E+04 .19991410E+04

FOR THE SUM FREQUENCY .60492770E+04
 THIRD ORDER SUSCEPTIBILITY HAS RE PART -.87115050E-38 CM6/ERG
 THIRD ORDER SUSCEPTIBILITY HAS IM PART .37430422E-42 CM6/ERG
 THIRD ORDER SUSCEPTIBILITY HAS MODULUS .87115050E-38 CM6/ERG

RESONANCES WITHIN A RANGE OF .1000000E+00 /CM CENTERED ABOUT EACH OF THE PUMP FREQUENCIES ARE INDICATED BY THE PROGRAM

THE PUMP FREQUENCIES ARE .20250680E+04 .20250680E+04 .19732850E+04

FOR THE SUM FREQUENCY .60234210E+04
 THIRD ORDER SUSCEPTIBILITY HAS RE PART -.95868550E-38 CM6/ERG
 THIRD ORDER SUSCEPTIBILITY HAS IM PART .34826775E-42 CM6/ERG
 THIRD ORDER SUSCEPTIBILITY HAS MODULUS .95868550E-38 CM6/ERG

RESONANCES WITHIN A RANGE OF .1000000E+00 /CM CENTERED ABOUT EACH OF THE PUMP FREQUENCIES ARE INDICATED BY THE PROGRAM

THE PUMP FREQUENCIES ARE .19991410E+04 .19991410E+04 .19991410E+04

FOR THE SUM FREQUENCY .59074230E+04
 THIRD ORDER SUSCEPTIBILITY HAS RE PART -.10406500E-37 CM6/ERG
 THIRD ORDER SUSCEPTIBILITY HAS IM PART .31681730E-42 CM6/ERG
 THIRD ORDER SUSCEPTIBILITY HAS MODULUS .10406500E-37 CM6/ERG

RESONANCES WITHIN A RANGE OF .1000000E+00 /CM CENTERED ABOUT EACH OF THE PUMP FREQUENCIES ARE INDICATED BY THE PROGRAM

THE PUMP FREQUENCIES ARE .19491410E+04 .19991410E+04 .20250680E+04

FOR THE SUM FREQUENCY .60233500E+04
THIRD ORDER SUSCEPTIBILITY HAS RE PART -.95265547E-38 CM6/ENG
THIRD ORDER SUSCEPTIBILITY HAS IM PART .36725773E-42 CM6/ENG
THIRD ORDER SUSCEPTIBILITY HAS MODULUS .95265547E-38 CM6/ENG

RESONANCES WITHIN A RANGE OF .10000000E+00 /CM CENTERED ABOUT EACH OF THE PUMP FREQUENCIES ARE INDICATED BY THE PROGRAM

THE PUMP FREQUENCIES ARE .19491410E+04 .19991410E+04 .19732850E+04

FOR THE SUM FREQUENCY .59715670E+04
THIRD ORDER SUSCEPTIBILITY HAS RE PART -.11493508E-37 CM6/ENG
THIRD ORDER SUSCEPTIBILITY HAS IM PART .28305723E-42 CM6/ENG
THIRD ORDER SUSCEPTIBILITY HAS MODULUS .11493508E-37 CM6/ENG

RESONANCES WITHIN A RANGE OF .10000000E+00 /CM CENTERED ABOUT EACH OF THE PUMP FREQUENCIES ARE INDICATED BY THE PROGRAM

THE PUMP FREQUENCIES ARE .19732850E+04 .19732850E+04 .19732850E+04

FOR THE SUM FREQUENCY .59198550E+04
THIRD ORDER SUSCEPTIBILITY HAS RE PART -.13898582E-37 CM6/ENG
THIRD ORDER SUSCEPTIBILITY HAS IM PART .19590024E-42 CM6/ENG
THIRD ORDER SUSCEPTIBILITY HAS MODULUS .13898582E-37 CM6/ENG

RESONANCES WITHIN A RANGE OF .10000000E+00 /CM CENTERED ABOUT EACH OF THE PUMP FREQUENCIES ARE INDICATED BY THE PROGRAM

THE PUMP FREQUENCIES ARE .19732850E+04 .19732850E+04 .20250680E+04

FOR THE SUM FREQUENCY .59716340E+04
THIRD ORDER SUSCEPTIBILITY HAS RE PART -.11965770E-37 CM6/ENG
THIRD ORDER SUSCEPTIBILITY HAS IM PART .25408519E-42 CM6/ENG
THIRD ORDER SUSCEPTIBILITY HAS MODULUS .11965770E-37 CM6/ENG

RESONANCES WITHIN A RANGE OF .10000000E+00 /CM CENTERED ABOUT EACH OF THE PUMP FREQUENCIES ARE INDICATED BY THE PROGRAM

THE PUMP FREQUENCIES ARE .19732850E+04 .19732850E+04 .19991410E+04

FOR THE SUM FREQUENCY .59457110E+04
THIRD ORDER SUSCEPTIBILITY HAS RE PART -.12617493E-37 CM6/ENG
THIRD ORDER SUSCEPTIBILITY HAS IM PART .24352396E-42 CM6/ENG
THIRD ORDER SUSCEPTIBILITY HAS MODULUS .12617493E-37 CM6/ENG

RESONANCES WITHIN A RANGE OF .10000000E+00 /CM CENTERED ABOUT EACH OF THE PUMP FREQUENCIES ARE INDICATED BY THE PROGRAM

THE PUMP FREQUENCIES ARE .20250680E+04 .19991410E+04 .19732850E+04
 FOR THE SUM FREQUENCY .5997440E+04
 THIRD ORDER SUSCEPTIBILITY HAS RE PART -.10487707E-37 CM6/ENG
 THIRD ORDER SUSCEPTIBILITY HAS IM PART .31783441E-42 CM6/ENG
 THIRD ORDER SUSCEPTIBILITY HAS MODULUS .10487707E-37 CM6/ENG

THAT'S ALL FOLKS

APPENDIX B: $\chi^{(1)}$ CODE

Program Structure and Performance

This program is quite similar to the $\chi^{(3)}$ code. It is, however, much less complex. Its essential steps are:

- (1) Calculation of rotational and vibrational terms, and partition functions
- (2) Calculation of rotational populations and all transition frequencies allowed by selection rules
- (3) Calculation of the frequency denominator which occurs in the sum over states
- (4) Calculation of CHIONE accounting for population in various vibrational states
- (5) Derivation of the absorption coefficient and the refractive index minus unity from the value of CHIONE
- (6) Evaluation of the k-vector mismatches if desired

Two subroutines are called in the course of the program. Subroutine ENERGY calculates the required energy levels and partition function. Subroutine CHI calculates the real and imaginary parts of CHI for a particular lower state vibrational level.

The data is input according to READ statements at the beginning of the main program, in a format very similar to that used by the $\chi^{(3)}$ code. All input variables should be expressed in cgs units unless otherwise specified. Unspecified variables will be preset to zero by the program.

The input variables for this program are as follows:

- LABEL is an alphanumeric array which stores the name of the molecule, for which the calculation is performed
- NV is the number of vibrational levels used in the calculation
- NJ is the number of rotational levels used in the calculation
- NOVT is the number of overtones used in the calculation

WE, WEXE, WEYE, WEZE are the familiar vibrational constants: ω_e , $\omega_e x_e$, $\omega_e y_e$, $\omega_e z_e$, respectively

BE, ALPHA, GAMMA, DE, BETA are the usual rotational constants: B_e , α_e , γ_e , D_e , δ_e , respectively

U(5,5) is a real array which contains the dipole moments for vibrational transitions between states labeled N and M (in Debye)

LINEW is a real array which stores the linewidths for vibrational and rotational transitions

POPU is a real array consisting of the initial distribution of population among the vibrational levels

TEMP is the temperature of the system being modeled (in Kelvin)

WS, WP are pump frequencies; the k-vector mismatches are calculated between the pairs of frequencies

DN is the population transfer between adjacent vibrational levels (used to compute the k-vector mismatch)

There are three labeled COMMON blocks in the program.

VIBCOM contains the vibrational constants WE, WEXE, WEYE, WEZE

ROTCOM contains the rotational constants BE, ALPHA, GAMMA, DE

BETA, TCOM contains the temperature inputted as TEMP

The output consists of various blocks listing the following:

- (1) All the input data
- (2) The input frequencies and the population transferred between adjacent vibrational levels
- (3) For each input frequency, the absorption coefficient and the refractive index minus unity
- (4) The k-vector mismatch

A complete calculation for one molecule, considering 1 vibrational level, 30 rotational levels, and 1 overtone takes less than a second on a CDC 6600, yielding results for 42 pairs of input frequencies.

Program Listing

74/74 OPT=2

FTN 4.6-4338

12/01/78 09.32.25

C	PROGRAM CHIONE(INPUT,OUTPUT,TAPE5=INPUT,TAPE6=OUTPUT)	CHIONE	2
C		CHIONE	3
C	THIS PROGRAM CALCULATES FIRST ORDER SUSCEPTIBILITIES AND RELATED	CHIONE	4
C	PROPERTIES FROM SPECTROSCOPIC DATA	CHIONE	5
C		CHIONE	6
C		CHIONE	7
C	INPUTS	CHIONE	8
C		CHIONE	9
C		CHIONE	10
C		CHIONE	11
C	LABEL(I), I=1,8	(8A10) CHIONE	12
C		CHIONE	13
C		CHIONE	14
C	NV,NJ,NOVT	(3I5) CHIONE	15
C		CHIONE	16
C	NV = NUMBER OF VIBRATIONAL LEVELS USED IN THIS CALCULATION	CHIONE	17
C	NJ = NUMBER OF ROTATIONAL LEVELS USED IN THIS CALCULATION	CHIONE	18
C	NOVT = NUMBER OF OVERTONES USED IN THIS CALCULATION	CHIONE	19
C		CHIONE	20
C		CHIONE	21
C	WE,WEXF,WEYE,WEZE	(4E15.8) CHIONE	22
C		CHIONE	23
C	THESE ARE THE VIBRATIONAL CONSTANTS (IN RECIPROCAL CM)	CHIONE	24
C		CHIONE	25
C		CHIONE	26
C	BE,ALPHA,GAMMA,DE,ETA	(5E15.8) CHIONE	27
C		CHIONE	28
C	THESE ARE THE ROTATIONAL CONSTANTS (IN RECIPROCAL CM)	CHIONE	29
C		CHIONE	30
C		CHIONE	31
C	FOR EACH VIBRATIONAL LEVEL, N---	CHIONE	32
C		CHIONE	33
C	U(M,N), M=1,NOVT+2	(5E15.8) CHIONE	34
C		CHIONE	35
C	U(M,N) = DIPOLE MOMENTS FOR VIBRATIONAL TRANSITIONS N TO M	CHIONE	36
C	(IN DEBYE)	CHIONE	37
C		CHIONE	38
C		CHIONE	39
C	LINEW(M,N), M=1,NOVT+2	(5E15.8) CHIONE	40
C		CHIONE	41
C	LINEWIDTHS (IN RECIPROCAL CM) FOR ALL OVERTONE TRANSITIONS NEEDED	CHIONE	42
C		CHIONE	43
C		CHIONE	44
C	POPI(N)	(5E15.8) CHIONE	45
C		CHIONE	46
C	INITIAL DISTRIBUTION OF POPULATION AMONG THE VIBRATIONAL LEVELS	CHIONE	47
C		CHIONE	48
C		CHIONE	49
C	TEMP	(1E15.8) CHIONE	50
C		CHIONE	51
C	TEMP = TEMPERATURE OF THE MODEL SYSTEM (KELVIN)	CHIONE	52
C		CHIONE	53
C		CHIONE	54
C	WS,WP,DN	(3F15.8) CHIONE	55
C		CHIONE	56
C	WS AND WP ARE PUMP FREQUENCIES; DN IS THE POPULATION TRANSFER BTW	CHIONE	57
C	ADJACENT VIBRATIONAL LEVELS. THE PROGRAM ENDS WHEN ALL ARE ZERO.	CHIONE	58

C		CHIONE	59
CS	DEBHG	CHIONE	60
CS	ANKAYS	CHIONE	61
CS	GOTOS	CHIONE	62
	REAL LINEW(5,5)	CHIONE	63
	DIMENSION DELTAE(500),U(5,5),LINEW(5,5),POPU(5)	CHIONE	64
	DIMENSION CHIE(5,2),CHIIM(5,2),LABEL(8)	CHIONE	65
	COMMON/VIBCOM/WE,WEXE,WEYE,WEZE	CHIONE	66
	COMMON/ROTCON/RE,ALPHA,GAMMA,DE,BETA	CHIONE	67
	COMMON/TCUM/TFMP	CHIONE	68
C		CHIONE	69
C	READ IN DATA	CHIONE	70
C		CHIONE	71
	READ(5,101) (LABEL(1),1=1,8)	CHIONE	72
101	FORMAT(8A10)	CHIONE	73
	WRITE(6,102) LABEL	CHIONE	74
102	FORMAT(1H1,/,5X, *CALCULATION OF THE FIRST ORDER SUSCEPTIBILITY	CHIONE	75
	AND RELATED PROPERTIES*,/,5X,8A10,/,)	CHIONE	76
	READ(5,103) NV,NJ,NOVT	CHIONE	77
103	FORMAT(3I5)	CHIONE	78
	WRITE(6,104) NV,NJ,NOVT	CHIONE	79
104	FORMAT(/,5X,*THIS CALCULATION USED*,15,* VIBRATIONAL LEVELS AND*,	CHIONE	80
	15,* ROTATIONAL LEVELS WITH*,15,* OVERTONES*)	CHIONE	81
	READ(5,105) WE,WEXE,WEYE,WEZE	CHIONE	82
105	FORMAT(5E15.8)	CHIONE	83
	WRITE(6,106)	CHIONE	84
106	FORMAT(/,5X,*VIBRATIONAL CONSTANTS:*,6X,*WE*,12X,*WEXE*,11X,*WEYE*	CHIONE	85
	*,11X,*WEZE*,12X,* (IN RECIPROCAL CM)*)	CHIONE	86
	WRITE(6,107) WE,WEXE,WEYE,WEZE	CHIONE	87
107	FORMAT(26X,5E15.8)	CHIONE	88
	READ(5,105) RE,ALPHA,GAMMA,DE,BETA	CHIONE	89
	WRITE(6,108)	CHIONE	90
108	FORMAT(/,5X,*ROTATIONAL CONSTANTS:*,7X,*BE*,12X,*ALPHA*,10X,	CHIONE	91
	GAMMA,11X,*DE*,12X,*BETA*,12X,* (IN RECIPROCAL CM)*)	CHIONE	92
	WRITE(6,109) RE,ALPHA,GAMMA,DE,BETA	CHIONE	93
	WRITE(6,109)	CHIONE	94
109	FORMAT(1H1,/,5X,*VIBRATIONAL TRANSITION MOMENTS (IN DEBYE)*,/,	CHIONE	95
	3X,*N*,11X,*N*0*,12X,*N*1*,12X,*N*2*,12X,*N*3*,12X,*N*4*)	CHIONE	96
	NOVT=NOVT+2	CHIONE	97
	DO 10 N=1,NV	CHIONE	98
	READ(5,105) (U(M,N),M=1,NOVT)	CHIONE	99
	NN=N-1	CHIONE	100
	WRITE(6,110) NN, (U(M,N),M=1,NOVT)	CHIONE	101
110	FORMAT(/,5X,15,5X,5E15.8)	CHIONE	102
10	CONTINUE	CHIONE	103
	WRITE(6,111)	CHIONE	104
111	FORMAT(/,5X,*TRANSITION LINEWIDTHS (IN RECIPROCAL CM)*,/,	CHIONE	105
	3X,*N*,11X,*N*0*,12X,*N*1*,12X,*N*2*,12X,*N*3*,12X,*N*4*)	CHIONE	106
	DO 20 N=1,NV	CHIONE	107
	READ(5,105) (L(NEW(M,N),M=1,NOVT)	CHIONE	108
	NN=N-1	CHIONE	109
	WRITE(6,112) NN, (L(NEW(M,N),M=1,NOVT)	CHIONE	110
112	FORMAT(/,5X,15,5X,5E15.8)	CHIONE	111
20	CONTINUE	CHIONE	112
	READ(5,105) (POPU(N),N=1,NV)	CHIONE	113
	WRITE(6,113)	CHIONE	114
113	FORMAT(/,5X,*THE INITIAL VIBRATIONAL LEVEL POPULATIONS*,/,	CHIONE	115

CHTONE 74/74 OPT=2

FTN 4.6-433B

12/01/78 09.32.25

```

      E22X,.00,14X,.01,.14X,.02,.14X,.03,.14X,.04)
      WRITE(6,114) (POPU(N),N=1,NV)
114  FORMAT(/,15X,5E15.8)
      READ(5,105) TEMP
      WRITE(6,115) TEMP
115  FORMAT(/,5X,*TEMPERATURE FOR THIS CALCULATION IS *.E15.8.* KELV*)
C
C      NORMALIZE THE POPULATION DISTRIBUTION
C
      PUPTOT=0.
      DO 30 N=1,NV
30  PUPTOT=PUPTOT+POPU(N)
      DO 40 N=1,NV
40  POPU(N)=POPU(N)/PUPTOT
C
C      READ IN WS,WP,DN; TERMINATE THE PROGRAM IF THEY ARE ALL ZERO
C
45  READ(5,105) WS,WP,DN
      IF(WS.EQ.0..AND.WP.EQ.0..AND.DN.EQ.0.) GO TO 1000
      WRITE(6,116) WS,WP,DN
116  FORMAT(/,5X,*THE PUMP FREQUENCIES ARE*.2(5X,E15.8),/,5X,*THE
      *POPULATION TRANSFERED BETWEEN ADJACENT LEVELS IS*.5X,E15.8)
C
C      BEGIN THE CALCULATION OF CHI AT WS AND WP; FIND ACOEF AND REMION
C
      DO 60 K=1,2
      W=WS
      IF(K.EQ.2) W=WP
      CHIRET=0.
      CHIIMT=0.
      DO 50 IGROUP=1,NV
      CALL ENERGY(IGROUP,NJ,NOVT,DELTA.E,0)
      CALL CHI(IGROUP,NJ,NOVT,W,Q,U,LINEW,DELTA.E,CHIRE(IGROUP,K),
      *CHIIM(IGROUP,K))
      CHIRET=CHIRET+POPU(IGROUP)*CHIRE(IGROUP,K)
50  CHIIMT=CHIIMT+POPU(IGROUP)*CHIIM(IGROUP,K)
      Z=SQRT(1+.4*.3.1415927*CHIRET)
      ACOEF=4*.3.1415927*W*CHIIMT/Z
      REMION=Z-1.
      WRITE(6,117) W,ACOE,REMION
117  FORMAT(/,5X,*FOR THE FREQUENCY *.E15.8,/,5X,*THE ABSORPTION COEFIC
      *IENT IS *.E15.8,/,5X,*THE REFRACTIVE INDEX MINUS UNITY IS *.E15.8)
      CONTINUE
      IF(NV.EQ.1) GO TO 45
C
C      BEGIN THE CALCULATION OF THE K-VECTOR MISMATCH
C
      ITOP=NV-1
      DO 70 I=1,ITOP
      ILOWER=I
      IUPPER=I+1
      WAVEM=WS*UN*(CHIRE(IUPPER,1)-CHIRE(ILOWER,1)-CHIRE(IUPPER,2)+
      *CHIRE(ILOWER,2))*2*.3.1415927
      IL=ILOWER-1
      IU=IUPPER-1
      WRITE(6,118) IL,IU,WAVEM
118  FORMAT(/,5X,*THE K-VECTOR MISMATCH VARIATION DUE TO POPULATION

```

CHTONE 116
CHTONE 117
CHTONE 118
CHTONE 119
CHTONE 120
CHTONE 121
CHTONE 122
CHTONE 123
CHTONE 124
CHTONE 125
CHTONE 126
CHTONE 127
CHTONE 128
CHTONE 129
CHTONE 130
CHTONE 131
CHTONE 132
CHTONE 133
CHTONE 134
CHTONE 135
CHTONE 136
CHTONE 137
CHTONE 138
CHTONE 139
CHTONE 140
CHTONE 141
CHTONE 142
CHTONE 143
CHTONE 144
CHTONE 145
CHTONE 146
CHTONE 147
CHTONE 148
CHTONE 149
CHTONE 150
CHTONE 151
CHTONE 152
CHTONE 153
CHTONE 154
CHTONE 155
CHTONE 156
CHTONE 157
CHTONE 158
CHTONE 159
CHTONE 160
CHTONE 161
CHTONE 162
CHTONE 163
CHTONE 164
CHTONE 165
CHTONE 166
CHTONE 167
CHTONE 168
CHTONE 169
CHTONE 170
CHTONE 171
CHTONE 172

CHTONE 74/1* OPT=2

FTN 4.6*4338

12/01/78 09.32.25

ETTRANSFER BETWEEN LEVELS*.15.* AND*.15.* IS *.E15.8)
70 CONTINUE
GO TO 45
1000 WRITE(6*120)
120 FURMAT(////.5X,*THAT#S ALL FOLKS*)
STOP
END

CHTONE 173
CHTONE 174
CHTONE 175
CHTONE 176
CHTONE 177
CHTONE 178
CHTONE 179

ENERGY 74/74 OPT=2

FTN 4.6+433B

12/01/78 09.12.25

	SUBROUTINE ENERGY(IIGROUN,NJ,NOVT,DELTAE,Q)	ENERGY	2
C		ENERGY	3
C	THIS SUBROUTINE CALCULATES THE NEEDED ENERGY LEVELS AND PARTITION	ENERGY	4
C	FUNCTIONS: ENERGY LEVEL DIFFERENCES ARE STORED LINEARLY IN	ENERGY	5
C	DELTAE. THE PARTITION FUNCTION IS STORED IN Q	ENERGY	6
C		ENERGY	7
C5	DEBUG	ENERGY	8
C5	ARRAYS	ENERGY	9
C5	GOTOS	ENERGY	10
	71MENSION DELTAE(500)	ENERGY	11
	COMMON/VIBCOM/WE,WEAE,WEYE,WEZE	ENERGY	12
	COMMON/ROTCOM/BE,ALPHA,GAMMA,DE,BETA	ENERGY	13
	COMMON/TCUM/TEMP	ENERGY	14
	IBRANC=-1	ENERGY	15
	LOWER=IGROUN-1	ENERGY	16
	UPPER=IGROUN-1	ENERGY	17
	ISTORE=0	ENERGY	18
	HE=2.*DE*(12.*BE**2-ALPHA*WE)/(3.*WE**2)	ENERGY	19
A	IKOT=0	ENERGY	20
	X=LOWER+0.5	ENERGY	21
	B=BE-ALPHA*X+GAMMA*X**2	ENERGY	22
	D=DE*BETA*X	ENERGY	23
11	Y=B*IKOT*(IKOT+1)-D*(IKOT*(IKOT+1))**2+HE*(IKOT*(IKOT+1))**3	ENERGY	24
	Z=WE*X-WEAE*X**2+WEYE*X**3+WEZE*X**4	ENERGY	25
	INDEX=IKOT+ISTORE+1	ENERGY	26
	DELTAE(INDEX)=-Y-Z	ENERGY	27
	IKOT=IKOT+1	ENERGY	28
	IF(IKOT.LE.NJ) GO TO 11	ENERGY	29
	IKOT=0	ENERGY	30
	X=UPPER+0.5	ENERGY	31
	B=BE-ALPHA*X+GAMMA*X**2	ENERGY	32
	D=DE*BETA*X	ENERGY	33
1A	JROT=IKOT+IBRANC	ENERGY	34
	Y=B*JROT*(JROT+1)-D*(JROT*(JROT+1))**2+HE*(JROT*(JROT+1))**3	ENERGY	35
	Z=WE*X-WEAE*X**2+WEYE*X**3+WEZE*X**4	ENERGY	36
	INDEX=IKOT+ISTORE+1	ENERGY	37
	DELTAE(INDEX)=DELTAE(INDEX)+Y+Z	ENERGY	38
	IKOT=IKOT+1	ENERGY	39
	IF(IKOT.LE.NJ) GO TO 18	ENERGY	40
	IKOT=0	ENERGY	41
24	JKOT=IKOT+IBRANC	ENERGY	42
	INDEX=IKOT+ISTORE+1	ENERGY	43
	IF(JKOT.LT.0) DELTAE(INDEX)=0.	ENERGY	44
	IKOT=IKOT+1	ENERGY	45
	IF(IKOT.LE.NJ) GO TO 24	ENERGY	46
	IF(IBRANC.EQ.-1) GO TO 27	ENERGY	47
	ITEST=IGROUN+NOVT-1	ENERGY	48
	IF(UPPER.LE.ITEST) GO TO 28	ENERGY	49
	R=BE-ALPHA/2.*GAMMA/4.	ENERGY	50
	Q=6.9503E-01*TEMP/R	ENERGY	51
	RETURN	ENERGY	52
27	IBRANC=1	ENERGY	53
	ISTORE=NJ+ISTORE	ENERGY	54
	GO TO A	ENERGY	55
2A	IBRANC=-1	ENERGY	56
	UPPER=UPPER+1	ENERGY	57
	ISTORE=NJ+ISTORE	ENERGY	58

ENFRGY 74/74 OPT=2

FTN 4.6+433B

12/01/78 09.32.25

GO TO 0
END

ENERGY 59
ENERGY 60

CHI 74/74 OPT=2

FTN 4.6+433B

12/01/78 09.32.25

```

SUBROUTINE CHI(N,NJ,NOVT,W,Q,U,LINEW,DELTAE,CHIRE,CHIIM)
C
C THIS SUBROUTINE CALCULATES THE REAL AND IMAGINARY PARTS OF CHI FOR
C PARTICULAR LOWER STATE VIBRATIONAL LEVEL
C
CS DEBING
CS ANWAYS
CS GUTOS
REAL L(LINEW(5,5))
DIMENSION DELTAE(500),U(5,5),LINEW(5,5)
COMMON/VIUCOM/WE,WFAE,WEYE,WEZE
COMMON/ROTCOM/BE,ALPHA,GAMMA,DE,BETA
COMMON/TCUM/TEMP
INOT=0
ISTORE=0
JSTORE=0
IBRANC=-1
SUMA=0.
SUMB=0.
SUMC=0.
SUMD=0.
CHIRE=0.
CHIIM=0.
6 INDEX=IROT+ISTORE+1
IF(DELTAE(INDEX).EQ.0) GO TO 16
JNDEX=JSTORE+1
Z=(DELTAE(INDEX)+W)**2+0.25*LINEW(JNDEX,N)**2
SUM1=(DELTAE(INDEX)+W)/Z
Z=(DELTAE(INDEX)-W)**2+0.25*LINEW(JNDEX,N)**2
SUM2=(DELTAE(INDEX)-W)/Z
SUMG=SUM1+SUM2
Z=(DELTAE(INDEX)+W)**2+0.25*LINEW(JNDEX,N)**2
SUM1=-0.5*LINEW(JNDEX,N)/Z
Z=(DELTAE(INDEX)-W)**2+0.25*LINEW(JNDEX,N)**2
SUM2=-0.5*LINEW(JNDEX,N)/Z
SUMH=SUM1+SUM2
15 Z=IROT+1
IF(IBRANC.EQ.-1) Z=IROT
SUMA=Z+SUMG+SUMA
SUMB=Z+SUMH+SUMB
IF(IBRANC.EQ.-1) GO TO 18
Z=U(JNDEX,N)**2
SUMC=Z+SUMA+SUMC
SUMD=Z+SUMB+SUMD
IF(JSTORE.LE.NOVT) GO TO 20
Z=IROT+(INOT+1)
HE=2.*DE*(12.*HE**2-ALPHA*WE)/(3.*WE**2)
Z=(RE-ALPHA*0.5+GAMMA*0.25)*Z-(DE*BETA*U.5)*Z**2+HE*Z**3
Z=(2*IROT+1)*EXP(-Z/6.9503F-01/TEMP)/U
CHIRE=SUMC*Z+CHIRE
CHIIM=SUMD*Z+CHIIM
IF(IROT.LE.NJ) GO TO 27
CHIRE=1.357E-1*CHIRE
CHIIM=1.357E-1*CHIIM
RETURN
16 SUMG=0.
SUMH=0.

```

```

CHI 2
CHI 3
CHI 4
CHI 5
CHI 6
CHI 7
CHI 8
CHI 9
CHI 10
CHI 11
CHI 12
CHI 13
CHI 14
CHI 15
CHI 16
CHI 17
CHI 18
CHI 19
CHI 20
CHI 21
CHI 22
CHI 23
CHI 24
CHI 25
CHI 26
CHI 27
CHI 28
CHI 29
CHI 30
CHI 31
CHI 32
CHI 33
CHI 34
CHI 35
CHI 36
CHI 37
CHI 38
CHI 39
CHI 40
CHI 41
CHI 42
CHI 43
CHI 44
CHI 45
CHI 46
CHI 47
CHI 48
CHI 49
CHI 50
CHI 51
CHI 52
CHI 53
CHI 54
CHI 55
CHI 56
CHI 57
CHI 58

```

CHI 74/74 OPT=2

FTN 4.6+4338

12/01/78 09.32.25

```
      GO TO 15
1A  ISTORE=ISTORE+NJ
      IBRANC=1
      GO TO 6
20  JSTORE=JSTORE+1
      ISTORE=ISTORE+NJ
      IBRANC=-1
      SUMA=0.
      SUMB=0.
      GO TO 6
27  IROT=IROT+1
      ISTORE=0
      JSTORE=0
      IBRANC=-1
      SUMA=0.
      SUMB=0.
      SUMC=0.
      SUMD=0.
      GO TO 6
      END
```

```
CHI 59
CHI 60
CHI 61
CHI 62
CHI 63
CHI 64
CHI 65
CHI 66
CHI 67
CHI 68
CHI 69
CHI 70
CHI 71
CHI 72
CHI 73
CHI 74
CHI 75
CHI 76
CHI 77
CHI 78
```

Sample Run

CALCULATION OF THE FIRST ORDER SUSCEPTIBILITY AND RELATED PROPERTIES
DEUTERIUM FLUORIDE

THIS CALCULATION USED 1 VIBRATIONAL LEVELS AND 30 ROTATIONAL LEVELS WITH 1 OVERTONES

VIBRATIONAL CONSTANTS:	WE	WEKE	WEYE	WEZE	(IN RECIPROCAL CM)
	.29985000E+04	.47190000E+02	.34000000E+00	.30300000E+02	
ROTATIONAL CONSTANTS:	BE	ALPHA	GAMMA	DE	BETA (IN RECIPROCAL CM)
	.11001700E+02	.30400000E+00	.35000000E+02	.59290000E+03	.14000000E+04

VIBRATIONAL TRANSITION MOMENTS (IN DEBYE)

N	N=0	N=1	N=2	N=3	N=4
0	.18140000E+01	.84100000E-01	-.83700000E-02		

TRANSITION LINEWIDTHS (IN RECIPROCAL CM)

N	N=0	N=1	N=2	N=3	N=4
0	.42300000E+00	.46000000E+00	.40400000E+00		

THE INITIAL VIBRATIONAL LEVEL POPULATIONS

	0	1	2	3	4
	.10000000E+01				

TEMPERATURE FOR THIS CALCULATION IS .30000000E+03 KELV

THE PUMP FREQUENCIES ARE .60000000E+04 .15400000E+04
 THE POPULATION TRANSFERRED BETWEEN ADJACENT LEVELS IS. .10000000E+04

FOR THE FREQUENCY .60000000E+04
 THE ABSORPTION COEFFICIENT IS .58100090E-04
 THE REFRACTIVE INDEX MINUS UNITY IS -.30664801E-04

FOR THE FREQUENCY .15400000E+04
 THE ABSORPTION COEFFICIENT IS .36584782E-03
 THE REFRACTIVE INDEX MINUS UNITY IS -.36218270E-03

THE PUMP FREQUENCIES ARE .60000000E+04 .15450000E+04
 THE POPULATION TRANSFERRED BETWEEN ADJACENT LEVELS IS. .10000000E+04

FOR THE FREQUENCY .60000000E+04
 THE ABSORPTION COEFFICIENT IS .58100090E-04
 THE REFRACTIVE INDEX MINUS UNITY IS -.30664801E-04

FOR THE FREQUENCY .15450000E+04
 THE ABSORPTION COEFFICIENT IS .36373412E-03
 THE REFRACTIVE INDEX MINUS UNITY IS -.35939920E-03

THE PUMP FREQUENCIES ARE .60000000E+04 .15500000E+04
 THE POPULATION TRANSFERRED BETWEEN ADJACENT LEVELS IS. .10000000E+04

FOR THE FREQUENCY .60000000E+04
 THE ABSORPTION COEFFICIENT IS .58100090E-04
 THE REFRACTIVE INDEX MINUS UNITY IS -.30664801E-04

FOR THE FREQUENCY .15500000E+04
 THE ABSORPTION COEFFICIENT IS .36164600E-03
 THE REFRACTIVE INDEX MINUS UNITY IS -.35444077E-03

THE PUMP FREQUENCIES ARE .6000000E+04 .1555000E+04
 THE POPULATION TRANSFERED BETWEEN ADJACENT LEVELS IS. .1000000E-04
 FOR THE FREQUENCY .6000000E+04
 THE ABSORPTION COEFFICIENT IS .5810009E-04
 THE REFRACTIVE INDEX MINUS UNITY IS -.3866480E-04
 FOR THE FREQUENCY .1555000E+04
 THE ABSORPTION COEFFICIENT IS .3595032E-03
 THE REFRACTIVE INDEX MINUS UNITY IS -.3539072E-03

THE PUMP FREQUENCIES ARE .6000000E+04 .1560000E+04
 THE POPULATION TRANSFERED BETWEEN ADJACENT LEVELS IS. .1000000E-04
 FOR THE FREQUENCY .6000000E+04
 THE ABSORPTION COEFFICIENT IS .5810009E-04
 THE REFRACTIVE INDEX MINUS UNITY IS -.3866480E-04
 FOR THE FREQUENCY .1560000E+04
 THE ABSORPTION COEFFICIENT IS .3575453E-03
 THE REFRACTIVE INDEX MINUS UNITY IS -.3511902E-03

THE PUMP FREQUENCIES ARE .6000000E+04 .1565000E+04
 THE POPULATION TRANSFERED BETWEEN ADJACENT LEVELS IS. .1000000E-04
 FOR THE FREQUENCY .6000000E+04
 THE ABSORPTION COEFFICIENT IS .5810009E-04
 THE REFRACTIVE INDEX MINUS UNITY IS -.3866480E-04
 FOR THE FREQUENCY .1565000E+04
 THE ABSORPTION COEFFICIENT IS .3555321E-03
 THE REFRACTIVE INDEX MINUS UNITY IS -.3485132E-03

THE PUMP FREQUENCIES ARE .6000000E+04 .1570000E+04
 THE POPULATION TRANSFERED BETWEEN ADJACENT LEVELS IS. .1000000E-04
 FOR THE FREQUENCY .6000000E+04
 THE ABSORPTION COEFFICIENT IS .5810009E-04
 THE REFRACTIVE INDEX MINUS UNITY IS -.3866480E-04
 FOR THE FREQUENCY .1570000E+04
 THE ABSORPTION COEFFICIENT IS .3535434E-03
 THE REFRACTIVE INDEX MINUS UNITY IS -.3458521E-03

THE PUMP FREQUENCIES ARE .6000000E+04 .1575000E+04
 THE POPULATION TRANSFERED BETWEEN ADJACENT LEVELS IS. .1000000E-04
 FOR THE FREQUENCY .6000000E+04
 THE ABSORPTION COEFFICIENT IS .5810009E-04
 THE REFRACTIVE INDEX MINUS UNITY IS -.3866480E-04

FOR THE FREQUENCY .19750000E+04
THE ABSORPTION COEFFICIENT IS .3815788E-03
THE REFRACTIVE INDEX MINUS UNITY IS -.3432144E-03

THE PUMP FREQUENCIES ARE .60000000E+04 .15800000E+04
THE POPULATION TRANSFERRED BETWEEN ADJACENT LEVELS IS .10000000E-04

FOR THE FREQUENCY .64000000E+04
THE ABSORPTION COEFFICIENT IS .58100090E-04
THE REFRACTIVE INDEX MINUS UNITY IS -.38064801E-04

FOR THE FREQUENCY .17000000E+04
THE ABSORPTION COEFFICIENT IS .34463827E-03
THE REFRACTIVE INDEX MINUS UNITY IS -.34059991E-03

THE PUMP FREQUENCIES ARE .60000000E+04 .15850000E+04
THE POPULATION TRANSFERRED BETWEEN ADJACENT LEVELS IS .10000000E-04

FOR THE FREQUENCY .60000000E+04
THE ABSORPTION COEFFICIENT IS .58100090E-04
THE REFRACTIVE INDEX MINUS UNITY IS -.38064801E-04

FOR THE FREQUENCY .15850000E+04
THE ABSORPTION COEFFICIENT IS .34772139E-03
THE REFRACTIVE INDEX MINUS UNITY IS -.33000010E-03

THE PUMP FREQUENCIES ARE .60000000E+04 .15900000E+04
THE POPULATION TRANSFERRED BETWEEN ADJACENT LEVELS IS .10000000E-04

FOR THE FREQUENCY .60000000E+04
THE ABSORPTION COEFFICIENT IS .58100090E-04
THE REFRACTIVE INDEX MINUS UNITY IS -.38064801E-04

FOR THE FREQUENCY .15900000E+04
THE ABSORPTION COEFFICIENT IS .34582799E-03
THE REFRACTIVE INDEX MINUS UNITY IS -.33543894E-03

THE PUMP FREQUENCIES ARE .60000000E+04 .15950000E+04
THE POPULATION TRANSFERRED BETWEEN ADJACENT LEVELS IS .10000000E-04

FOR THE FREQUENCY .64000000E+04
THE ABSORPTION COEFFICIENT IS .58100090E-04
THE REFRACTIVE INDEX MINUS UNITY IS -.38064801E-04

FOR THE FREQUENCY .15950000E+04
THE ABSORPTION COEFFICIENT IS .34395787E-03
THE REFRACTIVE INDEX MINUS UNITY IS -.33289192E-03

THE PUMP FREQUENCIES ARE .60000000E+04 .16000000E+04
THE POPULATION TRANSFERRED BETWEEN ADJACENT LEVELS IS .10000000E-04

FOR THE FREQUENCY .6000000E-04
 THE ABSORPTION COEFFICIENT IS .5810009E-04
 THE REFRACTIVE INDEX MINUS UNITY IS -.3866480E-04

FOR THE FREQUENCY .1600000E-04
 THE ABSORPTION COEFFICIENT IS .3421100E-03
 THE REFRACTIVE INDEX MINUS UNITY IS -.3303667E-03

THE PUMP FREQUENCIES ARE .6000000E-04 .1605000E-04
 THE POPULATION TRANSFERED BETWEEN ADJACENT LEVELS IS. .1000000E-04

FOR THE FREQUENCY .6000000E-04
 THE ABSORPTION COEFFICIENT IS .5810009E-04
 THE REFRACTIVE INDEX MINUS UNITY IS -.3866480E-04

FOR THE FREQUENCY .1605000E-04
 THE ABSORPTION COEFFICIENT IS .3402005E-03
 THE REFRACTIVE INDEX MINUS UNITY IS -.3278631E-03

THE PUMP FREQUENCIES ARE .6000000E-04 .1610000E-04
 THE POPULATION TRANSFERED BETWEEN ADJACENT LEVELS IS. .1000000E-04

FOR THE FREQUENCY .6000000E-04
 THE ABSORPTION COEFFICIENT IS .5810009E-04
 THE REFRACTIVE INDEX MINUS UNITY IS -.3866480E-04

FOR THE FREQUENCY .1610000E-04
 THE ABSORPTION COEFFICIENT IS .3384049E-03
 THE REFRACTIVE INDEX MINUS UNITY IS -.3253805E-03

THE PUMP FREQUENCIES ARE .6000000E-04 .1615000E-04
 THE POPULATION TRANSFERED BETWEEN ADJACENT LEVELS IS. .1000000E-04

FOR THE FREQUENCY .6000000E-04
 THE ABSORPTION COEFFICIENT IS .5810009E-04
 THE REFRACTIVE INDEX MINUS UNITY IS -.3866480E-04

FOR THE FREQUENCY .1615000E-04
 THE ABSORPTION COEFFICIENT IS .3367050E-03
 THE REFRACTIVE INDEX MINUS UNITY IS -.3229195E-03

THE PUMP FREQUENCIES ARE .6000000E-04 .1620000E-04
 THE POPULATION TRANSFERED BETWEEN ADJACENT LEVELS IS. .1000000E-04

FOR THE FREQUENCY .6000000E-04
 THE ABSORPTION COEFFICIENT IS .5810009E-04
 THE REFRACTIVE INDEX MINUS UNITY IS -.3866480E-04

FOR THE FREQUENCY .1620000E-04
 THE ABSORPTION COEFFICIENT IS .3349480E-03
 THE REFRACTIVE INDEX MINUS UNITY IS -.3204787E-03

THE PUMP FREQUENCIES ARE .40000000E+04 .16250000E+04
 THE POPULATION TRANSFERRED BETWEEN ADJACENT LEVELS IS. .10000000E-04
 FOR THE FREQUENCY .60000000E+04
 THE ABSORPTION COEFFICIENT IS .50100090E-04
 THE REFRACTIVE INDEX MINUS UNITY IS -.30004001E-04
 FOR THE FREQUENCY .10250000E+04
 THE ABSORPTION COEFFICIENT IS .33321397E-03
 THE REFRACTIVE INDEX MINUS UNITY IS -.31005062E-03

THE PUMP FREQUENCIES ARE .60000000E+04 .16300000E+04
 THE POPULATION TRANSFERRED BETWEEN ADJACENT LEVELS IS. .10000000E-04
 FOR THE FREQUENCY .60000000E+04
 THE ABSORPTION COEFFICIENT IS .50100090E-04
 THE REFRACTIVE INDEX MINUS UNITY IS -.30004001E-04
 FOR THE FREQUENCY .10200000E+04
 THE ABSORPTION COEFFICIENT IS .33150093E-03
 THE REFRACTIVE INDEX MINUS UNITY IS -.31005049E-03

THE PUMP FREQUENCIES ARE .60000000E+04 .16350000E+04
 THE POPULATION TRANSFERRED BETWEEN ADJACENT LEVELS IS. .10000000E-04
 FOR THE FREQUENCY .60000000E+04
 THE ABSORPTION COEFFICIENT IS .50100090E-04
 THE REFRACTIVE INDEX MINUS UNITY IS -.30004001E-04
 FOR THE FREQUENCY .10250000E+04
 THE ABSORPTION COEFFICIENT IS .32900956E-03
 THE REFRACTIVE INDEX MINUS UNITY IS -.31327820E-03

THE PUMP FREQUENCIES ARE .60000000E+04 .16400000E+04
 THE POPULATION TRANSFERRED BETWEEN ADJACENT LEVELS IS. .10000000E-04
 FOR THE FREQUENCY .60000000E+04
 THE ABSORPTION COEFFICIENT IS .50100090E-04
 THE REFRACTIVE INDEX MINUS UNITY IS -.30004001E-04
 FOR THE FREQUENCY .10400000E+04
 THE ABSORPTION COEFFICIENT IS .32813949E-03
 THE REFRACTIVE INDEX MINUS UNITY IS -.31091747E-03

THE PUMP FREQUENCIES ARE .60000000E+04 .19500000E+04
 THE POPULATION TRANSFERRED BETWEEN ADJACENT LEVELS IS. .10000000E-04
 FOR THE FREQUENCY .60000000E+04
 THE ABSORPTION COEFFICIENT IS .50100090E-04
 THE REFRACTIVE INDEX MINUS UNITY IS -.30004001E-04

THE ABSORPTION COEFFICIENT IS .2623894E-03
THE REFRACTIVE INDEX MINUS UNITY IS -.19332750E-03

THE PUMP FREQUENCIES ARE .6000000E-04 .1955000E-04
THE POPULATION TRANSFERRED BETWEEN ADJACENT LEVELS IS. .1000000E-04
FOR THE FREQUENCY .6000000E-04
THE ABSORPTION COEFFICIENT IS .5010009E-04
THE REFRACTIVE INDEX MINUS UNITY IS -.3866480E-04
FOR THE FREQUENCY .1955000E-04
THE ABSORPTION COEFFICIENT IS .2618894E-03
THE REFRACTIVE INDEX MINUS UNITY IS -.1917667E-03

THE PUMP FREQUENCIES ARE .6000000E-04 .1960000E-04
THE POPULATION TRANSFERRED BETWEEN ADJACENT LEVELS IS. .1000000E-04
FOR THE FREQUENCY .6000000E-04
THE ABSORPTION COEFFICIENT IS .5010009E-04
THE REFRACTIVE INDEX MINUS UNITY IS -.3866480E-04
FOR THE FREQUENCY .1960000E-04
THE ABSORPTION COEFFICIENT IS .2614421E-03
THE REFRACTIVE INDEX MINUS UNITY IS -.1902131E-03

THE PUMP FREQUENCIES ARE .6000000E-04 .1965000E-04
THE POPULATION TRANSFERRED BETWEEN ADJACENT LEVELS IS. .1000000E-04
FOR THE FREQUENCY .6000000E-04
THE ABSORPTION COEFFICIENT IS .5010009E-04
THE REFRACTIVE INDEX MINUS UNITY IS -.3866480E-04
FOR THE FREQUENCY .1965000E-04
THE ABSORPTION COEFFICIENT IS .2610153E-03
THE REFRACTIVE INDEX MINUS UNITY IS -.1886683E-03

THE PUMP FREQUENCIES ARE .6000000E-04 .1970000E-04
THE POPULATION TRANSFERRED BETWEEN ADJACENT LEVELS IS. .1000000E-04
FOR THE FREQUENCY .6000000E-04
THE ABSORPTION COEFFICIENT IS .5010009E-04
THE REFRACTIVE INDEX MINUS UNITY IS -.3866480E-04
FOR THE FREQUENCY .1970000E-04
THE ABSORPTION COEFFICIENT IS .2606091E-03
THE REFRACTIVE INDEX MINUS UNITY IS -.1871267E-03

THE PUMP FREQUENCIES ARE .6000000E-04 .1975000E-04
THE POPULATION TRANSFERRED BETWEEN ADJACENT LEVELS IS. .1000000E-04
FOR THE FREQUENCY .6000000E-04

THE ABSORPTION COEFFICIENT IS .58108898E-04
 THE REFRACTIVE INDEX MINUS UNITY IS -.38664801E-04
 FOR THE FREQUENCY .19750000E-04
 THE ABSORPTION COEFFICIENT IS .28022382E-03
 THE REFRACTIVE INDEX MINUS UNITY IS -.18559353E-03

THE PUMP FREQUENCIES ARE .60000000E-04 .19800000E-04
 THE POPULATION TRANSFERED BETWEEN ADJACENT LEVELS IS. .10000000E-04
 FOR THE FREQUENCY .60000000E-04
 THE ABSORPTION COEFFICIENT IS .58108898E-04
 THE REFRACTIVE INDEX MINUS UNITY IS -.38664801E-04
 FOR THE FREQUENCY .19800000E-04
 THE ABSORPTION COEFFICIENT IS .25985958E-03
 THE REFRACTIVE INDEX MINUS UNITY IS -.18406688E-03

THE PUMP FREQUENCIES ARE .60000000E-04 .19850000E-04
 THE POPULATION TRANSFERED BETWEEN ADJACENT LEVELS IS. .10000000E-04
 FOR THE FREQUENCY .60000000E-04
 THE ABSORPTION COEFFICIENT IS .58108898E-04
 THE REFRACTIVE INDEX MINUS UNITY IS -.38664801E-04
 FOR THE FREQUENCY .19850000E-04
 THE ABSORPTION COEFFICIENT IS .25951645E-03
 THE REFRACTIVE INDEX MINUS UNITY IS -.18254654E-03

THE PUMP FREQUENCIES ARE .60000000E-04 .19900000E-04
 THE POPULATION TRANSFERED BETWEEN ADJACENT LEVELS IS. .10000000E-04
 FOR THE FREQUENCY .60000000E-04
 THE ABSORPTION COEFFICIENT IS .58108898E-04
 THE REFRACTIVE INDEX MINUS UNITY IS -.38664801E-04
 FOR THE FREQUENCY .19900000E-04
 THE ABSORPTION COEFFICIENT IS .25919487E-03
 THE REFRACTIVE INDEX MINUS UNITY IS -.18103243E-03

THE PUMP FREQUENCIES ARE .60000000E-04 .19950000E-04
 THE POPULATION TRANSFERED BETWEEN ADJACENT LEVELS IS. .10000000E-04
 FOR THE FREQUENCY .60000000E-04
 THE ABSORPTION COEFFICIENT IS .58108898E-04
 THE REFRACTIVE INDEX MINUS UNITY IS -.38664801E-04
 FOR THE FREQUENCY .19950000E-04
 THE ABSORPTION COEFFICIENT IS .25889583E-03
 THE REFRACTIVE INDEX MINUS UNITY IS -.17952437E-03

THE PUMP FREQUENCIES ARE .00000000E+04 .20000000E+04
THE POPULATION TRANSFERED BETWEEN ADJACENT LEVELS IS. .10000000E-04

FOR THE FREQUENCY .60000000E+04
THE ABSORPTION COEFFICIENT IS .50100090E-04
THE REFRACTIVE INDEX MINUS UNITY IS -.30004001E-04

FOR THE FREQUENCY .20000000E+04
THE ABSORPTION COEFFICIENT IS .25061715E-03
THE REFRACTIVE INDEX MINUS UNITY IS -.17002221E-03

THE PUMP FREQUENCIES ARE .60000000E+04 .20050000E+04
THE POPULATION TRANSFERED BETWEEN ADJACENT LEVELS IS. .10000000E-04

FOR THE FREQUENCY .60000000E+04
THE ABSORPTION COEFFICIENT IS .50100090E-04
THE REFRACTIVE INDEX MINUS UNITY IS -.30004001E-04

FOR THE FREQUENCY .20050000E+04
THE ABSORPTION COEFFICIENT IS .25030150E-03
THE REFRACTIVE INDEX MINUS UNITY IS -.17052500E-03

THE PUMP FREQUENCIES ARE .60000000E+04 .20100000E+04
THE POPULATION TRANSFERED BETWEEN ADJACENT LEVELS IS. .10000000E-04

FOR THE FREQUENCY .60000000E+04
THE ABSORPTION COEFFICIENT IS .50100090E-04
THE REFRACTIVE INDEX MINUS UNITY IS -.30004001E-04

FOR THE FREQUENCY .20100000E+04
THE ABSORPTION COEFFICIENT IS .25012035E-03
THE REFRACTIVE INDEX MINUS UNITY IS -.17303497E-03

THE PUMP FREQUENCIES ARE .60000000E+04 .20150000E+04
THE POPULATION TRANSFERED BETWEEN ADJACENT LEVELS IS. .10000000E-04

FOR THE FREQUENCY .60000000E+04
THE ABSORPTION COEFFICIENT IS .50100090E-04
THE REFRACTIVE INDEX MINUS UNITY IS -.30004001E-04

FOR THE FREQUENCY .20150000E+04
THE ABSORPTION COEFFICIENT IS .25791000E-03
THE REFRACTIVE INDEX MINUS UNITY IS -.17354959E-03

THE PUMP FREQUENCIES ARE .60000000E+04 .20200000E+04
THE POPULATION TRANSFERED BETWEEN ADJACENT LEVELS IS. .10000000E-04

FOR THE FREQUENCY .60000000E+04
THE ABSORPTION COEFFICIENT IS .50100090E-04
THE REFRACTIVE INDEX MINUS UNITY IS -.30004001E-04

FOR THE FREQUENCY .20200000E+04
THE ABSORPTION COEFFICIENT IS .25773072E-03
THE REFRACTIVE INDEX MINUS UNITY IS -.17206950E-03

THE PUMP FREQUENCIES ARE .60000000E-04 .20250000E-04
THE POPULATION TRANSFERRED BETWEEN ADJACENT LEVELS IS. .10000000E-04

FOR THE FREQUENCY .60000000E-04
THE ABSORPTION COEFFICIENT IS .50100090E-04
THE REFRACTIVE INDEX MINUS UNITY IS -.30064001E-04

FOR THE FREQUENCY .20250000E-04
THE ABSORPTION COEFFICIENT IS .25754443E-03
THE REFRACTIVE INDEX MINUS UNITY IS -.17059454E-03

THE PUMP FREQUENCIES ARE .60000000E-04 .20300000E-04
THE POPULATION TRANSFERRED BETWEEN ADJACENT LEVELS IS. .10000000E-04

FOR THE FREQUENCY .60000000E-04
THE ABSORPTION COEFFICIENT IS .50100090E-04
THE REFRACTIVE INDEX MINUS UNITY IS -.30064001E-04

FOR THE FREQUENCY .20300000E-04
THE ABSORPTION COEFFICIENT IS .25742646E-03
THE REFRACTIVE INDEX MINUS UNITY IS -.16912456E-03

THE PUMP FREQUENCIES ARE .60000000E-04 .20350000E-04
THE POPULATION TRANSFERRED BETWEEN ADJACENT LEVELS IS. .10000000E-04

FOR THE FREQUENCY .60000000E-04
THE ABSORPTION COEFFICIENT IS .50100090E-04
THE REFRACTIVE INDEX MINUS UNITY IS -.30064001E-04

FOR THE FREQUENCY .20350000E-04
THE ABSORPTION COEFFICIENT IS .25731054E-03
THE REFRACTIVE INDEX MINUS UNITY IS -.16765941E-03

THE PUMP FREQUENCIES ARE .60000000E-04 .20400000E-04
THE POPULATION TRANSFERRED BETWEEN ADJACENT LEVELS IS. .10000000E-04

FOR THE FREQUENCY .60000000E-04
THE ABSORPTION COEFFICIENT IS .50100090E-04
THE REFRACTIVE INDEX MINUS UNITY IS -.30064001E-04

FOR THE FREQUENCY .20400000E-04
THE ABSORPTION COEFFICIENT IS .25721001E-03
THE REFRACTIVE INDEX MINUS UNITY IS -.16619893E-03

THE PUMP FREQUENCIES ARE .60000000E-04 .20450000E-04
THE POPULATION TRANSFERRED BETWEEN ADJACENT LEVELS IS. .10000000E-04

FOR THE FREQUENCY .60000000E-04
THE ABSORPTION COEFFICIENT IS .50100090E-04
THE REFRACTIVE INDEX MINUS UNITY IS -.30064001E-04

FOR THE FREQUENCY .20450000E-04
THE ABSORPTION COEFFICIENT IS .25715105E-03
THE REFRACTIVE INDEX MINUS UNITY IS -.16474296E-03

THE PUMP FREQUENCIES ARE .60000000E-04 .20500000E-04
THE POPULATION TRANSFERRED BETWEEN ADJACENT LEVELS IS. .10000000E-04

FOR THE FREQUENCY .60000000E-04
THE ABSORPTION COEFFICIENT IS .58100090E-04
THE REFRACTIVE INDEX MINUS UNITY IS -.30004001E-04

FOR THE FREQUENCY .20500000E-04
THE ABSORPTION COEFFICIENT IS .25711004E-03
THE REFRACTIVE INDEX MINUS UNITY IS -.16329135E-03

THAT'S ALL